DOTTORATO DI RICERCA IN
Scienze Applicate a Benessere e Sostenibilità

XXXVIII CICLO

COORDINATORE Prof. Carlo Baldari

INNOVATIVE EEG BIOMARKERS AND AI ALGORITHMS FOR THE EVALUATION OF PHYSIOLOGICAL AND PATHOLOGICAL AGING

Settore Scientifico Disciplinare: BIOS-06/A (ex BIO-09)

PhD candidate
Dr. Alessia Cacciotti

Scientific Supervisor
Prof. Fabrizio Vecchio

ABSTRACT

Aging is a biologically natural process that changes the structure and functions gradually at different levels, from the cells to the large-scale brain networks. Usually, physiological aging is associated with mild cognitive change; however, in a significant number of people, the process can become pathological and eventually result in Mild Cognitive Impairment (MCI) and Alzheimer's disease (AD).

Differentiating healthy from pathologic aging is still a hard scientific and clinical problem, especially in the preclinical and prodromal phases of neurodegenerative diseases. One method to study age-related brain changes is the electroencephalography (EEG), a non-invasive technique with a very high temporal resolution. Initial EEG studies have already contributed significantly to the understanding of age-related changes in brain oscillatory dynamics, but the combination of next-generation brain analytic methods, such as graph theory and entropy analysis, has the potential to reveal new biomarkers that can indicate not only physiological adaptations but also pathological deviations. Besides that, the new implementation of machine learning and artificial intelligence (AI) in the neurophysiological field represents a powerful tool for predictive and individualization purposes.

The current PhD project, titled ***"Identification of innovative EEG biomarkers and AI algorithms for physiological and pathological aging evaluation"***, aims to identify novel EEG biomarkers and implement AI models to distinguish between age groups and cognitive states. Specifically, the project is meant to achieve three main goals: (i) through connectivity and entropy analysis to validate novel EEG features that show statistically significant differences not only between young, adult, and elderly subjects but also between healthy elderly controls, MCI subjects, and AD patients; (ii) to implement AI algorithms that can track brain age changes among healthy people and differentiate healthy elderly people from pathological group, with the ultimate goal of facilitating early detection, prognostic assessment, and treatment planning.

120 healthy volunteers equally spread across three age groups (young, adult, and old) and 40 MCI as well as 40 AD patients were enrolled. Additionally, data from databases were included, for a total of 109 healthy elderly subjects, 75 MCI subjects, and 85 AD patients. Resting-state EEG in eyes-closed condition will be recorded from all participants. Healthy elderly, MCI subjects, and AD patients will be evaluated through a battery of neuropsychological tests. Functional connectivity will be computed along with graph theoretic measures, and signal complexity will be described by Approximate Entropy. Additionally, to both brain age estimation and physiological

versus pathological aging classification, optimization and feature selection methods will be used to pinpoint the most discriminative EEG-derived predictors. These analyses allow to significantly raise the classification's precision and reliability and reveal the neurophysiological features with the most significant diagnostic and prognostic value.

The research project would be a significant contribution to the emerging field of computational neurophysiology by facilitating the further application of EEG biomarkers and AI models. It would potentially lead to the implementation of robust biomarkers of aging which could be used for early detection of neurodegenerative processes, prognostic refinement, and, ultimately, the advancement of personalized therapy in the domain of age-related cognitive decline.

Table of contents

INTRODUCTION

Aging can be defined as a persistent decline in the age-specific fitness components of an organism due to internal physiological deterioration. It represents an inevitable biological process characterized by a progressive structural and functional decline, which manifests at multiple levels, from cellular to whole-body functions. Understanding how the brain changes over the course of aging is of fundamental importance for at least two reasons. On one hand, it enables a deeper comprehension of the neurobiological mechanisms underlying aging and how such changes affect cognitive functions. On the other, it offers the possibility to recognize and better characterize ***age-related pathologies, particularly neurodegenerative diseases such as Alzheimer's disease (AD)***.

AD represents one of the most common and severe neurodegenerative conditions in the elderly population. It is clinically characterized by progressive memory decline, impairment in at least one cognitive domain, and marked disturbances in social and occupational functioning. Due to the high prevalence and influence of AD, it is essential to make an early diagnosis to optimize patient care. A lot of work has been done during the last few years in the field of early biomarkers identification. This is particularly significant for prodromal states such as Mild Cognitive Impairment (MCI), which stands for a condition intermediate between normal aging and dementia. MCI is a clinical syndrome characterized by memory impairment that does not meet the clinical criteria for dementia.

Within this context, ***electroencephalography (EEG)*** has been the main methodological instrument to investigate brain function in aging. EEG is a non-invasive method that can measure the brain's electrical activity with a very high temporal resolution. Besides its standard application in clinical neurology, EEG has become a powerful tool for recording brain activity changes and monitoring neuroplasticity processes. Importantly, its integration with advanced computational methods, such as artificial intelligence (AI) and machine learning algorithms, opens new perspectives for the identification of innovative biomarkers of aging and neurodegeneration.

The present PhD thesis, titled ***"Innovative EEG biomarkers and AI algorithms for the evaluation of physiological and pathological aging"***, is organized into two major sections. The ***first section*** provides a theoretical and methodological overview: it discusses the biological and neurophysiological processes underlying aging, with particular attention to the alterations in brain connectivity and plasticity, and presents EEG as a fundamental tool for the evaluation of healthy and pathological trajectories of aging.

The ***second section*** describes the original experimental work that was done during the three years of the PhD program. It started with a series of preliminary studies that supported the main project, followed by the core investigation. The main research used EEG recordings to look at how aging changed functional connectivity and neural complexity in order to distinguish the physical changes in aging from the ones related to pathological decline. This work, through the combination of EEG-derived measures with AI approaches, is a step towards the fast-expanding field of computational neurophysiology, which is essentially the first goal of the next-generation early detection, and treatment strategies of neurodegenerative disorders.

FIRST PART

AGING

The aging process was originally defined by Harman as a “progressive accumulation of changes with time that are associated with or responsible for the ever-increasing susceptibility to disease and death which accompanies advancing age” [1]. Chronological age is the most powerful risk factor for a broad spectrum of debilitating conditions, particularly neurodegenerative disorders. The central nervous system is especially vulnerable to age-related perturbations: the incidence of Alzheimer’s disease, Parkinson’s disease, and related dementias rises exponentially with advancing age, and virtually all aged brains exhibit hallmark alterations such as synaptic degeneration, mitochondrial dysfunction, impaired proteostasis, neuroinflammatory activation, and accumulation of misfolded proteins including β-amyloid and hyperphosphorylated tau. As global life expectancy increases, the prevalence of these disorders is projected to escalate dramatically; for example, the number of individuals affected by Alzheimer’s disease is expected to more than double within the next two decades [2]. Deciphering the cellular and molecular mechanisms through which aging heightens vulnerability to neurodegeneration is therefore critical for identifying biomarkers of early pathological change and for developing targeted preventive and therapeutic interventions.

Brain aging is a long-term, multifactorial process, where the influences of genetics, molecules, cells, and the environment combine to degrade the brain's structural and functional aspects as well as cognitive abilities [3]. In contrast to acute neurological injury, aging is not a result of a single cause, but rather the outcome of gradual changes in metabolism, neurotransmission, vascular function, and immune regulation. The lifestyle factors like diet, physical activity, psychosocial stress, and exposure to environmental pollutants can influence these processes [4]. Delving into these mechanisms is necessary for early identification of vulnerable individuals, and then, creation of suitable interventions to mitigate age-related cognitive impairment and neurodegeneration.

GENETIC AND EPIGENETIC CONTRIBUTIONS

A growing body of evidence indicates that inherited genetic variation meaningfully shapes the pace and pattern of brain aging. Twin and family studies consistently show that roughly one-third to nearly half of the variability in late-life cognitive performance can be attributed to heritable factors, highlighting a strong genetic component alongside environmental influences

[5].

The most studied genetic contributor is the apolipoprotein E (APOE) gene. The ε4 variant of APOE has long been acknowledged as the major common risk factor for non-inherited Alzheimer's disease, but the impact of the gene is wider: ε4 carriers show faster cortical thinning and in general, they exhibit earlier memory decline even if they do not have dementia [6]. Besides the "longevity genes", which are involved in stress resistance, mitochondria maintenance, and neuronal survival, FOXO3A variants have been particularly linked to human longevity. It is considered to be the main regulator of the antioxidant response, apoptosis, and cellular stress resistance pathways [7]. Likewise, SIRT1, a NAD^+-dependent deacetylase, plays crucial roles in neural differentiation, mitochondrial function, and of supporting the nervous system in facing neurodegenerative processes [8, 9].

The genetic risk of disease can be seen as an initial bias which might be changed or worsened later by epigenetic drift, that is, the slow transition of the epigenome during life. The age-related changes of DNA methylation patterns, histone modifications and non-coding RNA profiles can for instance, inactivate or activate neuronal genes thereby altering transcriptional networks involved in synaptic plasticity, neuroinflammation, and metabolic regulation [10]. These epigenetic changes provide a mechanistic bridge between environmental exposures and the heritable architecture of the aging brain, helping to explain why individuals with similar genetic backgrounds may age very differently depending on lifestyle and environmental context.

NEUROCHEMICAL ALTERATIONS

Normal brain aging is accompanied by a series of neurochemical changes that influence cognition, mood, and neural plasticity. The most prominent is the alteration in the dopaminergic, serotonergic, and monoaminergic systems, which collectively regulate executive function, learning, and emotional balance. Dopamine, for instance, plays a crucial role in executive processes, motivation, and motor control. Both post-mortem and in-vivo studies suggest that dopaminergic signalling gradually decreases with age. The decrease is estimated to be between 3.7% and 14% per decade in normal aging, whereas dopamine synthesis was reported to be relatively unaffected or to show no consistent decline with age [11, 12]. In addition, longitudinal data provide a mechanistic explanation for the observed association between cortical and striatal D2/3 receptor availability and working memory performance, showing that over time there is a reduction in the latter that is linked to the former [13]. To that extent, dopaminergic changes could be the reason for slower cognitive processing, weaker

working memory, and subtle impairments in motor control, which can still be detected in non-demented older adults [14].

The serotonergic system, which is essential for mood regulation, adult neurogenesis, and synaptic plasticity, is also affected by aging. A number of in vivo and post-mortem studies conducted in humans point to a decline in the density of 5-HT receptors, especially in the case of 5-HT1A and 5-HT2A subtypes, as well as in serotonin transporter binding in the cortex and the hippocampus [15]. These alterations may be the cause of several symptoms frequently experienced in the elderly, such as depressed mood, disrupt sleep architecture, and difficulty in cognitive tasks requiring mental flexibility.

At the same time, monoamine oxidase (MAO), the enzyme that plays a pivotal role in dopamine and serotonin catabolism, is reported to have enhanced activity in old age. The upregulation of this enzymatic activity accelerates monoamine degradation and, at the same time, generates reactive oxygen species (ROS) like hydrogen peroxide. The oxidative insult that follows when antioxidant defences are overwhelmed can cause lipid peroxidation, mitochondrial dysfunction, and DNA damage and thus promote aging in neurons and make them more susceptible to neurodegenerative processes [16].

HORMONAL AND ENDOCRINE INFLUENCES

Endocrine changes represent a powerful yet often underappreciated driver of brain aging. Throughout life, circulating hormones interact with neuronal receptors to regulate synaptic plasticity, neurogenesis, and neuroinflammatory processes. As age advances, several key hormonal systems undergo profound alterations that collectively influence both cognitive and structural brain outcomes. Sex steroids, such as estrogens and androgens, exert broad neuroprotective effects by promoting synaptic spine formation, supporting cholinergic transmission, and attenuating neuroinflammation [17]. In women, the sharp decline in estrogen levels following menopause has been epidemiologically linked to a higher risk of cognitive impairment and Alzheimer's disease [18]. Evidence from observational and randomized trials of hormone replacement therapy (HRT) suggests that treatment initiated near the onset of menopause may confer cognitive benefits, whereas later initiation appears less effective or even detrimental [19]. Another crucial system involved in brain aging is the growth hormone/insulin-like growth factor 1 (GH/IGF-1) axis, which supports hippocampal neurogenesis and neuronal survival. The levels of GH and IGF-1 decline progressively with age, and lower IGF-1 concentrations have been associated with poorer episodic memory and reduced hippocampal

volume in older adults [20]. IGF-1 signaling plays a pivotal role in synaptic plasticity and long-term potentiation, processes central to learning and memory, and may therefore contribute to age-related cognitive decline [21]. However, the role of IGF-1 in brain aging is complex: in some contexts, it exerts protective effects, while in others it may promote pathological processes, such as those seen in Alzheimer's disease, depending on cellular signaling dynamics — a duality often referred to as the "Jekyll & Hyde" nature of IGF-1 [22]. In parallel, chronic activation of the hypothalamic–pituitary–adrenal (HPA) axis leads to sustained elevations in cortisol levels. While acute cortisol release is part of an adaptive stress response, prolonged exposure can damage hippocampal neurons, impair dendritic remodeling, and disrupt memory consolidation [23].

Collectively, these hormonal changes highlight how endocrine aging interacts with neural circuits to shape the structural integrity and functional capacity of the aging brain.

STRUCTURAL BRAIN CHANGES

Age-related structural modifications are the most visible hallmarks of brain aging and can be quantified through advanced neuroimaging. These alterations involve grey matter (GM), white matter (WM), and cerebrovascular networks, unfolding heterogeneously across cortical and subcortical regions. A summary of structural brain changes in normal aging is reported in Table 1.

- ***Global Brain Atrophy.*** Longitudinal MRI studies demonstrate that the total brain volume decreases by about 0.2–0.5 % per year from midlife, with a more pronounced decline after the age of 70 [24, 25]. The increase in the size of the ventricles is a reflection of this global atrophy and is a predictor of the Alzheimer's disease stage from MCI condition conversion [26]. The volumetric decline, in fact, is a result of neuronal soma shrinkage, reduced dendritic arborization, and loss of dendritic spines rather than a large-scale neuronal death [27].
- ***Regional Vulnerability.*** The prefrontal cortex, hippocampus, and temporal association cortices are the areas mainly subjected to age-related atrophy, whereas the occipital lobe is still relatively intact [28]. Volume reductions lead to a reduction in size of the hippocampal CA1 and dentate gyrus regions and, as consequence, impaired episodic memory [29, 30]. Likewise, there is a shrinkage of subcortical structures such as the caudate and thalamus, which causes disruption of the cortico-striatal and thalamo-cortical networks, vital for executive function [31].

- ***White-Matter Degeneration.*** Diffusion tensor imaging (DTI) is a reliable method to detect age-related reductions in fractional anisotropy (FA). This reduction is linked to a decrease in axonal density and demyelination [32, 33]. The frontostriatal and frontoparietal tracts are the most affected, supporting the "frontal aging hypothesis", that relates executive dysfunction with anterior WM degradation [34]. In addition, white-matter hyperintensities (WMHs), observable on T2-weighted MRI (Figure 1), are indicative of small-vessel ischemic injury and are associated with slow processing speed, gait disturbance, and increased risk of stroke and dementia [35].
- ***Synaptic and Dendritic Remodeling***. Examination of the brain after death reveals that synaptic loss, instead of neuronal death, is the main cellular basis for the volume decline of the aged brain. The decrease of dendritic spine density and simplification of arborization impairs cortical connectivity and neuroplasticity [36]. It is worth noting that synaptic integrity is a biological process that depends on stimulation: continuous intellectual activity and physical exercise have been proven to lessen these degenerative changes by facilitating synaptic maintenance and neurogenesis [37, 38].

Structure/Measure	*Typical Change (per decade)*	*Functional Consequence*
Total brain volume	↓ 0.2–0.5 %/year post-midlife	Global cognitive slowing
Prefrontal cortex	Marked cortical thinning	Executive dysfunction
Hippocampus (CA1, dentate)	Subfield atrophy	Episodic memory deficits
White-matter FA	Decline in frontostriatal tracts	Slower processing, attention deficits
White-matter hyperintensity	Increased lesion load	Gait disturbance, vascular cognitive impairment

Table 1. *Structural Brain Changes in Normal Aging*

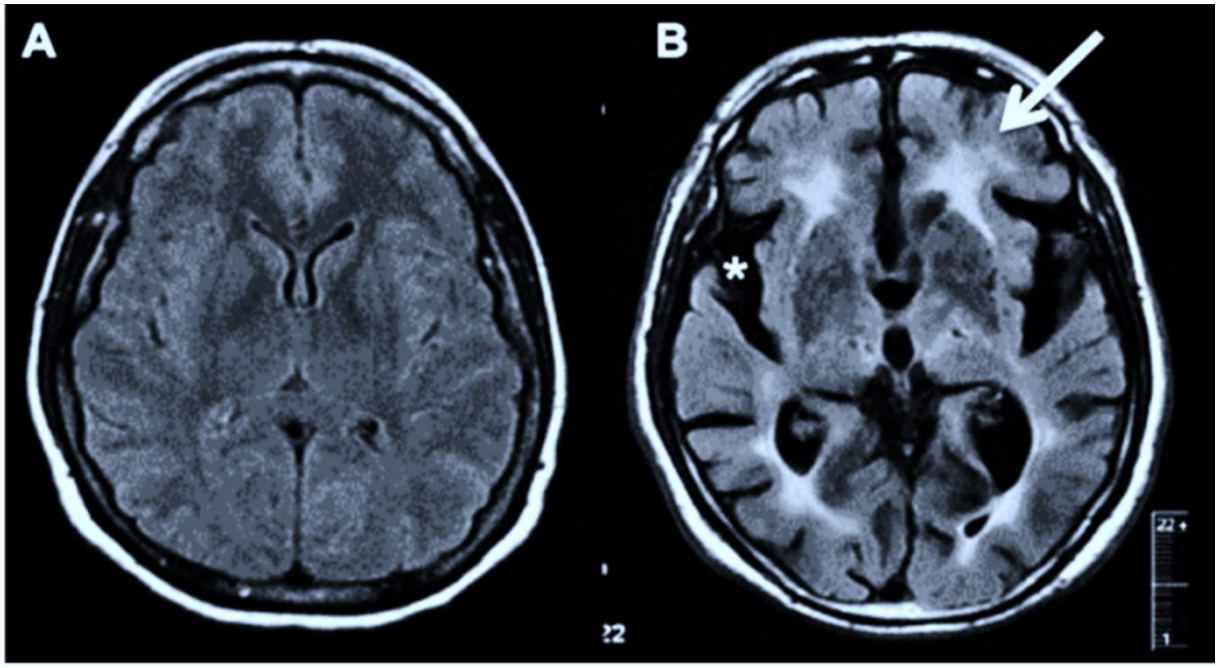

Figure 1. *Regional Patterns of Age-Related Atrophy. A: magnetic resonance imaging (MRI) of a normal 32-year-old woman. B: MRI of a 78 years old woman with temporal atrophy (asterisks) and white matter disease (white arrow)*

COGNITIVE AND FUNCTIONAL CONSEQUENCES

The structural brain alterations described above have direct repercussions on cognition, behaviour, and large-scale neural network dynamics. Cognitive aging is a highly heterogeneous process: while some domains remain relatively resilient, others exhibit a steady decline even in the absence of overt neurodegenerative disease. The pattern and extent of decline depend on the interplay between neural vulnerability, compensatory mechanisms, and lifestyle factors that promote or protect cognitive reserve. A summary of the main cognitive domains affected by aging is presented in Table 2.

Domains of Cognitive Change

Episodic memory is consistently the most sensitive domain to aging, showing progressive impairment in the ability to encode, store, and retrieve context-rich information [39]. Structural and functional MRI studies attribute this decline primarily to hippocampal atrophy and disruptions in the default-mode network (DMN), particularly the connectivity between the medial temporal lobe and posterior cingulate cortex [40, 41].

Working memory and executive functions—which depend heavily on the prefrontal cortex and frontoparietal circuits—also show gradual deterioration. Age-related thinning of the prefrontal cortex, combined with degeneration of long-range white-matter tracts, contributes to reduced

attentional control, multitasking difficulties, and slower decision-making [31, 42].

Decline in processing speed represents one of the most robust and generalized effects of aging on cognition. Slower information processing has been linked to widespread white-matter degradation and reduced efficiency of neural transmission [33, 43]. This slowing often precedes and predicts later cognitive decline across multiple domains [44].

In contrast, semantic memory (knowledge of facts and vocabulary) and procedural memory (skills and habits) are relatively preserved until late life, reflecting the selective nature of cognitive aging [45, 46]. This domain-specific resilience underscores the brain's capacity to maintain well-practiced cognitive functions even amidst structural deterioration.

Network Reorganization and Compensation

Functional neuroimaging has revealed that aging does not merely result in loss of activation but often involves adaptive reorganization of neural networks to maintain performance. Older adults frequently engage additional or alternative brain circuits compared with younger individuals—a phenomenon interpreted as compensatory recruitment rather than inefficiency [42, 47].

Three influential models illustrate these compensatory mechanisms:

1. *HAROLD (Hemispheric Asymmetry Reduction in Older Adults):* Older adults tend to exhibit more bilateral prefrontal activation during tasks that elicit unilateral activity in younger adults, suggesting the recruitment of contralateral regions to compensate for local inefficiency [48].
2. *CRUNCH (Compensation-Related Utilization of Neural Circuits Hypothesis):* This model posits that older adults show greater neural activation at lower task demands to maintain performance, but reach a ceiling earlier than younger adults, resulting in declining efficiency as task complexity increases [47].
3. *PASA (Posterior–Anterior Shift in Aging):* Functional activity tends to shift from posterior to anterior cortical regions, indicating greater reliance on prefrontal resources to compensate for occipitotemporal decline [49].

Together, these models highlight the dynamic interplay between neural decline and compensatory plasticity in the aging brain, supporting the concept of a "scaffolded" cognitive system that adapts to structural losses [50].

The combination of structural atrophy, white-matter deterioration, and compensatory reorganization manifests behaviourally as slower information processing, reduced attentional control, and diminished multitasking ability [43]. Nonetheless, these declines are not inevitable

nor irreversible. Ample evidence indicates that lifestyle factors—such as aerobic exercise, cognitive training, and social engagement—can bolster neural plasticity and preserve cognitive reserve, delaying or mitigating functional decline [51]. Physical activity enhances hippocampal volume and neurogenesis, while cognitive stimulation strengthens existing synaptic networks and promotes compensatory recruitment, underscoring the remarkable adaptability of the aging brain [38, 39].

Cognitive Domain	*Primary Neural Substrate*	*Typical Age-Related Change*
Episodic memory	Hippocampus, medial temporal lobe	Decline in encoding and retrieval
Working memory	Dorsolateral prefrontal cortex	Reduced capacity and slower updating
Processing speed	Global white-matter tracts	Generalized slowing
Semantic memory	Temporal neocortex	Relative preservation
Procedural memory	Basal ganglia, cerebellum	Relative preservation

Table 2. *Age-Related Cognitive Changes*

PHYSIOLOGICAL AGING

Healthy aging refers to the ability to grow older while maintaining physical vitality, cognitive competence, emotional stability, and independence, without the onset of neurodegenerative disease. Although aging inevitably entails structural and functional alterations in the brain, many individuals preserve a high quality of life and remain engaged in complex intellectual, social, and occupational activities well into advanced age [39, 52]. Understanding the biological and environmental factors that promote resilience is essential for distinguishing normal aging from pathology and for identifying strategies to sustain cognitive health across the lifespan.

MORPHOLOGICAL AND FUNCTIONAL BRAIN CHANGES

Neuroimaging studies consistently show that healthy aging is accompanied by gradual reductions in total brain volume, cortical thickness, and white-matter integrity [31]. Grey-matter loss is most pronounced in the prefrontal cortex and hippocampus, regions crucial for executive control and memory formation, while primary sensory and occipital cortices are relatively preserved [28, 53]. Functional MRI studies demonstrate that older adults exhibit altered connectivity within large-scale networks. In particular, the default mode network (DMN) shows reduced intra-network coherence, whereas compensatory increases in

frontoparietal network activity are observed during demanding cognitive tasks [40, 54]. This pattern reflects the brain's remarkable ability for neurocognitive scaffolding—the recruitment of alternative neural circuits to preserve performance despite structural decline [46]. Thus, aging should not be viewed solely as a degenerative process but also as one of plasticity, adaptation, and reorganization.

COGNITIVE CHARACTERISTICS OF HEALTHY AGING

Although mild declines in some cognitive domains are common, the overall cognitive profile of healthy older adults remains robust. Processing speed, working memory, and aspects of executive function typically decline modestly with age [41, 43]. These changes manifest as slower reaction times and reduced multitasking ability. In contrast, semantic memory, language comprehension, and emotional regulation often remain stable or even improve due to accumulated experience and knowledge [55, 56]. Primary visual and spatial reasoning abilities are also relatively preserved when sensory impairments are corrected. Importantly, profound episodic memory loss or dementia-like symptoms do not occur in normal aging unless there is concomitant neuropathology affecting the medial temporal lobe [57].

A defining feature of healthy aging is its remarkable interindividual variability. Some individuals maintain near-youthful cognition into their ninth decade, while others show significant decline at a similar chronological age [51]. In this context, the neural reserve hypothesis is particularly noteworthy. It refers to the brain's intrinsic capacity—such as greater synaptic density or efficient connectivity—that confers resilience to age-related changes [58]. The cognitive reserve concept extends this to the flexible recruitment of alternative networks and strategies, built through lifelong learning and intellectual engagement [59]. Functional imaging supports these ideas: older adults often exhibit bilateral prefrontal activation (HAROLD model) or increased activity at lower task demands (CRUNCH model), reflecting compensatory reorganization to maintain performance [47, 48].

A paradox in healthy aging is the frequent detection of neuropathological markers associated with Alzheimer's disease and other dementias in cognitively intact individuals. Autopsy studies have revealed amyloid-β plaques and neurofibrillary tangles even in older adults without cognitive symptoms [60, 61]. These findings suggest that neuropathological burden alone does not determine cognitive outcome. Individuals termed "super-agers" demonstrate preserved cognition despite significant amyloid accumulation, possibly due to enhanced synaptic plasticity, robust immune function, or protective genetic variants such as APOE ε2 [62].

Understanding these protective mechanisms is crucial for identifying targets that promote resilience to pathology.

PATHOLOGICAL AGING

Neurodegenerative diseases (NDs) comprise a diverse group of progressive disorders characterized by the selective loss of neurons and synapses within specific brain or spinal cord regions. Although each condition exhibits unique clinical features and topographical patterns of neuronal vulnerability, they share several pathogenic hallmarks: abnormal protein aggregation, mitochondrial dysfunction, oxidative stress, neuroinflammation, and impairment of proteostatic and autophagic systems [63]. The global burden of these disorders is very high and still growing exponentially as the average life expectancy goes up. The GBD Study 2019 shows that, taken together, neurological disorders are the number one cause of disability-adjusted life years (DALYs) globally (Figure 2), of which Alzheimer's disease and other dementias are the leading contributors among neurodegenerative conditions [64].

The major neurodegenerative diseases prevalence increases significantly with aging. The example of such is the incidence of Alzheimer's disease (AD) that approximately doubles every five years after age 65 and reaches nearly 30 % among those over 85 years [65]. Parkinson's disease (PD) is a condition that, according to current statistics, affects more than 10 million people worldwide. The prevalence of this disease is, however, expected to double in 2040 [66]. Frontotemporal lobar degeneration (FTLD) and amyotrophic lateral sclerosis (ALS) are less common, but they become the main contributors to years of life lost because they are usually the ones that start in adulthood and present earlier [67].

The economic impact is equally striking: the worldwide cost of dementia care alone is estimated to exceed US $1 trillion annually and is expected to double by 2030 [68]. Beyond economic measures, the human cost is profound, encompassing caregiver burden, loss of independence, and reduced quality of life for patients and families.

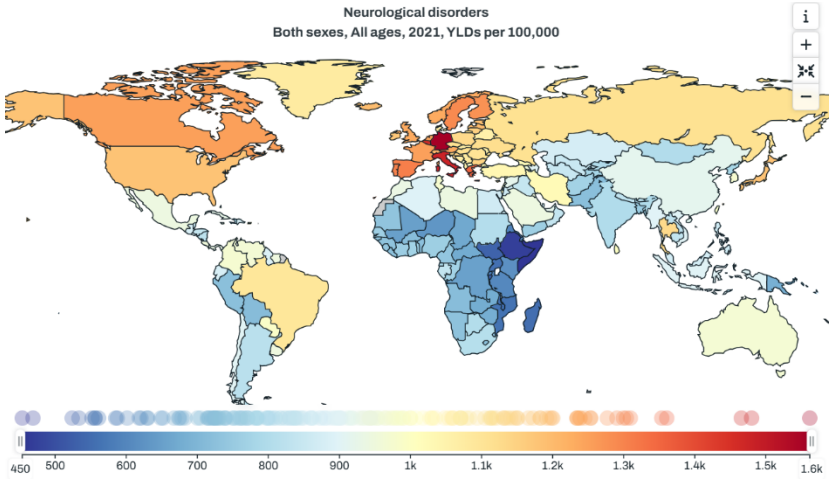

Figure 2. *Distribution of Disability Adjusted Life Years of neurodegenerative diseases at the global level available until the year 2021, according to the Institute for Health Metrics and Evaluation (IHME).*

SHARED PATHOGENIC MECHANISMS

- ***Protein Misfolding and Aggregation.*** A defining feature of most NDs is the accumulation of misfolded proteins that form toxic oligomers or insoluble fibrillar aggregates. Examples include amyloid-β and hyperphosphorylated tau in AD, α-synuclein in PD and dementia with Lewy bodies, TDP-43 in ALS and FTLD, and mutant huntingtin in Huntington's disease (HD) [69]. These proteins disrupt cellular homeostasis through multiple mechanisms: they impair synaptic transmission, trigger endoplasmic-reticulum stress, and interfere with axonal transport [70].
- ***Mitochondrial Dysfunction and Oxidative Stress.*** Mitochondria, being the powerhouses of the neurons, are heavily relied on for the production of ATP and calcium buffering. Damage to mitochondrial DNA, reduced electron transport chain activity and less mitophagy have been reported in neurodegenerative diseases, which thus result in the generation of a large number of reactive oxygen species (ROS). Oxygen radicals then attack all biological molecules including proteins, lipids, and nucleic acids initiating a self-perpetuating process of neuronal loss [71].
- ***Neuroinflammation and Immune Dysregulation.*** Microglia, the brain immune cells which keep homeostasis, are the main cause of neuroinflammation. Upon chronic activation microglia release pro-inflammatory cytokines (e.g., IL-1β, TNF-α) and reactive nitrogen species that cause further neuronal death [72]. While transient neuroinflammation may be beneficial, extensive activation leads to synaptic loss and disease spread. Recent genomic analyses point towards a significant role of innate immune system, as it identifies

genes such as TREM2 and CD33 involved in Alzheimer's disease and complement pathway genes in other dementias [73].

- ***Impaired Proteostasis and Autophagy.*** The maintenance of proteostasis—proper protein synthesis, folding, and degradation—is essential for neuronal health. Aging and genetic risk factors can compromise the ubiquitin-proteasome system and autophagic-lysosomal pathways, allowing toxic protein species to accumulate [74]. Therapeutic strategies aimed at enhancing autophagy or stabilizing proteostasis are therefore an active area of research.
- ***Excitotoxicity and Synaptic Dysfunction.*** Excessive activation of glutamate receptors leads to excitotoxic neuronal injury via calcium overload and free radical generation. Synaptic dysfunction, evident as impaired long-term potentiation and reduced dendritic spine density, is an early and consistent feature across many NDs, preceding overt cell death and clinical symptoms [75].

ALZHEIMER'S DISEASE (AD)

While all the neurodegenerative disorders present unique challenges, Alzheimer's disease remains the most prevalent and consequential. It accounts for roughly 60–70 % of all dementia cases and serves as the prototypical neurodegenerative disorder for studying age-related cognitive decline [65].

EPIDEMIOLOGY

AD is the most common cause of dementia worldwide and represents a major global health challenge. According to the World Alzheimer Report and the 2023 Alzheimer's Association data, an estimated 55 million people currently live with dementia of all types, and 60–70 % of these cases are attributable to AD [65]. Demographic projections indicate that, driven by population aging, the number of people with dementia will reach 78 million by 2030 and could surpass 139 million by 2050, with AD remaining the leading etiology (WHO, 2023).

Very large population-based studies indicate that the prevalence of AD increases exponentially with age, roughly doubling every five years after age 65. It is estimated that around 5–7% of the population aged 60 and above suffers from AD. The trend goes up to 15–20% for people aged 75 and over and to 25–35% for those 85 years and older. The incidence rate mirrors the same pattern and quite dramatically rises from about one case per 1,000 person-years in the

early 60s to more than 25 cases per 1,000 person-years beyond 90 years of age. Those trajectories are a manifestation of the close link between aging and neurodegenerative vulnerabilities that place AD among the most frequent chronic conditions in late life [76, 77].

Significant differences in the prevalence of the disease between the sexes are also present. Women account for almost two-thirds of all AD cases, a difference that can be only partially explained by the longer life expectancy of women. On the other hand, biological factors seem to contribute as well: postmenopausal estrogen reduction, sex-specific effects of the APOE ε4 allele, and differences in brain reserve, cardiovascular risk, and immune function that may elevate female vulnerability [78]. Additionally, socio-cultural factors, such as historically lower education levels and disproportionate caregiving roles, may play a part in the gender gap in AD prevalence and outcomes [78].

The differences in prevalence between various ethnic groups and regions of the world further complicate the picture. Prevalence is generally a little higher in North America and Western Europe than in some parts of Africa or South Asia. However, this difference could be partially explained by methodological differences raised due to diagnostic criteria and case ascertainment, variations in vascular health, education, lifestyle factors, medical care access and demographic aging patterns [76, 77].

The public health impact of AD is staggering. The world economic cost of the dementia disease exceeded USD $1.3 trillion in 2022 and is forecasted to almost double by 2030, according to the World Health Organization (2023). This is mainly attributable to the rising healthcare expenditures, institutional care, and economic value of the unpaid family caregiving [68]. Besides the monetary aspect, AD causes immense psychological and physical stress to caregivers, thus, elevating the rates of depression, anxiety, and social isolation among family members. In total, dementia is a significant contributor to the pool of disability-adjusted life years (DALYs) lost in aging societies and, thus, becomes one of the main causes behind dependence and living in institutions among the elderly population.

In conclusion, the disease of Alzheimer's comes out as one of the most important public health issues worldwide, thus illustrating the necessity of strategies on the public health level to be adopted, focusing on prevention, early diagnosis, and fair access to care. The sustained demographic transition and the enlarging burden in developing countries point to the pressing need for long-lasting, culturally-sensitive interventions aimed at alleviating both the personal and the societal cost of this escalating epidemic.

ETIOLOGY AND NEUROPATHOLGY

AD develops through a multifactorial and decades-long interplay of genetic, molecular, and environmental influences rather than a single causal event. The most influential explanatory model is the amyloid cascade hypothesis, which proposes that an imbalance between the production and clearance of amyloid-β (Aβ) peptides initiates a pathological sequence leading to tau hyperphosphorylation, synaptic dysfunction, and progressive neurodegeneration [79, 80]. Aβ is a derivative of amyloid precursor protein (APP), which is cleaved by β- and γ-secretases one after the other. On a physiological level, Aβ is made in a minimal quantity and is removed without any problem; however, if the production of the aggregation-prone Aβ42 isoform dramatically increases or the clearing of its route is blocked, then soluble oligomers are formed. They may eventually aggregate in fibrils and these fibrils are deposited as extracellular plaques mainly in the neocortex and hippocampus. These oligomeric species are neurotoxic: they disrupt synaptic signaling, block long-term potentiation—the electrophysiological basis of memory—and activate microglia, thus triggering the inflammatory and oxidative responses in a cascade manner [81].

Genetic studies provide convincing evidence for such a model. Chromosome Mutations in APP, PSEN1, and PSEN2 genes, which regulate γ-secretase activity, cause familial, autosomal-dominant forms of AD with almost complete penetrance and usually an early onset before 65 years of age [82]. In the case of the more common late-onset form of the disease, the first and most reliable risk factor is the apolipoprotein E (APOE) ε4 allele. The presence of one ε4 allele causes a moderate increase in the risk of AD, while two alleles cause higher risk, as well as an earlier age at onset. This effects attributed to facilitated aggregation and impaired clearance of Aβ [83]. Besides risk loci/proteins mentioned above, genome-wide association studies (GWAS) have identified other susceptibility genes, such as TREM2, CD33, CLU, and CR1, which are related to microglial activation and dysregulation of the innate immune system [84].

In addition to extracellular Aβ plaques, AD brains are characterized by another lesion: intracellular neurofibrillary tangles (NFTs) consisting of hyperphosphorylated tau [85]. Tau protein is an axonal microtubule-associated which plays an important role in cell transport. However, when it is excessively and abnormally phosphorylated it separates from microtubules, becomes misfolded, and combines with other proteins forming paired helical filaments that eventually merge to form NFTs. The tangles that Alzheimer follow a characteristic pattern: they initially appear in the transentorhinal cortex, then in the hippocampus and later in the association cortices. This pattern is in line with clinical transition from mild memory deficits to

global cognitive failure [86]. The density of tau tangles correlates far more closely with cognitive impairment than amyloid plaque burden, suggesting that tau pathology, while possibly triggered by Aβ, plays the central role in driving neurodegeneration [87].

In addition to plaques and tangles, the AD brain shows extensive loss of synapses and neurons, which is the most significant pathological correlate of cognitive decline. Quantitative studies have demonstrated that decreases in synaptic markers such as synaptophysin substantially precede neuronal death and strongly predict cognitive abilities [88]. Structural MRI demonstrates the atrophy of the hippocampus in the early stage and the thinning of the cortex in the temporal and parietal lobes, which are the brain areas involved in association processing and thus reflect the loss of synaptic connectivity underlying the observed atrophy.

Neuroinflammation is yet another essential layer of the AD iceberg. Microglia and astrocytes surround amyloid deposits, and when they are chronically activated, they release pro-inflammatory cytokines, complement proteins, and reactive oxygen species that further injure neurons and cause synaptic degeneration to extend in the area around the initial one [72]. Meanwhile, genetic variants in immune-related genes such as TREM2 and CD33, which influence the expression of glial-response genes and provide a biological link between inflammation and progression, have been identified as risk factors for late-onset AD [89].

Mitochondrial dysfunction and oxidative stress are additional key factors behind AD pathogenesis. Impaired electron transport, mitophagy, and excessive generation of reactive oxygen species (ROS) lead to lipid peroxidation, DNA damage, and energy failure creating a cycle of cellular injury that amplifies amyloid and tau toxicity [90]. At the same time, vascular pathology further exacerbates neurodegeneration. Chronic hypertension, diabetes, and small-vessel disease result in decreased brain perfusion and disruption of the blood−brain barrier (BBB), thus facilitating amyloid aggregation and tau phosphorylation through mechanisms induced by hypoxia and inflammation [91].

Together, these interacting mechanisms form a convergent picture of AD as a disorder of abnormal protein aggregation, chronic inflammation, mitochondrial failure, and vascular compromise. While the amyloid cascade hypothesis remains a cornerstone, contemporary models emphasize that Aβ accumulation acts as an early initiator, whereas tau propagation, synaptic loss, and glial activation are the primary drivers of neurodegeneration and clinical decline [92]. Rather than reflecting a single pathogenic pathway, AD represents the cumulative outcome of multiple biological insults interacting over decades to erode the integrity of neural networks and ultimately manifest as the clinical syndrome of dementia.

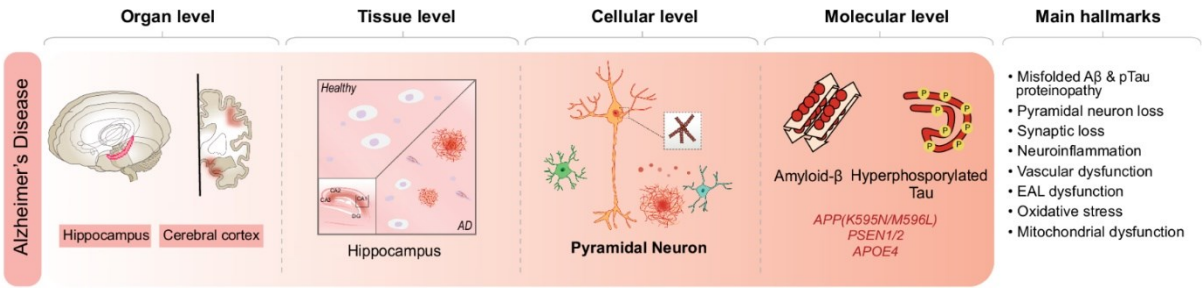

Figure 3. *Neuropathology of AD.*

DIAGNOSIS: CLINICAL CRITERIA, COGNITIVE SCALES, IMAGING AND BIOMARKERS

The diagnosis of Alzheimer's disease (AD) is no longer based solely on a clinician's impression of memory loss. Today it is a multi-layered process that combines clinical history, detailed cognitive testing, advanced brain imaging, and biological markers to capture both the symptoms and the underlying pathology of the disease. International recommendations—from the Diagnostic and Statistical Manual of Mental Disorders, Fifth Edition (DSM-5) to the frameworks proposed by the National Institute on Aging–Alzheimer's Association (NIA-AA) and the International Working Group (IWG)—all stress that AD should be defined by the progressive nature of cognitive decline together with objective evidence of amyloid and tau pathology [92-94]. A detailed medical and psychiatric history is collected, complemented by an interview with a family member or caregiver to document the onset, tempo, and daily-life consequences of cognitive symptoms. Standard laboratory investigations are performed to exclude potentially reversible causes of dementia, including thyroid dysfunction, vitamin B12 deficiency, metabolic derangements, or chronic infections. A thorough neurological examination helps to rule out other primary neurological conditions such as Parkinson's disease, normal-pressure hydrocephalus, or cerebrovascular disorders [95].

Based on the DSM-5 diagnostic criteria, the identification of a major neurocognitive disorder arising from AD would require the documentation of gradual and progressive impairment in one or more cognitive domains. These domains are typically memory but may also include attention, executive functioning, language, or visuospatial skills, with the deterioration being of such a degree that it hampers independence and the symptoms cannot be accounted for by delirium or another psychiatric disorder [96].

As the clinician's subjective impressions can vary, neuropsychological testing serves as an objective basis for the diagnosis. Short recapitulation instruments like the Mini-Mental State

Examination (MMSE) [97] and the Montreal Cognitive Assessment (MoCA) [98] are generally implemented for assessing global cognition and monitoring decline over time. If there is a necessity for more detailed information, a full neuropsychological battery is conducted to map out deficits in different cognitive domains. Specific memory, which is usually the first system that gets affected in AD, can be assessed with the Rey Auditory Verbal Learning Test (RAVLT), the California Verbal Learning Test, or the Wechsler Memory Scale [99]. The executive functions, among them set-shifting and inhibition, can be tested with the help of the Trail Making Test, Stroop Color–Word Test, or Wisconsin Card Sorting Test. The language component can be supported with the Boston Naming Test and verbal fluency tasks, whereas the visuospatial and constructional abilities can be measured by the Rey–Osterrieth Complex Figure Test or Clock Drawing Test. The attentional capacity and working memory can be very likely tested through Digit Span (forward and backward) or the Continuous Performance Test [100]. The continued use of these assays can show the gradual and selective impairment that differentiates Alzheimer's disease from normal aging and depression-induced cognitive inefficiency [101].

Neuroimaging provides a biological substrate to the clinical assessment. Structural MRI is routinely performed to exclude other causes of cognitive impairment and to quantify medial temporal lobe atrophy, particularly in the hippocampus, a hallmark of AD and a robust predictor of conversion from MCI to dementia [102]. Quantitative volumetric tools such as FreeSurfer allow accurate measurement of hippocampal volume and cortical thickness, enhancing diagnostic precision [103]. Functional imaging with fluorodeoxyglucose positron emission tomography (FDG-PET) typically reveals a pattern of hypometabolism in the posterior cingulate, precuneus, and temporoparietal association cortices, regions crucial for episodic memory and default mode network function [104]. Molecular imaging further specifies the changes induced by the disease: amyloid-PET tracers like ^{11}C-PiB and ^{18}F-florbetapir can reveal fibrillar amyloid-β deposition many years before the appearance of clinical symptoms, while tau-PET ligands such as ^{18}F-flortaucipir depict the distribution of neurofibrillary tangles and are in close correlation with disease severity [105].

Meanwhile, fluid biomarkers have evolved into a fundamental element of the diagnostic process that accompanies the modern era. Analysis of cerebrospinal fluid (CSF) portrays a typical pattern of lowered Aβ42 or a decreased Aβ42/Aβ40 ratio which points to amyloid deposition along with increased total tau (t-tau) and phosphorylated tau (p-tau181 or p-tau217) that indicate neurofibrillary pathology and neuronal damage [106]. Blood-based biomarkers have

lately also been utilized to offer a less invasive method. In fact, plasma p-tau181 and p-tau217 levels along with Aβ42/40 ratio not only agree very well with the corresponding CSF and amyloid-PET measurements but also can be used for the prediction of cognitive decline long before the appearance of clinical symptoms [107]. At the same time, neurofilament light chain (NfL) concentration levels in plasma serve as a non-specific source of axonal injury and neurodegeneration [108].

By combining the different biological indices, the A/T/N classification system represents a single biological model. Within this model, A stands for amyloid indicators such as CSF, Aβ42 or a positive amyloid-PET; T illustrates the presence of tau pathology as shown by increased CSF p-tau or positive tau-PET; N is the label for neurodegeneration, which can be quantified by MRI-supported hippocampal atrophy, FDG-PET hypometabolism, or elevated CSF t-tau. A patient with A+T+N+ is biologically defined as AD even at the preclinical stage. On the other hand, other combinations of biomarkers may reflect prodromal stages or an increased risk. The 2018 NIA–AA Research Framework [92], thus marked a major conceptual shift by defining AD not by its symptoms but by its underlying biological signature, enabling earlier and more accurate diagnosis, and paving the way for biomarker-guided therapeutic interventions.

A	T	N	Biomarker Category	
–	–	–	Normal	
+	–	–	Alzheimer's pathologic change	AD Continuum
+	+	–	Alzheimer's disease	
+	+	+	Alzheimer's disease	
+	–	+	Alzheimer's disease Concomitant non-Alzheimer's pathologic change	
–	+	–	Non-AD pathologic change	
–	–	+	Non-AD pathologic change	
–	+	+	Non-AD pathologic change	

Figure 4. *ATN biomarker profiles in relation to the AD continuum.*

CLINICAL COURSES AND STAGES

As illustrated in Figure 5, AD progresses as a slow and insidious continuum that unfolds years—often decades—before the onset of clinical dementia. Researchers and clinicians generally recognize three overlapping phases within this trajectory: the preclinical stage, mild cognitive impairment (MCI) due to AD, and Alzheimer's dementia [109]. These stages are not sharply delineated but represent successive points along a biological spectrum in which molecular alterations precede subtle cognitive changes, which in turn anticipate overt functional

decline.

During the preclinical phase, individuals are cognitively normal by conventional testing, yet biomarker studies reveal that neurodegenerative processes are already under way. Amyloid-β (Aβ) accumulation is typically the earliest detectable change and can be visualized with amyloid-PET imaging or inferred from reduced cerebrospinal fluid (CSF) Aβ42 concentrations and elevated phosphorylated tau (p-tau) levels [92, 110]. Recent advances in plasma biomarkers, including p-tau181, p-tau217, and the Aβ42/40 ratio, now enable less invasive detection of these early pathophysiological events, facilitating risk stratification and recruitment into prevention trials [107]. Even before measurable memory impairment, functional MRI and FDG-PET can demonstrate subtle disruptions in the default-mode network and reductions in cerebral glucose metabolism [111]. Importantly, however, biomarker positivity does not guarantee progression to symptomatic disease, as genetic background, vascular health, lifestyle, and cognitive reserve significantly modulate individual trajectories [59].

The next phase, mild cognitive impairment due to AD, marks the prodromal stage when cognitive deficits become objectively measurable though daily independence remains largely intact. Episodic memory, especially delayed recall of newly acquired information, is the most affected, but deficits in executive function, language, and visual-spatial processing may also be noticed [101].]. A neuropsychological examination is necessary for identification as it shows lower than expected performance of the patient's age and education level, although the patient may still be able to carry out daily activities. The rate of conversion from amnestic MCI to Alzheimer's dementia is reported in various longitudinal studies to be around 10–15 % on average per year, while the risk is substantially higher for APOE ε4 carriers or those biomarker-positive for Aβ and tau [92, 101]. At this stage, brain imaging frequently reveals hippocampal volume loss, diffuse cortical thinning, and reduced glucose metabolism in the posterior cingulate and temporoparietal regions, whereas the CSF and blood biomarkers reflect increasing tau pathology in line with spread neurofibrillary degeneration [102, 108].

The final and most incapacitating stage – Alzheimer's dementia – is characterized by severe and irreversible cognitive and functional decline, which extend across the whole of the brain. Alongside memory impairment, the decline in language, visuospatial and executive functions accelerates. Inability to perform the instrumental activities of daily living like managing money or medication, is the first stage of dependence, whereas later, patients will need the assistance of others even for basic care such as dressing, feeding, and personal hygiene. Neuropsychiatric symptoms, e.g., apathy, depression, anxiety, agitation, hallucinations, and in some cases

psychosis, are prevalent and thus, greatly contribute to the burden of the caregiver, as well as the probability of institutionalization [112]. The typical clinical journey from the time of diagnosis to death lasts around 8–10 years, however, the duration of survival may be anywhere between 3 and more than 15 years and depends on factors like age at onset, sex, genetic background and co-existing conditions [113]. Corresponding to the advanced stage, the phase neuropathologically is characterized by a massive accumulation of amyloid plaques, neurofibrillary tangles, synaptic loss, and neuroinflammation that lead, eventually, not only to severe cerebral atrophy but the disintegration of global networks [86].

In essence, neurodegenerative disorders, with AD being the main representative, constitute a staggering and increasing worldwide challenge for public health. The impressive speed with which advances are being made in molecular genetics, biomarker technology, and systems neuroscience is not only reshaping our comprehension of disease mechanisms but also facilitating an earlier and more precise diagnosis. However, an actually effective prevention or cure will implicate an integrated plan combining disease-modifying pharmacotherapy with lifestyle optimization and precision medicine measures. Cooperation across disciplines involving neuroscientists, clinical practitioners, data scientists, ethicists, and public-health professionals will be needed to make these scientific breakthroughs available to patients and society.

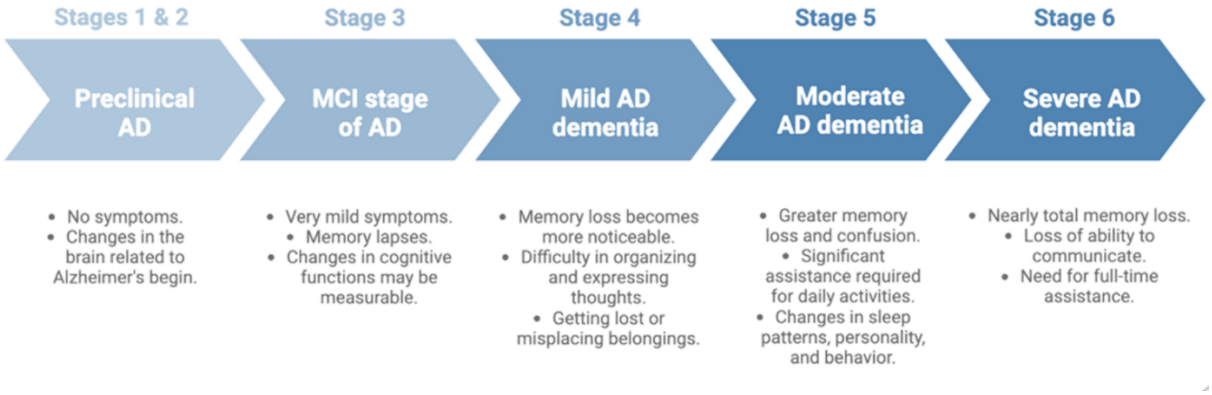

Figure 5. *Progressive stages of AD.*

MILD COGNITIVE IMPAIRMENT DUE TO ALZHEIMER'S DISEASE

Mild Cognitive Impairment (MCI) is the earliest stage with symptoms on the pathway from

normal aging to dementia, which can be distinguished by measurable cognitive decline in one or more domains with the preservation of daily functioning. When the underlying disease is AD, the condition is called MCI due to AD, a temporary stage that involves a high risk of dementia conversion. Therefore, the prodromal MCI phase constitutes a very important time for early detection and therapeutic intervention. Indeed, the clinical relevance of MCI due to AD is its capability to pinpoint patients with the highest likelihood of deterioration, thus enabling preventive measures and interventions to be administered at the appropriate time. The use of biomarkers has been greatly advanced lately, which also reflects on the possible role of neuroimaging, cerebrospinal fluid assay, and EEG-based functional markers in locating AD pathology at the very early MCI stage.

EPIDIEMOLOGY

Globally, MCI affects approximately 6–20% of adults aged 65 years and older, depending on the population studied and the diagnostic criteria applied [114-117], noting an increase with advancing age and differences related to educational attainment, assessment tools, and geographical region [118]. In a larger meta-analysis [119], the pooled global prevalence was 19.7% (95% CI: 18.3–21.1%) among adults older than 50 years. In community-dwelling populations, the estimated prevalence was 17.9% (95% CI: 16.0–19.8%), with regional estimates of ~17% in Asia, ~18% in Europe, ~20% in North America, ~18% in South America, and ~13% in Africa, emphasizing, however, the limited availability of high-quality studies in the latter region. An epidemiological meta-analysis study by an international consortium [120] showed that for the MCI condition, a prevalence of 5.9% can be estimated in a population with > 60 years, with an increment of the stratified age ranging from 4.5% between 60 and 69 years, to 5.8% between 70 and 79 years, and 7.1% between 80 and 89 years [121].

Studies analysing the progression from MCI to AD have reported annualized conversion rates ranging from approximately 8–17% for clinical samples and 5–12% for community samples [122, 123]. Regarding MCI due to AD, about one-third of affected people develop dementia within five years. However, some individuals with MCI revert to normal cognition or do not have additional cognitive decline. Evidence suggests that over a 5- to 10-year period after a diagnosis of MCI due to AD, 30% to 50% of people progress to AD [123, 124]. Within the MCI population, up to 15% people who have amnestic MCI are estimated to progress to AD in that period, and research indicates that progression to dementia may be more likely for people with this subtype of MCI due to AD.

The differences in the reported prevalence of MCI worldwide are due to the lack of standardized cut-off for neuropsychology test scores, use of population versus clinic-based cohorts, and algorithmic versus clinical approaches to assign the MCI diagnosis [125].

ETIOLOGY, NEUROPATHOLGY AND RISK FACTORS

The pathophysiology of MCI due to AD largely mirrors that of Alzheimer's disease, but its clinical manifestation remains subtle, with a predominance of memory impairment in the amnestic subtype. The etiology of MCI due to AD lies in the progressive accumulation of neuropathological changes typical of AD, notably amyloid-β plaques and tau-related neurofibrillary tangles. Tau pathology is very significant in the medial temporal lobe during the MCI stage, particularly in patients with amnestic presentations. These pathological hallmarks lead to synaptic dysfunction, neuronal injury, and eventually, neurodegeneration.

Beyond neuropathological mechanisms, numerous different factors are responsible for individuals becoming MCI due to AD. They may generally be considered as non-modifiable and modifiable risk factors.

Non-modifiable factors like age, genetic predisposition, and sex are beyond individual control but important for singling out the susceptible populations. Age is the most influent risk factor: the occurrence of MCI increases exponentially with age, especially after 65 years old, and so does the risk of conversion to AD with every decade. From a genetic perspective, the ε4 allele of the APOE gene is the most significantly recognized single genetic risk factor of AD. The individuals with one or two alleles of APOE ε4 will develop amyloid pathology fastest, have earlier cognitive decline, and are at a higher risk of MCI progression to dementia. In addition, family history plays a significant role. A positive family history, particularly if it concerns the first-degree relatives, is correlated with higher risk of MCI as well as earlier age of onset, reflecting the influence of both genetic and environmental factors. Finally, several studies suggest that females are at greater risk for developing AD from MCI and may also have a higher incidence of amnestic MCI, potentially due to hormonal changes, differences in life expectancy, or patterns of brain aging [126, 127].

In contrast to non-modifiable factors, modifiable risk factors offer valuable opportunities for early intervention and prevention strategies aimed at delaying or potentially halting the progression of cognitive decline. These include aspects related to cardiovascular health, lifestyle habits, mental wellbeing, and medication use. Recognizing and addressing these factors is essential not only for risk stratification but also for the development of personalized

preventive approaches tailored to individuals' clinical and psychosocial profiles. A substantial body of evidence has established that chronic medical conditions such as hypertension, diabetes mellitus, hyperlipidemia, coronary artery disease, stroke, and obesity are strongly associated with an increased risk of both MCI and AD [128, 129]. In particular, a study by Sanford [129] highlighted how multimorbidity—defined as the presence of four or more comorbid conditions—significantly raises the likelihood of developing MCI, especially when two or more of these conditions include hypertension, coronary artery disease, hyperlipidemia, and osteoarthritis. In addition to chronic conditions, pharmacological factors can also negatively affect cognitive function. Several commonly prescribed medication classes are associated with memory impairment and increased risk of cognitive decline. These include opioids, benzodiazepines and other anxiolytics, non-benzodiazepine hypnotics such as zolpidem, muscle relaxants, antiepileptics, and a range of anticholinergic agents—including certain antihistamines, antidepressants, urinary incontinence medications, and antipsychotics [130]. Besides that, lifestyle and behavioural factors play a crucial role in modulating cognitive functions. Physical inactivity is still one of the major contributing factors. Regular aerobic exercise has been proven to increase neurogenesis, lower systemic inflammation, improve cerebrovascular function, and finally, increase cognitive performance, especially in old people. Likewise, lower educational attainment and less engagement in mentally stimulating activities are associated with increased risk of MCI and dementia. On the other hand, higher education, bilingualism, and indwelling intellectual and social activities have been demonstrated to build up brain reserve, thus, postponing the clinical appearance of neurodegenerative pathology. Healthy lifestyle behaviours that include following the Mediterranean diet, quitting smoking, moderate alcohol intake, regular physical activity, and participation in social activities are all linked to the reduced risk of cognitive decline [101, 131].

Psychological and neuropsychiatric factors also have a significant influence. Depression is strongly associated to cognitive and functional decline and may also serve as an independent risk factor for advancement from MCI to dementia. Depression has been related to the shrinkage of the hippocampus, less neuroplasticity, and the dysfunction of the stress response system, which may lead to an accelerated neurodegeneration process [129]. Similarly, prolonged psychological stress as well as social isolation are becoming more and more acknowledged as sources of cognitive decline due to their effect on neuroendocrine and immune pathways [131]. Lastly, sleep disturbances, especially insomnia and obstructive sleep apnea (OSA), have been correlated with impaired glymphatic clearance of amyloid-β, a major protein in AD

pathogenesis. New evidence points out that sleep disruption may not only aggravate cognitive symptoms but also play a direct role in amyloid accumulation in the brain [132]. A summary of risk and protective factors for cognitive decline is reported in Figure 6.

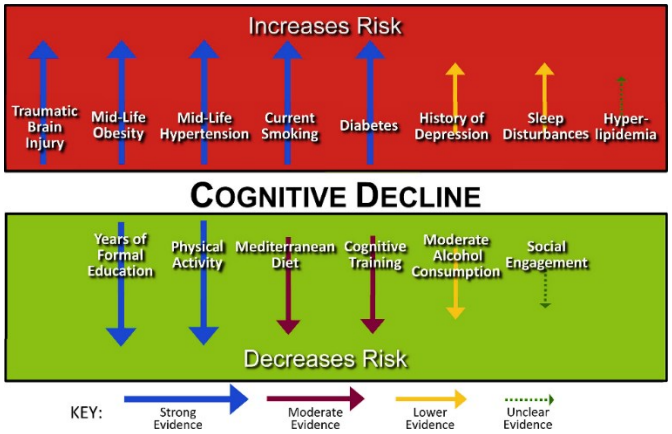

Figure 6. *Risk and protective factors for cognitive decline.*

DIAGNOSIS: CLINICAL CRITERIA, COGNITIVE SCALES, IMAGING AND BIOMARKERS

Although the term MCI was initially used by researchers at New York University referring to Stage 3 of the Global Deterioration Scale (GDS) [133], MCI was fully characterized by Petersen and colleagues at the Mayo Clinic [134]. They described individuals with isolated memory concerns beyond what was expected for their age, demonstrating memory impairment on objective testing yet did not fulfill the criteria for dementia. MCI was therefore considered to represent a borderline stage between normal aging and very early dementia. This early definition of amnestic MCI was found inadequate, as it became evident that not all patients with MCI progressed to dementia and that memory impairment was not the only cognitive domain affected [135]. In fact, MCI can be broadly classified as either amnestic or non-amnestic, depending on the primary cognitive domain affected [129]. Moreover, the deficits may involve a single cognitive domain or be multidomain, potentially affecting one or more of the following six cognitive domains: learning and memory, language, complex attention, executive function, social cognition, and visuospatial function. Amnestic MCI is characterized by predominant memory loss and is more likely to progress to Alzheimer's disease, while non-amnestic MCI, in which memory is relatively preserved, is less common and may instead lead to non-Alzheimer dementias [129, 136].

Further development came in 2003 with the convening of a Key Symposium, which led to the publication of international criteria for MCI and broadening of the construct from earlier

versions that had focused only on memory impairment [137, 138]. These criteria included cognitive complaints from the patient or family members, deficits in any cognitive domain and not only memory, preserved overall general function but increasing difficulties in activities of daily life, and no dementia.

In this context, it is worth noting that a feature that can accompany the symptomatic debut of AD is the presence of subjective cognitive concerns, referring to self-perceived changes in cognitive functioning. Over the years, this phenomenon has been described using a variety of terms, including subjective cognitive impairment (SCI) [139], subjective cognitive complaints (SCC) [140], subjective memory impairment (SMI) [141], and subjective memory complaints (SMC) [142], resulting in a heterogeneous and fragmented terminology across the literature. To address this inconsistency, the Subjective Cognitive Decline Initiative (SCD-I) working group proposed a unified framework in 2014. They introduced the term subjective cognitive decline (SCD) and provided an operationalized definition to guide research and clinical assessment [143]. According to this consensus, SCD refers to a self-experienced decline in cognitive abilities relative to a previously normal state, despite the absence of objective impairment on standardized cognitive testing. Whether this condition may or may not represent an increased risk for progression to MCI and/or dementia is still a controversial issue [144]. However, a consistent body of evidence indicates that SCD actually represents a risk factor for future cognitive decline, for MCI and AD dementia [144, 145] . Dubois and colleagues [146, 147] specify that the SCD per se cannot be considered as a “proxy” for preclinical AD, in line with studies reporting that the percentage of amyloid PET positivity is independent from rates of memory complaints [148, 149]. However, SCD individuals with evidence of pathophysiological AD biomarker positivity (SCD plus) represent a category at risk for clinical AD [143].

More recently, the American Psychiatry Association's Diagnostic and Statistical Manual of Mental Disorders 5th Edition (DSM-V) included a predementia phase called mild neurocognitive disorders (mild NCD) (Diagnostic and statistical manual of mental disorders: DSM-5™, 5th ed, 2013 [96]). The criteria for mild NCD closely resemble the MCI criteria adopted in the Key Symposium of 2003. It is characterized by a decline in one or more cognitive domains (e.g., memory, executive function, attention, language, visuospatial skills), both subjectively and objectively observable by clinical assessment and neuropsychological testing. However, this decline does not interfere with the individual's ability to perform daily activities independently and cannot be attributed to delirium or other psychiatric conditions [150]. DSM-

V does not propose specific neuropsychology test cut-off scores for diagnosing mild NCD. The DSM-V approach involves the characterization of the syndrome, mild or major NCD, and then a subsequent task of determining its etiology, such as AD, frontotemporal degeneration, Lewy body disorders or vascular cognitive impairment. Finally, in the 2018, the 11th Revision of the International Classification of Diseases (ICD 11) by the World Health Organization (WHO) adopted the definition of mild neurocognitive disorder in alignment with the DSM-V diagnostic criteria [150].

At approximately the same time, the National Institute on Aging and the Alzheimer's Association (NIA-AA) convened a work group to discuss the MCI due to AD criteria [151]. The initial criteria were published in 2011 [151] and revised in 2018 [92]. The criteria closely resemble the core clinical criteria proposed by the 2003 Symposium and are based on:

1. Subjective cognitive complaints (typically memory);
2. Objective cognitive impairment (typically measured by performance below norms on standardized tests);
3. Preserved independence in functional abilities;
4. No dementia.

The revision noted that neurobehavioural disturbance may be an important feature of the clinical presentation and that cognitive deficits may result in a mild but noticeable impact on the complex activities of daily living. The NIA-AA also suggested research criteria to help determine the etiology of MCI using biomarkers to differentiate MCI due to AD from MCI due to other reasons. In this context, the two main helpful biomarkers are amyloid-beta (Aβ) deposition and neuronal injury [151]. According to the NIA-AA workgroup, valid indicators of Aβ deposition are: cerebrospinal fluid concentrations of Aβ42 (CSF Aβ42) and positron emission tomography (PET) amyloid imaging; valid indicators of neuronal injury are: CSF tau/phosphorylated tau, hippocampal volume or medial temporal atrophy by volumetric measures or visual rating, rate of brain atrophy, fluoro-deoxyglucose (FDG) PET imaging and SPECT perfusion imaging.

This framework allows for classification into “MCI due to AD – high likelihood,” “intermediate likelihood,” or “unlikely,” depending on the concordance between symptoms and biomarkers evidence [151]. Individuals who exhibit both a positive Aβ biomarker and a positive biomarker of neuronal injury have the highest likelihood that their cognitive impairment is attributable to AD pathology. When only one class of biomarkers is positive—either Aβ or neuronal injury—and the other has not been tested or is unavailable, the diagnosis falls into the intermediate

likelihood category. Conversely, a confirmed absence of both amyloid deposition and neuronal injury biomarkers strongly suggests that the cognitive decline observed in MCI is unlikely to be due to AD.

Based on the model proposed by NIA-AA Research Framework [92], AT(N) biomarkers can be used individually or in combination to determine the likelihood that MCI is due to underlying Alzheimer's pathology. When both A and T biomarkers are positive (A+T+), with or without evidence of neurodegeneration (N+), the condition is typically classified as "MCI due to AD – high likelihood". The use of this biomarker-based framework enhances diagnostic accuracy, supports risk stratification, and facilitates early intervention and participation in clinical trials targeting preclinical and prodromal AD [92]. Within this framework, MCI becomes a clinical stage along a broader continuum of AD pathology.

Furthermore, the NIA-AA guidelines and the subsequent AT(N) research framework emphasize that, even in the context of biomarker-based diagnoses, the diagnosis of MCI requires objective evidence of cognitive decline based on standardized neuropsychological testing. Cognitive assessments are essential identifying measurable deficits in one or more cognitive domains, to distinguish MCI from both normal aging and overt dementia, and monitoring the trajectory of the condition. Although they do not specify the use of particular screening tests, there are some commonly used ones including, the Montreal Cognitive Assessment (MoCA), which is particularly sensitive to subtle changes across multiple domains [98]; the Mini-Mental State Examination (MMSE), which offers a brief global measure of cognitive function, although it is less sensitive to early-stage impairment [97]; and the Clinical Dementia Rating (CDR) scale, which evaluates both cognitive and functional performance and is often used to classify MCI when the global score is 0.5 [152].

Additional neuropsychological tests such as the Wechsler Memory Scale (WMS) for detailed memory profiling, the Trail Making Test (TMT) for executive function and attention, and the Alzheimer's Disease Assessment Scale – Cognitive Subscale (ADAS-Cog) are frequently used, particularly in research and clinical trials [153, 154].

Functional assessment tools are also crucial to establish the preserved independence that characterizes MCI. Instruments such as the Functional Activities Questionnaire (FAQ) [155], the Lawton-Brody Instrumental Activities of Daily Living (IADL) scale [156], and the Disability Assessment for Dementia (DAD) scale are used to evaluate instrumental daily activities and ensure that deficits do not meet the threshold for dementia.

Moreover, behavioural and neuropsychiatric symptoms are increasingly recognized as part of

the AD prodromal phase. The Neuropsychiatric Inventory (NPI) is commonly used to assess symptoms such as depression, apathy, anxiety, and agitation, which may co-occur with or precede cognitive impairment and are considered important for differential diagnosis and prognosis [157].

ELECTROENCEPHALOGRAPHY (EEG)

Electroencephalography (EEG) is an electrophysiological method used to record the electrical activity generated by the human brain. Owing to its high temporal resolution, EEG is particularly valuable for investigating dynamic cerebral processes [158]. Clinically, it is widely employed in the assessment of patients with suspected neurological disorders, including Alzheimer's disease, epilepsy, Parkinson's disease, and various forms of dementia. Beyond its clinical applications, EEG also represents an essential tool in cognitive neuroscience, neurolinguistics, psychology, and psychophysiological research.

The origins of EEG date back to the early 20th century, when the German psychiatrist Hans Berger made a groundbreaking contribution to neurological and psychiatric diagnostics [159] (Figure 7). Berger began by recording brain activity in individuals with cranial abnormalities, employing a highly sensitive Siemens double-coil galvanometer (sensitivity: 130 mV/cm) together with low-impedance surface electrodes. In 1929, he published the first scientific report on human EEG, introducing the concepts of "alpha waves" and "beta waves," and demonstrating that the alpha rhythm disappears when the eyes are open [159]. His work went far beyond the mere description of EEG patterns: Berger applied mathematical analyses to quantify wave characteristics in an attempt to uncover meaningful distinctions among them. In doing so, he laid the foundation for what is now recognized as quantitative EEG [160].

More than ninety years after its introduction, EEG remains a robust, cost-effective, and widely accessible diagnostic technique for exploring brain electrophysiology. Advances in digital technology have considerably enhanced its precision and expanded its applications, enabling the use of EEG beyond traditional laboratory and clinical settings [161].

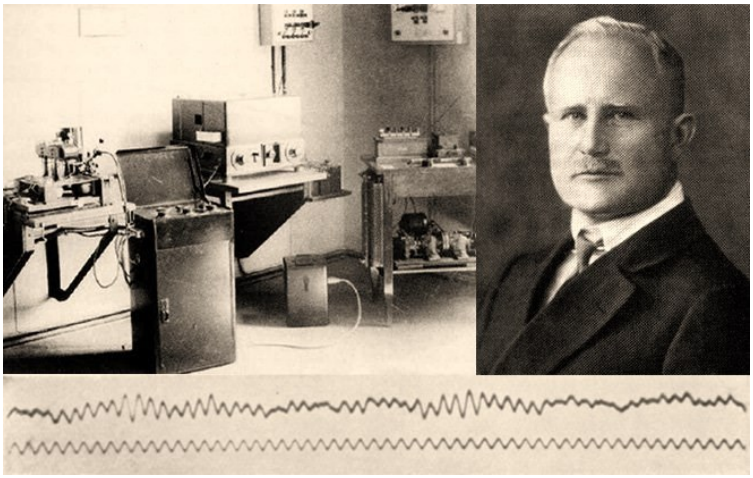

Figure 7. *Hans Berger's first EEG recording (1924).*

EEG POTENTIALS

In 1891, Heinrich Wilhelm Gottfried Waldeyer first introduced the term "neuron" to describe the functional unit of the nervous system. Structurally, a nerve cell consists of three principal components: the cell body, or soma, which resembles that of other cell types; multiple short extensions known as dendrites, which receive incoming signals from other neurons and convey them to the soma; and a single elongated projection, the axon, which transmits signals away from the cell body toward other neurons or muscle cells. Communication between an axon and its target cell occurs at specialized junctions termed synapses (Figure 8) [162].

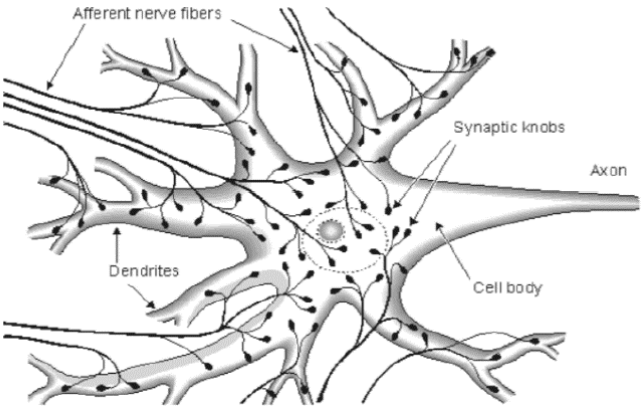

Figure 8. *Components of a single neuron: the cell body (soma), dendrite, axon, afferent nerve fibers, and synaptic terminals.*

Nerve cells are characterized by two fundamental properties: excitability—the ability to produce a rapid and substantial change in membrane potential in response to minimal stimuli—

and conductivity—the capacity to transmit signals to other neurons. The neuronal cell membrane, a semipermeable barrier enclosing the cytoplasm, generates and propagates electrochemical impulses along its surface [163]. These properties arise from the neuron's ability to maintain a negative resting membrane potential, typically around –70 mV relative to the extracellular space, and to generate action potentials (brief voltage discharges) in response to synaptic inputs. The difference in potential between the intracellular compartment and ground can be measured to calculate the transmembrane voltage (mV) [164]. With non-invasive techniques, however, it is not possible to record the activity of a single neuron; electroencephalography instead reflects the summed activity of billions of neurons.

Neurons can be broadly classified into two major types: pyramidal and non-pyramidal cells. Pyramidal neurons (Figure 9A) typically possess a soma shaped like a teardrop or triangular pyramid. They feature a prominent apical dendrite extending from the pointed end of the soma, together with a cluster of shorter basal dendrites emerging from the rounded base. Pyramidal cells represent the most abundant excitatory neurons in the brain. Their primary role is to integrate synaptic inputs and transform them into patterned trains of action potentials. As "projection neurons," they often send axons over long distances, sometimes even beyond the brain itself [165]. In the cerebral cortex, pyramidal neurons are organized into cortical layers, where their axon terminals form corticocortical connections arranged in column-like domains, or palisades. Their dendritic trees are aligned in parallel and oriented perpendicular to the cortical surface, allowing these neurons to act as dipole sources that generate the so-called "dipolar fields".

Non-pyramidal neurons (Figure 9B), by contrast, are characterized by smaller cell body and dendrites that extend radially in multiple directions, displaying substantial morphological diversity. They contribute primarily to local cortical circuitry, regulating excitability and transmission, and are essential for maintaining the modular organization of the cortex [166]. However, because EEG signals are most effectively detected when current dipoles are oriented perpendicular to the cortical surface, non-pyramidal neurons make only a negligible contribution to scalp EEG recordings [167].

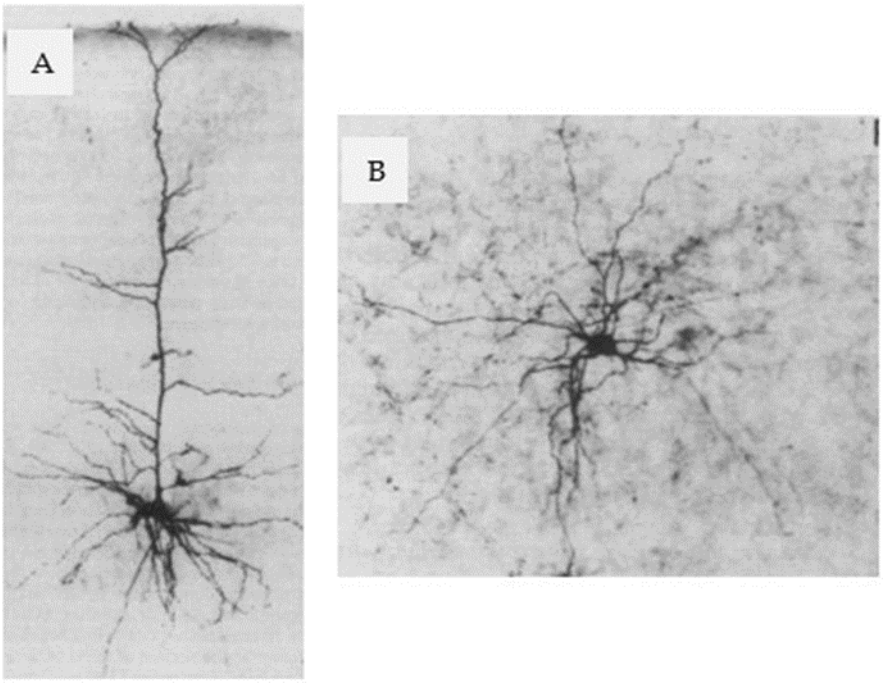

Figure 9. *Type of pyramidal cells. (A) Photomicrograph of a pyramidal neuron. (B) Photomicrograph of a non-pyramidal neuron.*

Therefore, the oscillatory signals recorded on the scalp with electroencephalography (EEG) primarily reflect the spatial and temporal summation of excitatory and inhibitory postsynaptic potentials (EPSPs and IPSPs) generated by cortical pyramidal neurons in the cerebral cortex [167] . During an excitatory postsynaptic potential, neurotransmitter molecules are released into the synaptic cleft and bind to receptors on the postsynaptic membrane, increasing its permeability to sodium ions (Na^+). The influx of Na^+ produces a net inward positive current, which depolarizes the membrane and brings the neuron closer to the threshold for firing an action potential. In contrast, an inhibitory postsynaptic potential occurs when neurotransmitter binding opens potassium (K^+) or chloride (Cl^-) channels. The resulting outward flow of K^+ or inward flow of Cl^- generates a net negative current, hyperpolarizing the membrane and decreasing the likelihood of action potential initiation [168].

Because these postsynaptic potentials arise synchronously across large populations of vertically oriented pyramidal neurons, their individual dipole fields combine to create measurable voltage fluctuations at the scalp. This large-scale summation of local field potentials underlies the rhythmic EEG oscillations detected in non-invasive recordings.

EEG INSTRUMENTATION

Although no single configuration is ideal for every EEG application, a set of fundamental requirements must be met to obtain reliable recordings. Electrical signals generated by human brain activity are typically below 100 μV in amplitude and under 100 Hz in frequency, and can be measured non-invasively through electrodes placed on the scalp.

Electrodes and Skin–Electrode Interface

Electrodes serve as the primary-interface that change biopotential activity into measurable electrical signals. Generally, EEG electrodes are metallic and might be of various designs: cup, disc, needle, and microelectrode types. In the majority of neurophysiological experiments, silver/silver-chloride (Ag/AgCl) electrodes are considered the most suitable since the AgCl surface rapidly stabilizes its electrochemical equilibrium, minimizing polarization artifacts. The correct measurement of electrodes performance not only depends on the types of electrodes but also on skin preparation. After a light abrasion, a conductive electrolyte—usually an EEG gel or paste—is applied to the scalp to decrease stratum corneum resistance and hence reduce the contact impedance. At the electrode–electrolyte–skin interface, ions accumulate and undergo ion–electron exchange, thus, making recording stable.

The contact impedance of each electrode with the skin should be between 1 kΩ and 10 kΩ. Most of the time, research settings are involved in bringing the contact impedance values to less than 5 kΩ in order to increase the quality of the signal. The impedance lower than ~1 kΩ may indicate the existence of short circuits between electrodes, while noise and distortion of the signal are at an elevated level if values go beyond ~10 kΩ [169].

Signal Acquisition and Amplification

As shown in Figure 10, a complete EEG system comprises electrodes, a signal-acquisition unit, amplification circuitry, and facilities for display and analysis. Each electrode lead connects to a jack box, which routes signals to an electrode selector capable of configuring referential or bipolar montages [167]. Inside the jack box, the primary circuitry often includes an analog-to-digital (A/D) converter, enabling direct interfacing with the computer system so that digitized samples can be stored and processed.

Because cortical signals are on the order of microvolts, differential amplifiers are required to magnify voltage differences between electrode pairs for visualization. Modern EEG amplifiers typically achieve a common-mode rejection ratio (CMRR) of at least 80 dB, and often around 100 dB, which helps eliminate electrical interference from environmental noise. Maintaining

this high CMRR requires differential input impedances of at least 1 MΩ (preferably 10 MΩ) to prevent signal attenuation.

Filtering and Calibration

To reduce artifacts, EEG channels are equipped with analog filters, including a notch filter at 50 Hz (or 60 Hz in the United States) to suppress mains interference, as well as adjustable high-pass and low-pass filters to define the recording bandwidth. Additional controls typically include calibration signals, baseline adjustments, and sensitivity settings to optimize the display of voltage fluctuations [170].

Overall, these integrated components—electrodes, skin preparation, amplification, filtering, and digitization—ensure that the inherently low-amplitude electrical activity of the brain can be accurately recorded, processed, and visualized for clinical and research applications.

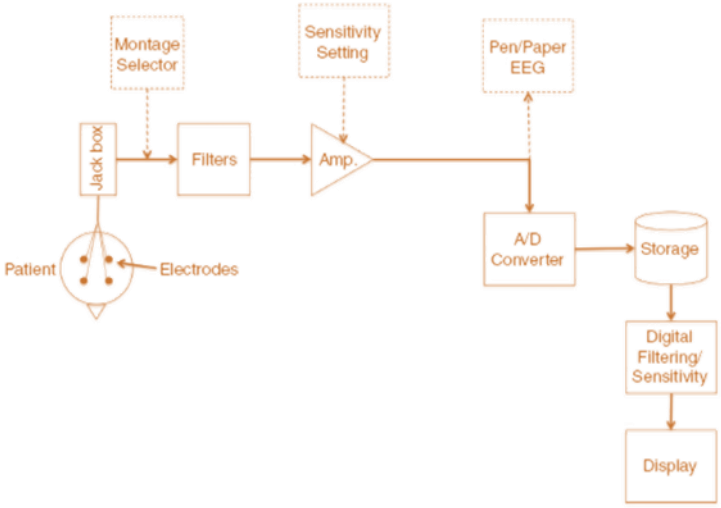

Figure 10. *Schematic representation of EEG amplifiers. Scalp electrodes transmit biopotential signals to a jack box, which routes them through filters and amplifiers for signal conditioning. Components shown within the dashed boxes depict elements of traditional analog EEG systems—such as the montage selector, sensitivity controls, and pen-and-paper recording. In modern digital EEG systems, the amplified signal is converted by an analog-to-digital (A/D) converter, stored for subsequent analysis, and displayed on a computer monitor.*

ELECTRODE PLACEMENT AND EEG MONTAGE

Accurate monitoring of electroencephalographic (EEG) activity requires the simultaneous recording of signals from as many scalp regions as possible. Recording from too few channels increases the likelihood of missing or mislocalizing electrical events, whereas using a greater number of channels improves spatial resolution and reduces the risk of interpretive errors. For

most clinical and research applications, a minimum of 19 simultaneous channels is generally considered essential to capture the principal cortical sources of EEG activity.

Standard Electrode Placement Systems

Several internationally recognized systems define how electrodes are positioned on the scalp, including the 10–20 system, its higher-density 10–10 system, and the even denser 10–5 system [171, 172]. Among these, the International 10–20 system remains the clinical standard, with all other systems representing systematic extensions of this framework (Figure 11). The name "10–20" refers to the proportional distances—10 % or 20 % of specific head measurements—used to guide electrode placement.

Electrode locations are determined relative to anatomical landmarks:

- Nasion: the depressed area between the eyes at the bridge of the nose
- Inion: the prominent bump at the posterior midline of the skull
- Preauricular points: small notches of cartilage just anterior to the ear canals

Each electrode site is labeled with a letter and a number. Letters denote the underlying cerebral region (Fp = frontopolar, F = frontal, C = central, P = parietal, T = temporal, O = occipital). Odd numbers indicate the left hemisphere, even numbers the right, while "Z" (from the German Zentral) designates the midline. Additional sites such as "A" identify auricular (mastoid) locations. Alongside scalp electrodes, auxiliary sensors for respiration, muscle activity (EMG), and electrocardiography (ECG) are often included to enhance diagnostic accuracy.

The basic 10–20 system employs 19 electrodes, whereas the 10–10 and 10–5 systems add proportionally spaced intermediate sites, providing higher spatial sampling and improved localization of cortical generators. These dense-array configurations are particularly valuable for high-resolution or source-localization EEG studies [173].

EEG MONTAGES

A montage is the standardized arrangement of recording electrodes and the method by which their signals are combined to create a topographic representation of brain electrical activity. Montages can be categorized by their spatial layout and by the type of electrical reference used.

Spatial organization

- Unpaired: a single channel records activity from one electrode pair.
- Paired channel: comparable left–right channels are displayed in parallel.
- Paired group: chains of electrodes on one hemisphere are compared with matching chains on the opposite side.

Montages may be longitudinal (anterior–posterior orientation) or transverse (side-to-side orientation).

Reference configuration

- Bipolar montage: each channel records the potential difference between two adjacent active electrodes. Channels are often arranged in longitudinal or transverse "chains," providing high spatial resolution and good artifact rejection.
- Referential montage: each channel represents the voltage difference between an active electrode and an electrically "neutral" reference site, typically located at the vertex (Cz), an ipsilateral mastoid, or a common-average reference.

Modern digital EEG systems allow the raw data—initially recorded with a single common reference—to be re-montaged post hoc into multiple bipolar or referential configurations, offering flexibility for clinical interpretation and advanced analyses [172, 174, 175].

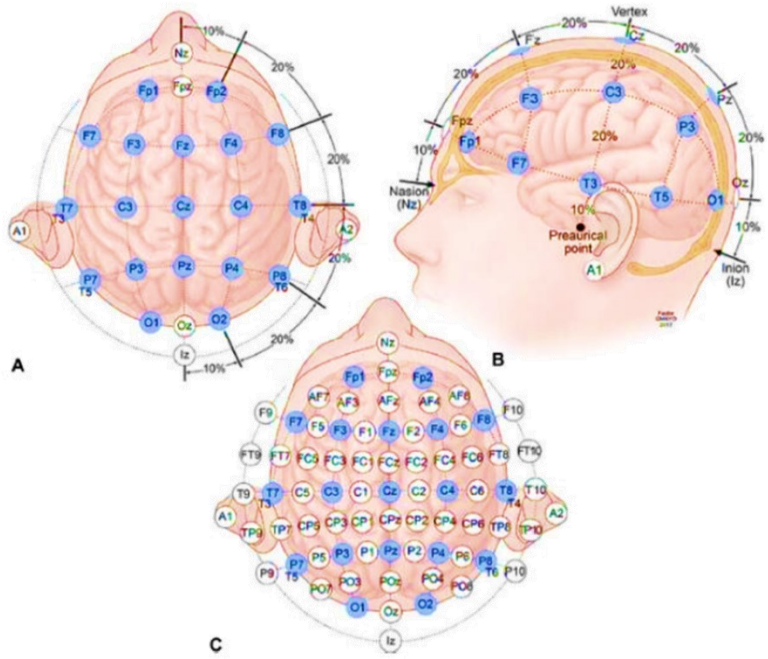

Figure 11. *International 10–20 Electrode Placement System. Top (A) and side (B) views illustrate electrode positions spaced at 10 % or 20 % of measured cranial distances. Panel (C) depicts the augmented high-density extension of the 10–20 system. Electrodes overlie frontal, temporal, central, parietal, and occipital regions, enabling standardized and reproducible recordings across diverse cortical areas.*

EEG RHYTMS

EEG activity is conventionally divided into distinct frequency bands, or rhythms, each reflecting specific neurophysiological and cognitive states. At the cellular level, these oscillations arise from the synchronous activity of large populations of cortical pyramidal neurons, primarily in superficial cortical layers. Such synchronization may occur as isolated, large-amplitude potentials or as continuous, rhythmic field potentials. The regularity of these discharges determines whether the oscillations exhibit a narrow or broad spectral bandwidth. In general, the amplitude of EEG oscillations decreases as frequency increases, consistent with the idea that higher-frequency rhythms involve smaller or less synchronized neuronal assemblies [176].

The overall EEG spectrum spans approximately 0.01–100 Hz, with ultra-slow components near 0.01 Hz representing slow cortical potentials that are often attenuated in routine clinical recordings because of high-pass filtering. Within this range, five principal frequency bands are recognized: delta (δ), theta (θ), alpha (α), beta (β), and gamma (γ) (Figure 12) [176]. Hans Berger first described alpha and beta rhythms in 1929, while W. Grey Walter later introduced the delta and theta designations. The term gamma was coined by Jasper and Andrews in 1938 to describe oscillations above 30 Hz. These canonical bands are not rigid categories but rather reflect dominant peaks within a continuous spectrum, and their relative power varies with age, vigilance state, cognitive demands, and pathology.

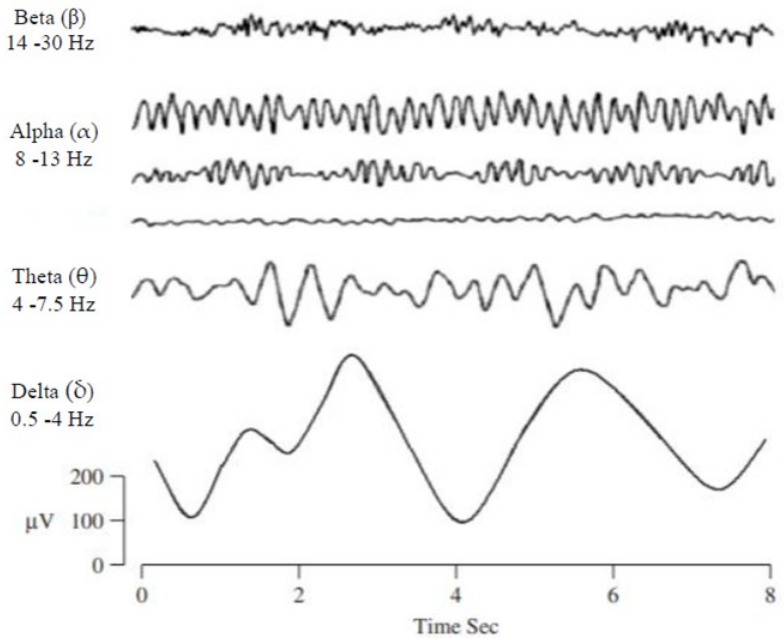

Figure 12. *Principal EEG Rhythms. Delta (0.5–4 Hz), theta (4–8 Hz), alpha (8–12 Hz), beta (12–30 Hz), and gamma (>30 Hz) frequency bands, shown with their characteristic waveforms.*

DELTA RHYTHM (δ)

The delta band (0.5–4 Hz) is the slowest and typically the highest-amplitude EEG rhythm [177, 178]. Delta activity is most prominent during the deepest stages of non–rapid eye movement (NREM) sleep and plays a key role in homeostatic sleep regulation. In infants and young children, delta activity is abundant during wakefulness and gradually diminishes with maturation as faster rhythms emerge. In awake adults, persistent focal or diffuse delta activity often indicates structural brain abnormalities such as tumors, ischemic lesions, or encephalopathy [179, 180]. Delta power also increases transiently during tasks that require sustained internal attention, suggesting a role in large-scale network coordination.

THETA RHYTHM (θ)

Theta oscillations (4–7.5 Hz) are believed to originate from thalamocortical and hippocampal circuits [178, 179, 181]. They appear during drowsiness and the transition to early sleep but are also strongly linked to episodic memory encoding, working memory maintenance, and cognitive control. Enhanced frontal-midline theta activity is observed during tasks demanding sustained attention, error monitoring, or mental effort. In meditative and creative states, theta synchronization has been associated with internalized awareness and access to unconscious processes [182]. Developmentally, theta power is high in childhood and declines with age, serving as a marker of brain maturation and emotional regulation.

ALPHA RHYTHM (α)

The alpha rhythm (8–13 Hz) is the predominant EEG pattern in visually relaxed but awake adults and is frequently referred as the posterior dominant rhythm [183-185]. The rhythm is prominent over the occipital and parietal areas and has the shape of a nearly sinusoidal waveform (Figure 13). Alpha power increases when eyes are closed and decreases during eyes open condition, sensory stimulation, or cognitive engagement [186]. Alpha oscillations are considered to control the flow of information within cortical networks by functioning as an inhibitory mechanism which gates the most irrelevant sensory input. In addition, alpha activity has been associated with memory, processing speed, and attentional control tasks [187]. The subbands comprise alpha1 (8–10 Hz) which is related to relaxed wakefulness and alpha2 (10–13 Hz) that exhibited stronger modulation by attentional and semantic processing demands. The presence of abnormal alpha may signal cortical dysfunction such as in dementia or traumatic

brain injury.

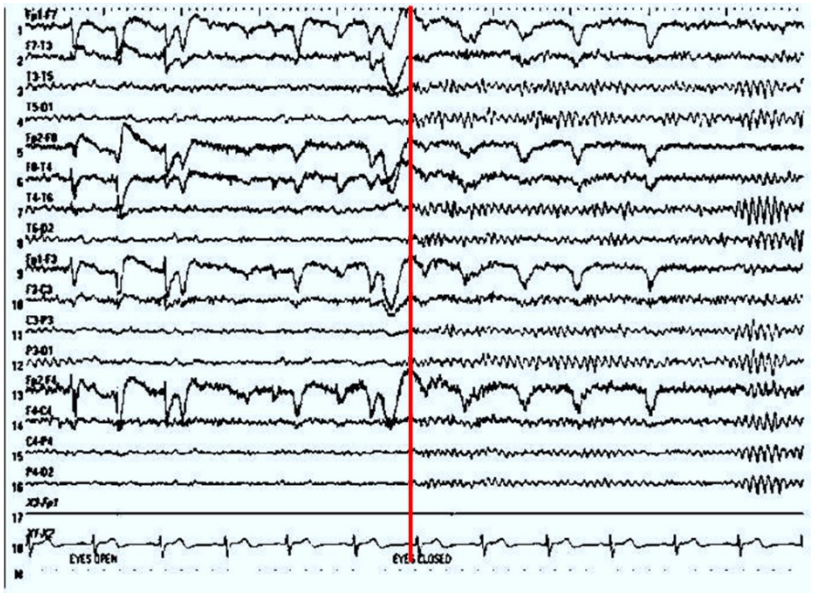

Figure 13. *Effect of Eye Closure on Alpha Activity. These traces demonstrate the increase in occipital alpha power in eye close condition and its attenuation with eye opening.*

BETA RHYTHM (β)

The beta band (14–26 Hz) predominates during active wakefulness and is associated with focused attention, sensorimotor processing, and cognitive engagement [188]. Beta activity is most pronounced over the frontal and central cortices, with a specific Rolandic mu rhythm that attenuates during voluntary movement or somatosensory stimulation [189, 190]. Beta oscillations facilitate top–down control and are thought to support the maintenance of the current sensorimotor or cognitive state. They are often subdivided into beta1 (14–20 Hz), related to relaxed alertness, and beta2 (20–26 Hz), which is enhanced during intense mental or motor activity. Excessive or abnormal beta activity may be observed in conditions such as anxiety disorders or during benzodiazepine use.

GAMMA RHYTHM (γ)

Gamma oscillations encompass frequencies above 30 Hz, sometimes extending beyond 100 Hz [63]. Though typically low in amplitude and more challenging to detect with scalp EEG, gamma activity is implicated in higher-order cognitive operations such as perceptual binding, attention, memory formation, and sensorimotor integration. Gamma power increases in association with sensory processing and learning, and focal gamma responses can help localize cortical regions

responsible for specific motor functions, such as finger or tongue movements [191, 192]. High-frequency gamma (>60 Hz) has become a key target for research using high-density EEG and magnetoencephalography (MEG) to study neural synchrony and consciousness.

EEG ARTIFACTS

EEG recordings inevitably contain artifacts, that is, electrical signals not generated by intrinsic brain activity. Because neural potentials vary in amplitude, duration, and morphology, it is impossible to obtain an entirely artifact-free trace. For this reason, understanding the mechanisms and sources of artifact formation is essential for accurate interpretation and for the design of effective preprocessing methods. Artifacts are commonly classified as either non-physiological (exogenous artifact), when their origin lies in the recording equipment or surrounding environment, or physiological (endogenous artifact), when they arise from the participant's own bioelectric or biomechanical activity [193].

EXOGENOUS ARTIFACT

Exogenous artifacts originate from external or technical sources that interfere with the EEG acquisition system rather than from the participant's own physiology.

The most common contributors are electrodes, the headbox and amplifier, interconnecting cables, and environmental electromagnetic fields.

- Electrode-related artifact are particularly frequent. Mechanical displacement or a brief loss of contact at the electrode–skin interface can generate abrupt voltage shifts known as electrode pops. Poor or uneven scalp preparation can result in high or unequal impedance across electrodes, producing slow baseline drifts or intermittent spikes [194]. Drying of conductive paste, formation of salt bridges between neighboring electrodes, or a gel bridge—where the conductive gel connects adjacent electrodes—may lead to spurious synchronization and false coherence between channels. Frayed or broken wires and loose connectors add further instability.
- Power-line interference at 50 Hz (or 60 Hz in some regions) is still a typical disturbance. It happens when the alternating current from the power mains is coupled with the recording circuitry. This is generally due to the recording equipment not being grounded properly or high electrode impedance. A combination of keeping the impedances under about 5 kΩ, ensuring

proper grounding, and using a notch filter is the usual repertoire of the measures taken to avoid the defect [194].

- Environmental sources may also pollute the recordings. The noise is a result of the radio frequency emitting devices such as ventilators, infusion pumps, wireless routers, or fluorescent lighting. Even mobile phones or laptops placed close to the amplifier may be culprits. Besides that, mechanical vibrations and patient movements through electrode cables can cause the so-called microphonic noise. Changing magnetic fields rapidly, for instance, can be a result of the MRI system or a big transformer, which eventually leads to currents in the leads. Electrostatic discharges coming from the clothes or the bed can cause transient high amplitude spikes that can spread to different channels [195].
- Cable movement may also induce artifact. Slight cable displacement induces movement of the oscillatory signals, especially during the patient repositioning. In some hospital settings, radiofrequency (RF) interference from telemetry systems or electrosurgical equipment can introduce high-frequency artifacts. Sources of this type of artifacts are electrodes, headbox, amplifier, cables and environment [196].

ENDOGENOUS ARTIFACT

Endogenous artifacts are generated by the participant's own physiological or biomechanical activity but do not reflect cortical electrical processes.

- Ocular activity. The eye functions as an electrical dipole, with the cornea being electropositive relative to the retina. Any eye movement or blink alters the orientation of this corneo-retinal dipole, producing slow potential shifts detectable by scalp electrodes, especially in the frontal regions. Blinks usually have abrupt, high-amplitude deflections [197]. The duration of the depolarization is about 0.2-0.4 seconds. This quite rapide changes in corneal position and eyelid movement alter local conductance [195]. Electro-oculographic (EOG) signals are generally larger than cortical EEG and occupy overlapping frequencies. So, a dedicated EOG channel is highly recommended for detecting and regressing ocular artifacts [198].
- Muscle (electromyographic, EMG) activity. Along with the production of sound, contraction of cranial, facial, or scalp muscles can lead to a noise that covers the frequency band from near-DC to over 200 Hz and can mask neural signals in the alpha and beta bands. This broadband noise is also produced by the action of swallowing, clenching the jaw, or even by subtle facial tension. Independent Component Analysis (ICA) or simultaneously recorded

surface EMG is generally used to disentangle the EMG and EEG sources [197].

- Cardiac activity. The heart's electrical field is a potential EEG confound, as it produces rhythmic deflections on the scalp regular with electrocardiogram (ECG) signals. The pulse or ballistocardiographic artifact (i.e., arising when an electrode is positioned over a pulsating artery) is more challenging to address. The mechanical expansion with each heartbeat causes slow periodic waves around 1 Hz when the electrode is over a pulsating artery, which can easily be confused with delta activity. It is worth noting that these pulse waves always precede the ECG R-wave by a certain interval, thus identification becomes easier [196].
- Respiratory activity. In this case, the artifact is caused by breathing movements that displace the head or chest and thus create low-frequency baseline drifts. It is also possible that the ventilator cycle may cause rhythmic fluctuations on the EEG of a patient under mechanical ventilation [198].
- Sweat-related artifacts. These artifacts are related to changes in skin conductivity due to accumulated perspiration, resulting in slow (<1 Hz) baseline shifts. Along with this, heavy sweating condition may also cause salt bridges to form between the electrodes placed closely, resulting in false voltage asymmetries or spurious synchrony [199].
- Movement-related artifacts. Head or limb movements are usually accompanied by irregular, high-amplitude deflections; however, tremor in neurodegenerative diseases such as Parkinson’s disease introduces rhythmic activity that can be indistinguishable from genuine cortical oscillations. Jaw clenching, teeth grinding (bruxism), or tongue movements are a mixture of mechanical and EMG effects whereby there is the addition of both slow drifts and high-frequency noise [198].
- Other physiological artificats. Beyond these common sources, additional endogenous phenomena may appear. Glossokinetic artifacts arise when tongue movements change the dipole between the tongue tip and base, detectable especially in inferior frontal electrodes. Ballistocardiographic artifacts are particularly relevant in simultaneous EEG–fMRI recordings, where head motion coupled to the cardiac cycle induces complex artifacts in both modalities. Skin-potential changes from the sympathetic nervous system—sometimes called the galvanic skin response—create slow potential shifts during emotional arousal. Even subtle postural adjustments or coughing can superimpose transient broadband noise [198].

A simple example of common exogenous and endogenous artifact is shown in Figure 14.

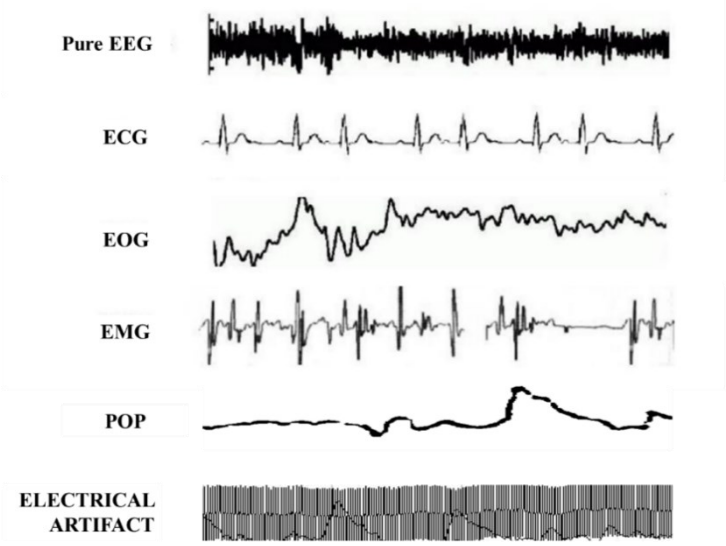

Figure 14. *Common Physiological Artifacts in EEG Recordings: Ocular, Muscular, and Cardiac. This figure presents the most frequent types of artifacts that can affect EEG data, specifically highlighting ocular, muscular, and cardiac artifacts. (Urigüen & Garcia-Zapirain, 2015).*

ARTIFACT REMOVAL TECHNIQUES

Eliminating artifacts from EEG recordings is essential for reliable analysis of neural activity. Exogenous artifacts can often be minimized through preventive measures such as careful scalp preparation, secure electrode attachment, proper grounding, and recording in an electromagnetically shielded environment. Simple analog or digital filtering (for example, applying a 50/60 Hz notch filter to suppress power-line interference) can further attenuate residual non-physiological noise.

In contrast, endogenous or biological artifacts—including ocular, muscular, cardiac, and movement-related activity—are more challenging to eliminate because they overlap in frequency and amplitude with genuine brain signals. Removal therefore typically requires a combination of manual inspection and advanced computational methods [194].

A traditional approach is the manual rejection of artifact-contaminated epochs. Here, continuous EEG data are segmented into shorter time windows (epochs), which are visually inspected by an experienced reviewer. Artifacts were removed from the data before the subsequent analysis in this study. To explain, artifacts might be large-amplitude deflections caused by the eye blink that can be sudden electrode pops or high-frequency EMG bursts. Although this technique conserves data integrity and can be easily executed, it is a lengthy procedure and may lead to a significant loss of the data, especially in long recordings or in the case of participants who are prone to movement.

Nowadays, the preprocessing pipelines commonly use Independent Component Analysis (ICA) that is a blind-source–separation method and hypothetically considers that the EEG recorded is an instantaneous linear combination of independent sources from the brain and non-brain. ICA separates the multichannel EEG into several independent components where each one represents a single time course and scalp topography. To identify the noise sources, spatial distributions, and temporal patterns also assist. These components can be further removed or weakened to reconstruct the EEG after the cardiac, ocular, and muscle activity signal components are recognized by their typical spatial maps and temporal patterns. The method is popular because it makes it possible to obtain pure neural signals while not having to throw away large chunks of data although there is a need for quite some data, high SNR, and expert interpretation to avoid the loss of real cortical activity [200].

In addition to the methods of manual rejection and ICA, the development of automated as well as semi-automated algorithms has also been reported. In the case of Principal Component Analysis (PCA), Canonical Correlation Analysis (CCA), and wavelet decomposition, the methods may be used for the isolation and suppression of the artifact-related features in the time-frequency domain. In the case of adaptive filters, reference signals, such as an electrooculogram (EOG) for eye saccades or an electromyogram (EMG) for muscle activity, can be used for the subtraction of the correlated noise from ECG channels. The most recent evolutions include machine learning-based classifiers and hybrid pipelines that can integrate different methods for fast, automatic, and almost user-free clean EEG data [201, 202].

In reality, removal of artifacts to the optimal extent is usually the result of a multi-step strategy which includes preventive measures during data acquisition, thorough visual inspection, and the usage of one or more computational algorithms that are appropriate for the type and the level of contamination of the dataset. Such a combined system leads to the preservation of the most authentic neural information while the impact of the artifactual signals on the EEG recordings is minimized.

EEG IN PHYSIOLOGICAL AND PATHOLOGICAL AGING

EEG offers a unique, non-invasive window onto the functional organization of the aging brain. Across the life span, characteristic changes in EEG rhythms and network properties reveal

alterations in neuronal synchronization, information transfer, and neuroplastic capacity.

By combining classical spectral measures with network-level metrics, EEG provides insight into both the progressive changes of healthy aging and the pathological disconnection that accompany dementia [203, 204].

Power Spectral Density (PSD):

PSD quantifies the distribution of EEG power across frequency bands—delta (1–4 Hz), theta (4–8 Hz), alpha (8–13 Hz), beta (13–30 Hz), and gamma (>30 Hz)—and is one of the most reproducible EEG markers of aging.

- *Physiological aging:* Normal aging is related to a mild global slowing of the dominant rhythm. A number of studies demonstrate a gradual increase in theta power along with a subtle decrease of posterior alpha and frontal beta power starting from the sixth decade of life [182, 205]. The sequence probably indicates less thalamocortical drive and slower cortical oscillatory dynamics, but cognition is still preserved most of the time, as compensatory networks are able to maintain global communication.
- *Pathological aging:* A spectral reorganization is much stronger in MCI and AD. Common findings consist of a substantial increase in delta and theta power, very often fronto-temporal or diffuse, along with a drastic reduction of alpha and beta activity, especially in posterior association cortices [206, 207]. The theta/alpha power ratio is an extensively validated marker of disease progression and, thus, it is the best predictor of conversion from MCI to AD in longitudinal cohorts [208]. Beta desynchronization is associated with attention and executive function deficits, whereas posterior alpha slowing is indicative of memory-related networks degradation. In line with a disrupted fast inhibitory–excitatory balance, gamma activity (>30 Hz) also frequently diminishes.

Functional Connectivity (FC)

EEG-based FC is a measure of temporally correlated activity or phase synchronization of oscillations between different brain regions, which allows one to capture network communication within the brain at a millisecond time scale.

- *Physiological aging:* Results of research indicate a gradual loss of long-range alpha and beta coherence with aging being the main cause of reduction in the integration of distant cortical hubs such as frontal and parietal regions [209, 210]. Still, a lot of older people are able to maintain sufficient cognition, which is an evidence of compensatory local reorganization.
- *Pathological aging:* Pathological aging is characterized by a more dramatic

disconnection syndrome. Patients exhibit reduced intra- and inter-hemispheric connectivity, particularly in the default-mode and memory networks, with greatest reductions in alpha-band coherence. Frontal hyper-connectivity sometimes emerges as a compensatory response, but it often fails to restore global efficiency and may even suppress parietal activity [211, 212]. These FC alterations correlate strongly with episodic-memory and executive deficits, making FC a robust biomarker of cognitive decline [213].

Graph-Theoretical Network Properties

Graph theory models the brain as a network of nodes (electrodes or cortical regions) and edges (functional connections), enabling quantitative assessment of local and global efficiency.

- *Physiological aging:* Healthy older adults show a modest decline in clustering coefficient and a slight increase in characteristic path length, reflecting a slow erosion of both local and global network efficiency while largely preserving the "small-world" topology essential for efficient information transfer [214, 215].
- *Pathological aging:* These changes become far more pronounced in pathological aging. Numerous studies demonstrate marked reductions in clustering and significant lengthening of path length, signifying breakdown of local neighborhood communication and global integration [200, 214]. The resulting loss of small-world organization is strongly associated with memory impairment, language difficulties, and executive dysfunction. Graph-theoretical metrics derived from EEG are increasingly used to track disease progression and to evaluate interventions such as cognitive training or non-invasive brain stimulation.

Entropy

Entropy provides a measure of the complexity or unpredictability of EEG time series.

- *Physiological aging:* Physiological aging shows a moderate increase in entropy, reflecting a gradual alteration in neural signal variability and dynamical range while cognitive performance remains relatively stable [216].
- *Pathological aging:* Patients exhibit a significant entropy decline, particularly in parietal and temporal regions critical for memory and association processing [217]. · Lower entropy is a measure that points to less information processing capacity and can signal a reduction in the adaptability of cortical circuits. Some localized entropy changes have been reported in a few MCI stage studies, which could signify a brief compensatory plasticity phase before the general neurodegeneration takes place [29].

All these EEG signatures—spectral slowing, reduced functional connectivity, disrupted small-world topology, and alteration in entropy—combine to clarify the mechanism by which brain dynamics change with age. While in normal aging the changes are slow and partially compensated, in MCI and AD they are faster and correlate with the clinical severity.

Such parameters may help local differential diagnosis at an early stage, keep track of disease progression, and be used as a source of data in pharmacological or neuromodulatory trials.

Interventions, for example, that bring back posterior alpha power or work to network efficiency by energy consumption reduction are thus considered potential biomarkers of therapeutic efficacy.

SECOND PART

STUDY 1

EEG ENTROPY INSIGHTS IN THE CONTEXT OF PHYSIOLOGICAL AGING AND ALZHEIMER'S AND PARKINSON'S DISEASES: A COMPREHENSIVE REVIEW [218]

Published as:

Cacciotti A, *Pappalettera C, Miraglia F, Rossini PM, Vecchio F. EEG entropy insights in the context of physiological aging and Alzheimer's and Parkinson's diseases: a comprehensive review. Geroscience. 2024 Dec;46(6):5537-5557. doi: 10.1007/s11357-024-01185-1.*

OBJECTIVE

This review aims to highlight the growing relevance of entropy measures in neuroscience, particularly for analysing EEG signals to assess brain complexity and irregularity. It emphasizes how nonlinear approaches—such as approximate entropy (ApEn), sample entropy (SampEn), multiscale entropy (MSE), and permutation entropy (PermEn)—can detect subtle neural alterations that traditional linear methods might miss. The review explores the application of these measures in the context of healthy brain aging and neurodegenerative diseases, especially Alzheimer's disease (AD) and Parkinson's disease (PD). Overall, it supports the potential of entropy analysis as a biomarker for early diagnosis, disease monitoring, and the development of personalized therapeutic strategies.

ABSTRACT

Over time, entropy measures have become a significant topic of interest in the field of neuroscience to explain the nonlinear behaviour of the brain. In this regard, entropic analysis of EEG signals can be considered as a useful tool for decoding the complexity and irregularity of the electrical activity of the brain. The use of entropy measures instead of linear ones deepens the comprehension of the brain dynamics, which is especially useful in revealing the underlying mechanisms of brain aging as well as of various acute/chronic-progressive neurological disorders. This review, by going through various applications of entropy in the study of normal

brain aging and neurodegenerative diseases, including Alzheimer's disease (AD) and Parkinson's disease (PD), is putting emphasis on the importance of entropy analysis and its ability to discriminate between physiological and pathological conditions. Several entropy measures like approximate entropy (ApEn), sample entropy (SampEn), multiscale entropy (MSE), and permutation entropy (PermEn) are here considered for characterizing the health status of the brain. The use of entropic analysis in monitoring the degree of complexity and irregularity of EEG signals can be of great help for clinical practices to achieve early diagnosis and treatment monitoring and disease management.

METHODS

Entropy based measures

Entropy is a fundamental concept that originates from thermodynamics and information theory, where it is used to quantify the degree of uncertainty, disorder, or complexity within a system. In physical systems, high entropy is associated with randomness and uniform distributions, whereas low entropy corresponds to more ordered, concentrated configurations. This concept has been successfully extended to neuroscience, where entropy allows researchers to explore the dynamic behaviour of neural systems by measuring the complexity of brain activity.

In the context of brain function, the brain is seen as a complex, dynamic system that continuously adapts to internal and external changes. Neural signals—particularly those captured through electroencephalography (EEG)—reflect a wide range of activities, from highly regular to highly chaotic patterns. Entropy-based measures provide a mathematical framework for quantifying this variability, allowing for distinctions between different brain states, whether physiological (e.g., healthy aging) or pathological (e.g., Alzheimer's or Parkinson's disease) [219].

Shannon and Conditional Entropy

The foundation of entropy analysis lies in Shannon entropy, developed within the field of information theory. It was originally designed to evaluate the amount of information carried in messages transmitted through noisy communication channels. In its basic form, Shannon entropy quantifies the average level of uncertainty associated with a random variable. When applied to a discrete variable V, whose outcomes occur with probabilities $p(v_i)$, Shannon entropy is defined as [220, 221]:

$$H(V) = -\sum_{x \in X} p(v) \log p(v)$$

This formula captures how unpredictable the outcomes are: entropy is zero when all outcomes are identical (i.e., fully predictable), and reaches its maximum when all outcomes are equally likely. From the concept of Shannon entropy different metrics has been derived, such as permutation entropy (PermEn) [222].

Beyond this, Conditional Entropy (CE) provides a means to evaluate the remaining uncertainty in one variable given knowledge of another. If two random variables, *V* and *W*, have a joint probability distribution *p(V,W)*, conditional entropy quantifies how much uncertainty remains about *V* once *W* is known:

$$H(V|W) = \sum_{k,j} z_{kj} \log\left(\frac{q_j}{z_{kj}}\right)$$

While more complex to compute, CE is useful when interdependencies between variables must be taken into account—such as the influence of different brain regions on each other. Different metrics have been derived from the concept of CE, like approximate entropy (ApEn) [223], sample entropy (SampEn) [224], and multiscale entropy (MSE) [225].

Permutation Entropy (PermEn)

Permutation Entropy offers a way to assess the complexity of a time series by focusing not on the amplitude of values but on the temporal order in which they appear. It is particularly useful for identifying dynamic changes in signals and is relatively robust to noise.

To compute PermEn, the EEG time series is first embedded into delay vectors, which are constructed using two parameters: the embedding dimension m, and the time lag τ. These vectors are then converted into ordinal patterns (i.e., permutations of ranks), and the relative frequency of each permutation is used to compute entropy:

$$PermEN\ (m, L) = -\sum_{i=1}^{m!} p(\pi) \ln p(\pi)$$

The more diverse the orderings of the values, the higher the entropy, indicating greater signal complexity [222].

Approximate Entropy (ApEn)

Approximate Entropy is another widely used method for quantifying signal regularity. It examines the likelihood that similar patterns in a time series remain similar over time. The method begins by calculating the distance between short sequences of data and assessing how many remain within a given threshold r. The similarity function is:

$$C_i^m(r) = \frac{1}{N-(m-1)} \sum_{j \neq i} \Theta\{r - d(X(i), X(j))\}$$

With:

$$\Theta\{\mathrm{x}\} = \begin{cases} 1, & x \geq 0 \\ 0, & x < 0 \end{cases}$$

From this, the Approximate Entropy is computed as:

$$ApEn\ (m, r) = \phi^m(r) - \phi^{m+1}(r)$$

ApEn is relatively easy to compute and is suitable for shorter time series, but it has limitations, such as being sensitive to signal length and including self-matches, which may bias the results [226].

Sample Entropy (SampEn)

Sample Entropy is a refinement of ApEn that improves reliability by excluding self-matches from its computation. It evaluates the probability that sequences similar for m points remain similar when an additional point is considered. The result is expressed as:

$$SampEn\ (m, r) = -\ln \frac{A}{B}$$

Where A and B refer to the counts of matched sequences of length m+1 and m, respectively. SampEn is more robust to noise and less dependent on data length, making it suitable for physiological data like EEG [224].

Multiscale Entropy (MSE)

Multiscale Entropy (MSE) represents an advanced method for analysing the complexity of physiological signals like EEG by considering not only short-term fluctuations, but also how information unfolds over longer time scales. The method operates in two main steps. Initially, it performs a coarse-graining of the time series: this is basically averaging the original signal over non-overlapping windows of different lengths, the scale factor γ. Thus, each scale gives a new, lower-resolution version of the signal, showing the system's behaviour at progressively slower temporal resolutions. Finally, the algorithm uses a standard entropy measure—usually Sample Entropy (SampEn)—to each coarse-grained time series. By doing this for several scale factors, MSE obtains an entropy profile that indicates how the complexity of the signal changes at different time scales. The technique is particularly useful in the study of the nervous system as it accounts for both fast neuronal variations and slow, integrative, processes, thus providing a more complete picture of brain dynamics than single-scale entropy methods [225].

RESULTS

Physiological Aging

Complex patterns arise from EEG entropy measures during healthy aging. In a majority of cases aged population exhibits increased entropy of slow oscillations such as delta and theta while they show decreased entropy of fast bands like beta and gamma. This change in brain dynamics is indicative of a shift, wherein slow local and processes become more irregular whereas fast integrative rhythms lose complexity. Multiscale entropy (MSE) gives some more clues: aging is usually characterized by higher entropy at the fine scale and lower entropy at the coarse scale, suggesting a retained local adaptability but impaired long-range temporal integration. The differences highlight the distinctive features of the aging brain during cognitive task performance, which is characterized by compensatory increases in short-scale entropy concomitant with reduced complexity at broader scales. The figure 15 presents a graphical summary of the results.

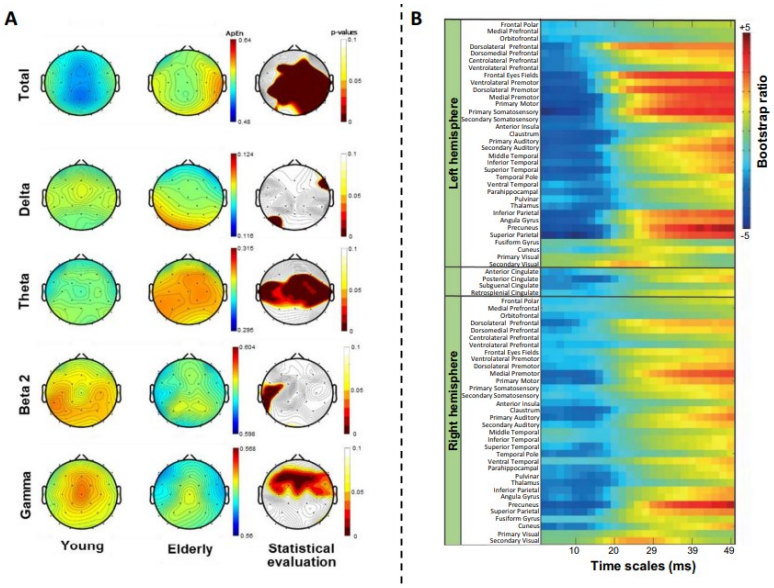

Figure 15. *Entropy changes during normal aging were examined across EEG frequency bands (panel A) and time scales (panel B), highlighting differences in neural processing across brain regions.*

Alzheimer's Disease (AD)

Patients with AD consistently exhibit reduced entropy, especially in the alpha band and at fine temporal scales, indicating a general loss of neural flexibility and irregularity. ApEn and SampEn studies highlight diminished complexity in temporal regions, which are particularly vulnerable to AD pathology. MSE analyses further confirm lower entropy at short time scales, suggesting early disruption of fast neural processes. Genetic factors appear to influence these patterns: patients carrying protective alleles show relatively preserved entropy in higher-

frequency bands (alpha, beta, gamma), pointing to better maintenance of network dynamics despite disease burden. A visual representation of the results is reported in Figure 16.

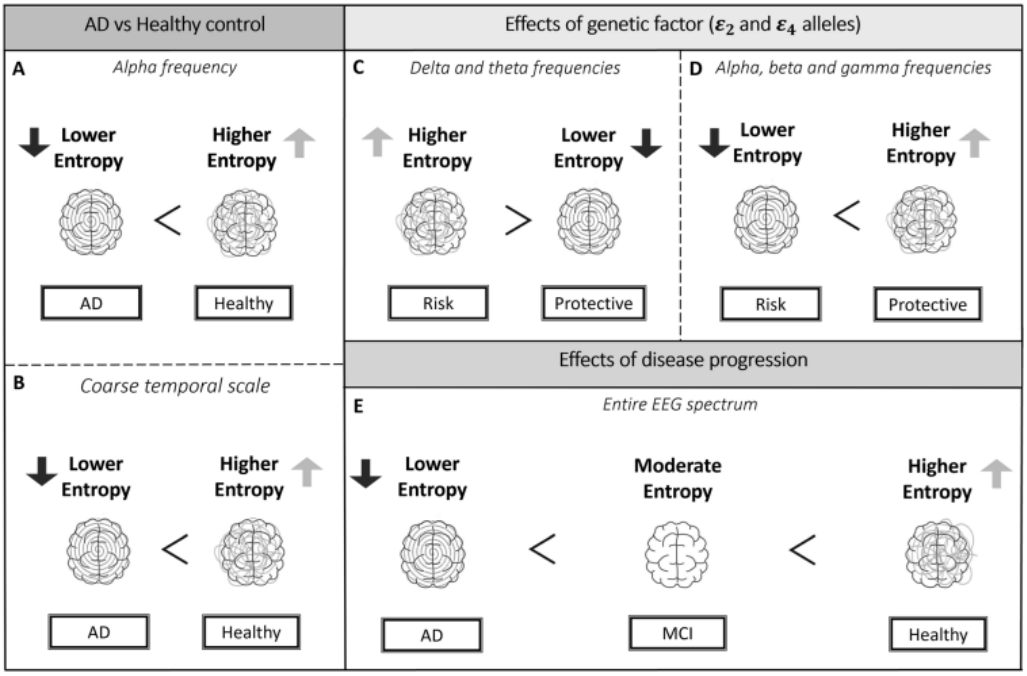

Figure 16. *The figure provides a graphical overview of findings on entropy modulation in Alzheimer's disease (AD). Blue upward arrows represent increased entropy values, while green downward arrows indicate reductions. The first section of the figure illustrates how AD patients differ from healthy elderly individuals in the alpha band, with the patients showing consistently lower entropy both in this frequency range and at coarse temporal scales. The second section highlights the role of genetic factors: in the lower frequency bands, subjects carrying protective alleles (epsilon 2) exhibit lower entropy compared to those with risk alleles (epsilon 4), whereas in the higher frequency bands the opposite trend emerges, with protective carriers showing higher entropy values. Finally, the third section depicts how entropy changes along the continuum from healthy aging to mild cognitive impairment (MCI) and Alzheimer's disease. Here, a clear gradient can be observed, with healthy elderly displaying the highest entropy, MCI subjects presenting intermediate values, and AD patients showing the lowest entropy across the frequency spectrum.*

Parkinson's Disease (PD)

The entropy results of PD are more diverse and seem to be dependent on the stage of the disease and the method of analysis. There are studies that find an increase in ApEn in advanced PD in line with the idea of greater irregularity of the signal in a later stage of the disease. As a matter of fact, reduction of PermEn in various frequency bands has been related to early-stage PD. MSE analysis revealed increased entropy at coarse scales in PD patients during sleep, suggesting a disruption of large-scale temporal organization.

DISCUSSION AND CONCLUSION

Entropy measures are capable to characterise not only physiological aging but also neurodegenerative pathology. In fact, the complex phenomenon of entropy changes in different frequency bands observed in aging brains of healthy individuals reflects a gradual reorganization of brain networks in which compensatory mechanisms maintain local adaptability while disrupt long-range integration. Concerning pathological aging, a very characteristic feature of AD is the consistent pattern observed across multiple neurophysiological and structural metrics, reflecting a loss of the brain's flexibility and complexity. This decline manifests at various levels (neural activity, network connectivity, and synaptic integrity) all of which collectively define the core pathology of AD. In PD, the concept is far more complex whereby entropy is reduced initially to reflect the loss of neural variability but later it increases most probably due to those mechanisms or pathological noise associated with the disease. Additionally, pharmacological treatment in PD is demonstrated to be a functional change alongside clinical interventions by the modulation of entropy.

Summing up, entropy stands out as a potent and minimally invasive tools for investigating brain dynamics. Its usefulness in discerning not only the loss, but also the compensation in the neural systems makes it especially beneficial for the study of the aging processes as well as for the discrimination of normal aging from such pathological conditions as AD and PD. What lies ahead is the task of standardizing analytic methods, combining entropy with other biomarkers, and uncovering its longitudinal predictive capacity for disease progression and treatment effects monitoring.

STUDY 2

APPROXIMATE ENTROPY ANALYSIS ACROSS ELECTROENCEPHALOGRAPHIC RHYTHMIC FREQUENCY BANDS DURING PHYSIOLOGICAL AGING OF HUMAN BRAIN [219]

Published as:

*Pappalettera C, **Cacciotti A**, Nucci L, Miraglia F, Rossini PM, Vecchio F. Approximate entropy analysis across electroencephalographic rhythmic frequency bands during physiological aging of human brain. Geroscience. 2023 Apr;45(2):1131-1145. doi: 10.1007/s11357-022-00710-4.*

OBJECTIVE

This study aimed to investigate the effects of physiological aging on the human brain by analysing EEG signal complexity using approximate entropy (ApEn). The goal was to determine whether ApEn can capture age-related changes in brain activity across different frequency bands and assess its potential as a biomarker for brain aging. Additionally, the authors evaluated the classification performance of ApEn features in distinguishing young and elderly participants using support vector machine (SVM) models.

ABSTRACT

Aging is the inevitable biological process that results in a progressive structural and functional decline associated with alterations in the resting/task-related brain activity, morphology, plasticity, and functionality. In the present study, we analysed the effects of physiological aging on the human brain through entropy measures of electroencephalographic (EEG) signals. One hundred sixty-one participants were recruited and divided according to their age into young (n = 72) and elderly (n = 89) groups. Approximate entropy (ApEn) values were calculated in each participant for each EEG recording channel and both for the total EEG spectrum and for each of the main EEG frequency rhythms: delta (2-4 Hz), theta (4-8 Hz), alpha 1 (8-11 Hz), alpha 2

(11-13 Hz), beta 1 (13-20 Hz), beta 2 (20-30 Hz), and gamma (30-45 Hz), to identify eventual statistical differences between young and elderly. To demonstrate that the ApEn represents the age-related brain changes, the computed ApEn values were used as features in an age-related classification of subjects (young vs elderly), through linear, quadratic, and cubic support vector machine (SVM). Topographic maps of the statistical results showed statistically significant difference between the ApEn values of the two groups found in the total spectrum and in delta, theta, beta 2, and gamma. The classifiers (linear, quadratic, and cubic SVMs) revealed high levels of accuracy (respectively 93.20 ± 0.37, 93.16 ± 0.30, 90.62 ± 0.62) and area under the curve (respectively 0.95, 0.94, 0.93). ApEn seems to be a powerful, very sensitive-specific measure for the study of cognitive decline and global cortical alteration/degeneration in the elderly EEG activity.

METHODS

Participants

A total of 161 healthy volunteers participated in the study and were divided into two age-based groups: 72 young adults (38 females; mean age = 24.8 ± 3.4 years; education = 14.3 ± 2.6 years) and 89 older adults (47 females; mean age = 69.4 ± 4.4 years; education = 10.9 ± 3.7 years). Exclusion criteria included current treatment with psychotropic or vasoactive medications and any history of neurological or psychiatric disorders. All participants were right-handed, as confirmed by the Handedness Questionnaire [227], and provided informed consent in accordance with the Declaration of Helsinki.

EEG Recording and Pre-processing

EEG data were collected using a 32-channel Easycap system (Brain Products) with electrodes positioned according to the Augmented International 10–20 system. The Fpz electrode served as the reference, and one electrode as the ground, yielding 31 usable EEG channels. Recordings were performed at a 1000 Hz sampling rate with electrode impedance kept below 5 kΩ. Each participant underwent a 6-minute eyes-closed resting-state session while seated in an electrically shielded, sound-attenuated, dimly lit room. Data were processed with custom MATLAB scripts based on the EEGLAB toolbox [228]. Signals were down-sampled to 512 Hz and filtered with a 0.2–47 Hz band-pass FIR filter. Continuous data were segmented into 2-s epochs, and artifacts such as muscle or cardiac activity were removed through expert visual inspection followed by Infomax ICA decomposition [210]. Approximately 5 minutes of artifact-free data were retained per participant.

Entropy Analysis

The complexity of brain activity was quantified using Approximate Entropy (ApEn), which is robust to noise and sensitive to subtle changes in signal regularity. For each participant, ApEn was calculated for every channel and frequency band—delta (2–4 Hz), theta (4–8 Hz), alpha 1 (8–11 Hz), alpha 2 (11–13 Hz), beta 1 (13–20 Hz), beta 2 (20–30 Hz), and gamma (30–45 Hz)—and for the full spectrum (0.2–47 Hz) [229]. Parameters were set to m = 2 and r = 0.2 × variance(x), where x denotes a 2-s epoch. ApEn values range from 0 (highly regular) to 2 (highly random) [230]. The ApEn values were computed using home-made MATLAB software.

The calculation proceeded as follows [226]:

1. A point-by-point comparison is made between each data sequence of length m and all other sequences. If the distance between points is less than the tolerance factor r, a match is scored. All the matches are counted as:

$$N_i = \sum_{i=1, i \neq k}^{N} \|Y_i - Y_k\|_\infty < r$$

where Y_i is the m-dimensional vector sequence, defined as a delayed reconstruction of the time series $\{y(i)\} = [y(1), y(2), \dots, y(N)]$, where i ranges from 1 to N, number of data points:

$$Y_i = [y(i), y(i+1), \dots, y(i+m+1)]$$

2. The comparison is performed on each successive m+1-long sequence, starting form the first sequence of m+1 points.
3. The number of matches is converted to a natural logarithm value and afterwards normalized by the number of data points (N):

$$\Phi_m = (N - m + 1)^{-1} \sum_{i=1}^{N-m+1} \log(N_i)$$

Finally, the ApEn is calculated using the following expression:

$$\text{ApEn} = \Phi_m - \Phi_{m+1}$$

Additionally, using the algorithm implemented in MATLAB, topographical maps of ApEn values across the scalp were generated for each frequency band and for the total spectrum to examine spatial distributions and age-related modulations.

Statistical evaluation

The two-tailed unpaired Student's t-test was performed to analyse the ApEn values to highlight

the statistical differences in each frequency band (total, delta, theta, alpha 1, alpha 2, beta 1, beta 2, and gamma) between groups (young, elderly). To account for multiple comparisons, the Bonferroni correction was performed on MATLAB. The function maintains the same threshold for the hypothesis rejection ($p<0.05$) but changes the p-values of the statistical analysis according to the number of comparisons.

Classification Procedures

To determine whether ApEn features could reliably discriminate between young and older participants, a supervised machine-learning pipeline based on Support Vector Machines (SVMs) was implemented in MATLAB.

Two datasets were considered. The first one is the full feature set, containing all the ApEn values from all 31 EEG channels across 7 frequency bands, totaling 217 features (31×7). The second one is the reduced feature set, containing 21 features selected via forward stepwise regression. At each iteration the algorithm added the feature with the lowest F-test p-value (< 0.05) that significantly reduced the model's residual sum of squares, thereby eliminating variables with near-zero variance or strong collinearity.

Three SVM kernels were evaluated: Linear SVM using a linear kernel, Quadratic SVM with polynomial kernel, and Cubic SVM with polynomial kernel [231]. The sequential minimal optimization (SMO) algorithm solved the quadratic optimization problem at each training step, ensuring efficient computation. For each kernel and feature set, model performance was evaluated with stratified tenfold cross-validation repeated 100 times to enhance reliability [232]. In each iteration the data were randomly partitioned into ten equally sized folds: nine folds were used for training and one for testing, rotating through all folds. Performance metrics included mean accuracy, standard deviation across folds, sensitivity, specificity, and the area under the ROC curve (AUC). The classifier achieving the highest mean accuracy was considered optimal, as the binary classification (young vs. elderly) involved balanced groups and did not require prioritizing false negatives or positives. This pipeline provided a rigorous assessment of the ability of ApEn-derived EEG features to capture age-related brain dynamics.

RESULTS

A significant group effect emerged for ApEn values in the total spectrum and in the delta, theta, beta 2, and gamma frequency bands. The total-spectrum analysis was included to enable direct comparison with prior entropy studies in the literature.

Within the total spectrum, statistically significant differences were observed in centro-parietal,

right occipital, and right temporal regions, where older adults exhibited higher ApEn values than younger participants.

For the delta band, significant effects appeared in the left occipital and right frontotemporal areas: older adults showed higher ApEn values in the left occipital region, whereas in the right frontoparietal region they displayed lower values compared to the younger group.

In the theta band, the elderly group demonstrated markedly higher ApEn values across the entire central region.

For beta 2, a significant difference was found in the centro-temporal region, with older adults presenting lower ApEn values than younger adults.

In the gamma band, older participants also exhibited significantly reduced ApEn values in the frontocentral region.

No significant group differences emerged for the alpha 1, alpha 2, or beta 1 frequency ranges.

Topographic ApEn maps and electrode-wise p-values (Bonferroni-corrected) are presented in Figure 17 and Table 3, respectively.

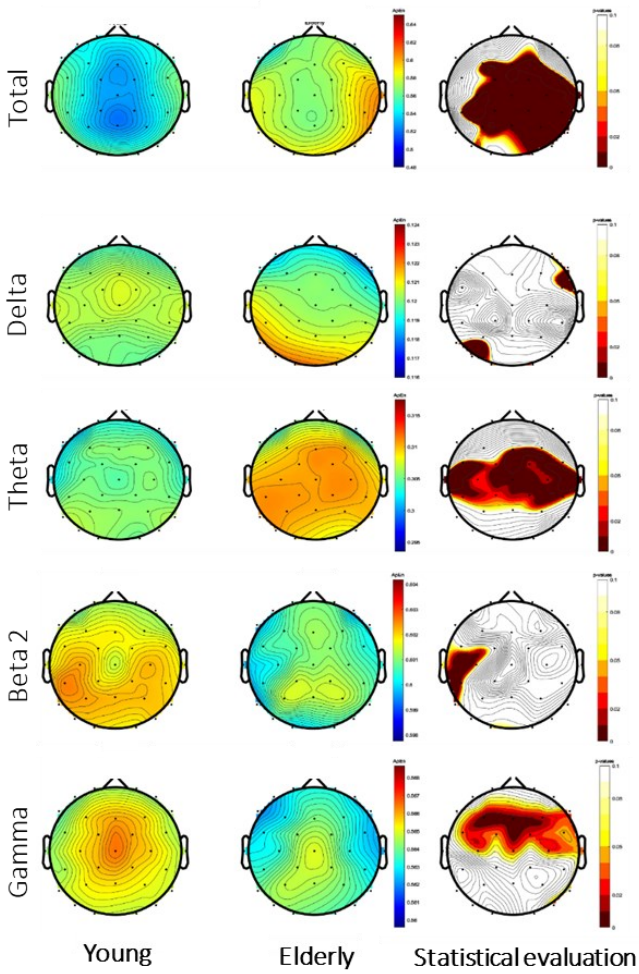

Figure 17. *Topographical Maps of ApEn values. Topographical maps were generated to illustrate the spatial*

distribution of ApEn values and the statistically significant differences between the two groups. Each row corresponds to a specific EEG frequency band (total, delta, theta, alpha 1, alpha 2, beta 1, beta 2, gamma). For each band, the first column depicts the ApEn topography of the young group and the second column that of the elderly group. Entropy magnitude is represented on a color scale, where warmer hues (red) indicate higher ApEn values and cooler hues (blue) indicate lower values. For every frequency band, the colorbar range was set from the minimum to the maximum ApEn value observed across both groups, extending to ±2 standard deviations. The final column displays the scalp distribution of Bonferroni-corrected p-values reflecting significant group differences.

Channel	*Total*	*Delta*	*Theta*	*Beta 2*	*Gamma*
Fp1	–	–	–	–	–
Fp2	–	–	–	–	–
AF7	–	–	–	–	–
AF8	–	0.034419	–	–	–
F7	–	–	–	–	–
F3	0.045618	–	–	–	0.003588
Fz	1.86E-06	–	0.035483	–	0.002459
F4	8.88E-06	–	–	–	0.017365
F8	–	0.00145	–	–	0.033302
FC5	–	–	0.024336	–	0.036875
FC1	7.38E-05	–	0.026024	–	0.041576
FC2	1.84E-06	–	0.016836	–	0.0236994
FC6	0.001513	0.008887	–	–	0.046002
T7	–	–	0.001656	–	–
C3	0.002459	–	0.030691	0.037925	0.041576
Cz	3.47E-05	–	0.003536	–	0.032632
C4	7.25E-07	–	0.015533	–	0.030968
T8	7.38E-05	0.0035288	0.021555	–	0.032632
CP5	0.045618	–	0.023193	0.004028	–
CP1	4.62E-05	–	0.026411	–	–
CP2	1.36E-06	–	0.012672	–	–
CP6	1.13E-07	–	0.024336	–	–
P7	–	0.03362	–	0.001698	–
P3	0.000215	–	–	–	–

Table 3. *Statistical p-values. Significant Bonferroni-corrected p-values for each channel and in each frequency band.*

For the classification analyses, each SVM variant (linear, quadratic, and cubic) was trained using two approaches: (1) the complete set of ApEn features from all electrodes and frequency bands, and (2) a reduced set of 21 features identified through feature selection. Classifier performance—summarized as mean ± SE for accuracy, AUC, specificity, and sensitivity—was averaged across 100 iterations of tenfold cross-validation. The best-performing models and their receiver operating characteristic (ROC) curves with 95% confidence intervals are reported in Table 4 and Figure 18.

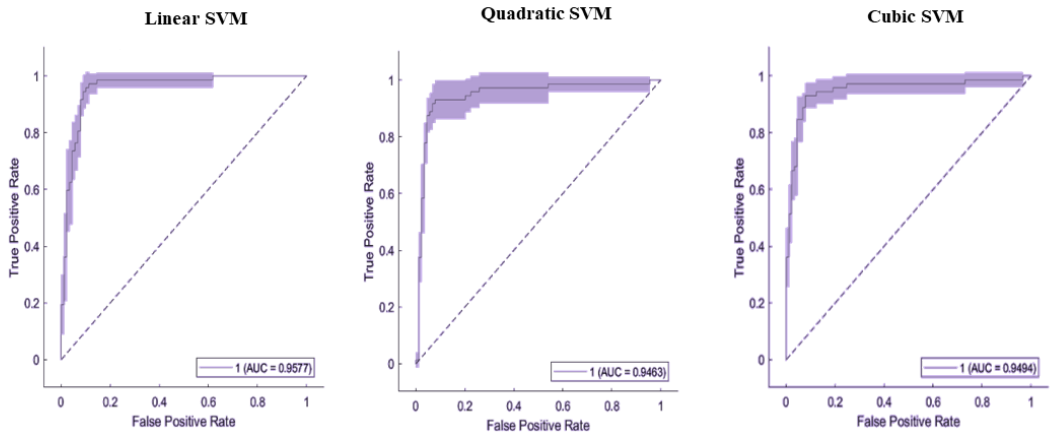

Figure 18. *ROC curve of the SVM classifiers. Mean receiver operating characteristic (ROC) curves with 95 % confidence intervals illustrating classification performance for the 161 participants using features selected through stepwise regression and classified with linear, quadratic, and cubic SVM models. Corresponding AUCs were 0.95, 0.94, and 0.93 respectively reflecting excellent discriminative ability for all three classifiers.*

		All Features		
Classifier	***Accuracy (%)***	***AUC***	***Specificity (%)***	***Sensitivity (%)***
SVM linear	89.45 ± 2.46	0.89	91.96 ± 2.00	87.78 ± 3.1
SVM quadratic	89.45 ± 2.56	0.93	88.92 ± 2.77	89.86 ± 3.61
SVM cubic	90.11 ± 2.14	0.92	93.21 ± 2.59	87.78 ± 2.26
		After the Features selection		
Classifier	***Accuracy (%)***	***AUC***	***Specificity (%)***	***Sensitivity (%)***
SVM linear	93.20 ± 1.42	**0.96**	91.40 ± 1.31	94.30 ± 2.25
SVM quadratic	93.16 ± 1.81	**0.95**	94.29 ± 1.37	92.2 ± 2.38
SVM cubic	90.62 ± 1.86	**0.95**	90.0 ± 2.24	90.97 ± 3.64

Table 4. *SVMs performances. Linear, quadratic, and cubic SVM performance values represented by mean±SE before and after the feature selection.*

DISCUSSION AND CONCLUSION

This study explored how healthy aging influences the complexity of resting-state brain activity, using entropy across a broad range of EEG frequency bands and scalp regions, and then testing whether these measures could distinguish younger from older adults with machine-learning methods. The results show a clear age-related fingerprint of neural complexity and point to ApEn as a promising marker of the aging process.

These findings, when considered together, suggest a complex reorganization of neural activity with age rather than a simple increase or decrease in signal irregularity. The increased ApEn in slow rhythms like delta and theta implies that the aging brain is functioning with greater large-

scale variability, which in turn might permit more flexible communication across distributed networks and could be a way of preserving functional capacity. In contrast, the lower ApEn observed in the faster beta 2 and gamma rhythms points to a decrease in the precision and stability of high-frequency neural activities that are usually involved in rapid information exchange, fine sensory integration, and cognitive control. The fact that these alterations are localized in centro-parietal and frontotemporal areas indicates that aging affects not only those brain regions that are most engaged in attention, memory, and executive functions but also that it is not a diffuse process but selectively expressed in these areas.

The classification results also uncover evidence to the physiological relevance of these entropy changes. ApEn-based feature-supported vector machine classifiers successfully differentiating between the younger and older subjects with an accuracy of over 90% in most cases and an accuracy of 93% after feature selection which was the highest achieved value. The strong predictive power at an individual level demonstrates that the identified alterations are consistent and robust, thus the changes identified can capture the most important aspects of the brain's electrical activity which are related to chronological age.

Summing up, these findings present healthy aging as a vibrant and intricately reorganized brain network pattern. The simultaneous presence of increased variability in slower oscillations and decreased complexity in faster ones could be the brain's attempt to keep a proper balance between flexibility and efficiency: when the precision of local high-frequency circuits is diminished, the system may take the role of broader slower rhythms to support not only stable cognition but also behaviour. Thus, the entropy profile observed in this case is not simply a sign of decay but rather evidence of an adaptive strategy with which the brain reorganizes its activity to functionally preserve even when structural and metabolic changes coexist. The very fact that these entropy measures can so well discriminate the elderly from the young implies that ApEn might be a potential biomarker for monitoring the normal aging trajectory, thereby offering insight into the brain's resource reallocations for maintaining cognitive performance throughout life.

STUDY 3

ELECTROENCEPHALOGRAPHIC COMPLEXITY AND COGNITIVE DECLINE: INSIGHTS FROM APPROXIMATE ENTROPY ACROSS AGING AND DEMENTIA [In preparation]

Alessia Cacciotti, *Anna Fabbrocino, Chiara Pappalettera, Franca Deriu, Paolo Maria Rossini, Fabrizio Vecchio. In preparation*

OBJECTIVE

This study aimed to investigate alterations in electroencephalographic (EEG) signal complexity across the continuum from healthy aging to Mild Cognitive Impairment (MCI) and Alzheimer's Disease (AD). Specifically, changes in Approximate Entropy (ApEn) within the total EEG spectrum and across the main EEG frequency bands was evaluated, as well as their associations with cognitive and functional performance. Furthermore, the discriminative potential of ApEn features was evaluated using a Random Forest classifier combined with Recursive Feature Elimination (RFE) to distinguish between Healthy Elderly, MCI, and AD participants. By integrating group-level comparisons, machine learning classification, and neuropsychological correlations, the study aimed to identify frequency- and region-specific entropy patterns that may serve as electrophysiological markers of cognitive decline and support early diagnosis and clinical stratification.

ABSTRACT

Physiological aging involves gradual modifications of brain activity patterns (including the electric one), sometimes leading to pathological outcomes. Understanding changes in EEG brain signal complexity from healthy aging to MCI and AD may provide insights into cognitive decline and support early diagnosis. EEG data were collected from 269 participants divided into three groups: Healthy Elderly (n = 109), MCI (n = 75), and AD patients (n = 85). Approximate Entropy (ApEn) was computed for the Total EEG Spectrum and frequency bands.

A Random Forest classifier with a One-vs-One strategy and Recursive Feature Elimination (RFE) was used for group discrimination. In parallel, group comparisons and correlations with neuropsychological scores were performed to further investigate the functional relevance of these entropy changes by assessing their association with cognitive and functional performance. Significant group differences in Total ApEn were found, particularly in central brain regions, with progressive decreases from Healthy Elderly to MCI and AD. Frequency-specific patterns emerged: (i) Delta ApEn was increased in AD across the scalp; (ii) Alpha 1 ApEn showed frontal decreases and occipital increases in AD, whit MCI intermediate pattern; (iii) Gamma ApEn was markedly reduced in AD compared to both Healthy Elderly and MCI, showing central and frontal localization, and extending to occipital regions when comparing MCI to AD.. The classifier achieved 66.9% accuracy, with sensitivities of 80.73% (Healthy Elderly), 42.67% (MCI), and 70.59% (AD), and specificities of 79.12%, 89.18%, and 85.39% respectively. Positive correlations were found between ApEn and cognitive scores in both the Total EEG Spectrum and Gamma band, conversely, Delta and Alpha1 ApEn showed negative correlations with cognitive and functional scores.

The distinct entropy patterns observed across frequency bands and scalp/brain regions may contribute to developing more refined and objective tools for early diagnosis and clinical stratification.

METHODS

Participants

A total of 269 individuals took part in the study: 109 Healthy Elderly (58 females; mean age = 72.5 ± 1.6 years; education = 13.5 ± 0.4 years), 75 MCI participants (51 females; mean age = 74.4 ± 1.1 years; education = 12.0 ± 0.9 years), and 85 AD patients (59 females; mean age = 74.3 ± 1.5 years; education = 12.9 ± 0.8 years). The three groups were comparable in age and education, though not fully balanced for sex. Healthy Elderly were required to be ≥60 years old and free from neurological, psychiatric, or sleep disorders (screened using the Pittsburgh Sleep Quality Index). AD patients were aged ≥60 years and diagnosed according to NIA–AA clinical core criteria. Exclusion criteria for AD included psychosis, genetic or metabolic diseases, other neurological conditions, and any uncompensated medical illness or substance abuse potentially affecting cognition or mood. MCI inclusion criteria comprised objective memory impairment, preserved daily autonomy (IADL score), and a Clinical Dementia Rating of 0.5. Exclusion criteria were absence of memory deficits, diagnosis of dementia, extrapyramidal signs,

psychiatric or neurological disorders, substance abuse, cognitive-enhancing medications, or severe medical conditions.

All participants were right-handed, as verified by the Handedness Questionnaire [227]. The study adhered to the Declaration of Helsinki and the World Medical Association's ethical principles (1997) and received approval from the IRCCS San Raffaele Roma Ethics Committee. Written informed consent was obtained from all participants.

Neuropsychological Assessment

All participants underwent an extensive neuropsychological evaluation assessing both global and domain-specific cognition. General cognitive function was measured using the Mini-Mental State Examination (MMSE) and the Addenbrooke's Cognitive Examination (ACE), providing complementary assessments of orientation, attention, memory, language, fluency, and visuospatial skills.

Functional autonomy was evaluated using the Instrumental Activities of Daily Living (IADL) scale and its quantitative version (IADL-Q). Executive and attentional functions were assessed with the Digit Symbol Substitution Test (DSST), targeting processing speed and sustained attention.

Mean ± SE scores for all cognitive and functional measures across groups (Healthy Elderly, MCI, and AD) are summarized in Table 5.

	MMSE	*ACE_R*	*ADL*	*A-IADL-Q*	*DSST*	*ACER_AO*	*ACER_ME*	*ACER_FL*	*ACER_LIN*	*ACER_VS*
Healthy Elderly	29.4±0.1	92.9±0.5	5.9±0.0	8.0±0.0	42.8±1.0	17.9±0.0	22.4±0.3	11.5±0.2	25.8±0.1	15.1±0.1
MCI	27.7±0.4	83.1±1.6	5.8±0.2	7.6±0.3	29.3±1.7	17.1±0.2	17.8±0.9	9.9±0.4	24.1±0.5	14.2±0.4
AD	19.4±1.0	59.5±2.4	4.6±0.3	1.9±0.5	11.9±1.9	13.8±0.7	9.6±0.9	5.3±0.6	20.2±1.2	10.4±0.6

Table 5. *Mean (± standard error) scores for each cognitive and functional assessment across the three groups: Healthy, Mild Cognitive Impairment (MCI), and Alzheimer's Disease (AD). MMSE refers to the Mini-Mental State Examination, a global measure of cognitive functioning. ACE-R is the Addenbrooke's Cognitive Examination – Revised, a multidomain cognitive screening test, with the following subtests: AO (Attention and Orientation), ME (Memory), FL (Fluency), LIN (Language), and VS (Visuospatial). ADL indicates Activities of Daily Living, assessing basic functional abilities, while A-IADL-Q is the Amsterdam Instrumental Activities of Daily Living Questionnaire, which evaluates complex daily functioning. DSST corresponds to the Digit Symbol Substitution Test, measuring processing speed and attention.*

EEG Acquisition and Preprocessing

EEG signals were recorded using a 61-channel EasyCap (Brain Products) following the 10–20

system, referenced to Fpz. Vertical and horizontal EOGs were monitored to track ocular activity. Electrode impedance was kept below 5 kΩ, and data were sampled at 1000 Hz. Participants completed a 6-minute eyes-closed resting-state session in a sound-attenuated, dimly lit, electrically shielded room.

Preprocessing was performed in MATLAB using EEGLAB [228]. Data were down-sampled to 512 Hz, band-pass filtered between 0.2–47 Hz, and segmented into 2-s non-overlapping epochs. Artifactual epochs were discarded through expert visual inspection, followed by Infomax Independent Component Analysis (ICA) to remove ocular and muscular components. At least 3 minutes of artifact-free EEG data were retained per participant for subsequent analyses.

Entropy Analysis

ApEn was computed for each electrode and frequency band using a custom MATLAB routine. EEG data were filtered into seven canonical bands (Delta 2–4 Hz, Theta 4–8 Hz, Alpha 1 8–11 Hz, Alpha 2 11–13 Hz, Beta 1 13–20 Hz, Beta 2 20–30 Hz, Gamma 30–45 Hz) and for the Total band (0.2–47 Hz) [230]. ApEn values were averaged across epochs to obtain a single entropy score per electrode and band. The algorithm parameters were $m = 2$ and $r = 0.2 \times \text{std}(x)$, where x represents each 2-s epoch. ApEn values ranged from 0 (highly regular) to 2 (maximally irregular) [226].

Scalp topographies were generated by interpolating ApEn values across electrodes, visualizing spatial distributions of EEG complexity and region-specific modulations associated with aging and cognitive decline.

Statistical Evaluation

Pairwise group comparisons (Healthy Elderly vs MCI, MCI vs AD, and Healthy Elderly vs AD) were conducted using two-tailed unpaired Student's t-tests for each electrode and frequency band (Total, Delta, Theta, Alpha 1, Alpha 2, Beta 1, Beta 2, Gamma). An initial significance level of $p < 0.05$ was applied, followed by false discovery rate (FDR) correction for multiple comparisons. Only FDR-corrected p-values below the adjusted threshold were considered significant.

Machine Learning

A Random Forest (RF) classifier was implemented to discriminate among the three groups (Healthy Elderly, MCI, AD). Given the multiclass design, a one-vs-one (OvO) strategy was employed [233]. Feature selection was performed using Recursive Feature Elimination (RFE) with an RF estimator to identify the most informative features while reducing dimensionality.

Model performance was assessed via 5-fold cross-validation [232], and metrics included overall

accuracy, class-specific sensitivity (true-positive rate), and specificity (true-negative rate). This approach minimized overfitting and ensured robust generalization to unseen data.

Correlation Analysis

To explore associations between ApEn and cognitive performance, correlation analyses were conducted across ten regions of interest (ROIs: frontal, central, parietal, temporal, and occipital in each hemisphere) for both Total and frequency-specific bands.

ApEn values within each ROI were averaged across constituent electrodes. Correlation matrices were visualized using a color scale from blue (–1) to red (+1), where only significant correlations were displayed, and brightness reflected significance strength. This approach enabled an intuitive mapping of regional associations between EEG entropy and cognitive functioning across domains and frequency ranges.

RESULTS

ApEn topographical representation

To understand how brain complexity modulates in relation to pathological aging, ApEn has been evaluated in three distinct groups (Healthy Elderly, MCI subjects and AD patients) through EEG Total Spectrum and typical frequency bands. Significant differences between groups were calculated and are presented in Figure 19. The new significance thresholds identified by the FDR correction for each comparison and frequency band are reported in Table 6.

Statistically significant differences in ApEn values among the three groups were identified in the Total EEG spectrum and were visualized using a symmetric matrix representation (Figure 19A). In the comparison between Healthy Elderly and AD patients, the differences continued to predominantly affect the central region and additionally extended to the parietal area. Conversely, no statistically significant differences were found between the MCI and AD groups across any region. These findings likely reflect a progressive decrease in ApEn within the central region, as illustrated by scalp distribution patterns transitioning from Healthy Elderly to MCI subjects, and subsequently to AD patients, within the Total EEG spectrum.

When examining the distinct EEG frequency bands, statistically significant differences emerged specifically within the Delta, Alpha 1, and Gamma bands.

A highly statistically significant result was observed in the Delta frequency band (Figure 19B). The difference in entropy distribution in AD patients is evident across the entire scalp, where an increase in ApEn values is observed compared to the other two groups. However, this

increase is slightly less pronounced when comparing AD patients specifically to the MCI group. In contrast, this group exhibited a slight decrease in ApEn in the frontal regions compared to Healthy Elderly, accompanied by a modest increase in the occipital areas. Consequently, statistical significance was reached only at two electrodes corresponding to these respective areas.

In the Alpha 1 band (Figure 19C), AD patients consistently exhibited an increase in ApEn compared to Healthy Elderly, which, in this case, was confined exclusively to the occipital regions. Conversely, the frontal areas were characterized by a reduction in complexity. This pattern, however, was not observed in MCI subjects, who showed a marked increase in ApEn in the frontal regions relative to both Healthy Elderly and AD patients. Regarding the occipital distribution, MCI group displayed a pattern similar to that of AD patients, though with higher entropy levels compared to Healthy participants. These observed differences culminated in a statistically significant effect localized in the centro-frontal electrodes in the comparison between MCI subjects and AD patients. By contrast, no statistically significant differences were found between Healthy Elderly and MCI subjects in this frequency band.

The final observed difference was identified in the Gamma frequency band (Figure 19D). Statistically significant differences within this band were evident in the comparisons between Healthy Elderly and AD groups, as well as between MCI and AD groups. Specifically, AD patients demonstrated a pronounced reduction in entropy across the entire scalp relative to both Healthy Elderly and MCI subjects. In the comparison between Healthy Elderly and AD subjects, these statistically significant differences were primarily localized to electrodes overlying the central and frontal cortices. Conversely, in the MCI versus AD comparison, significant alterations extended beyond the central and frontal regions to include occipital areas.

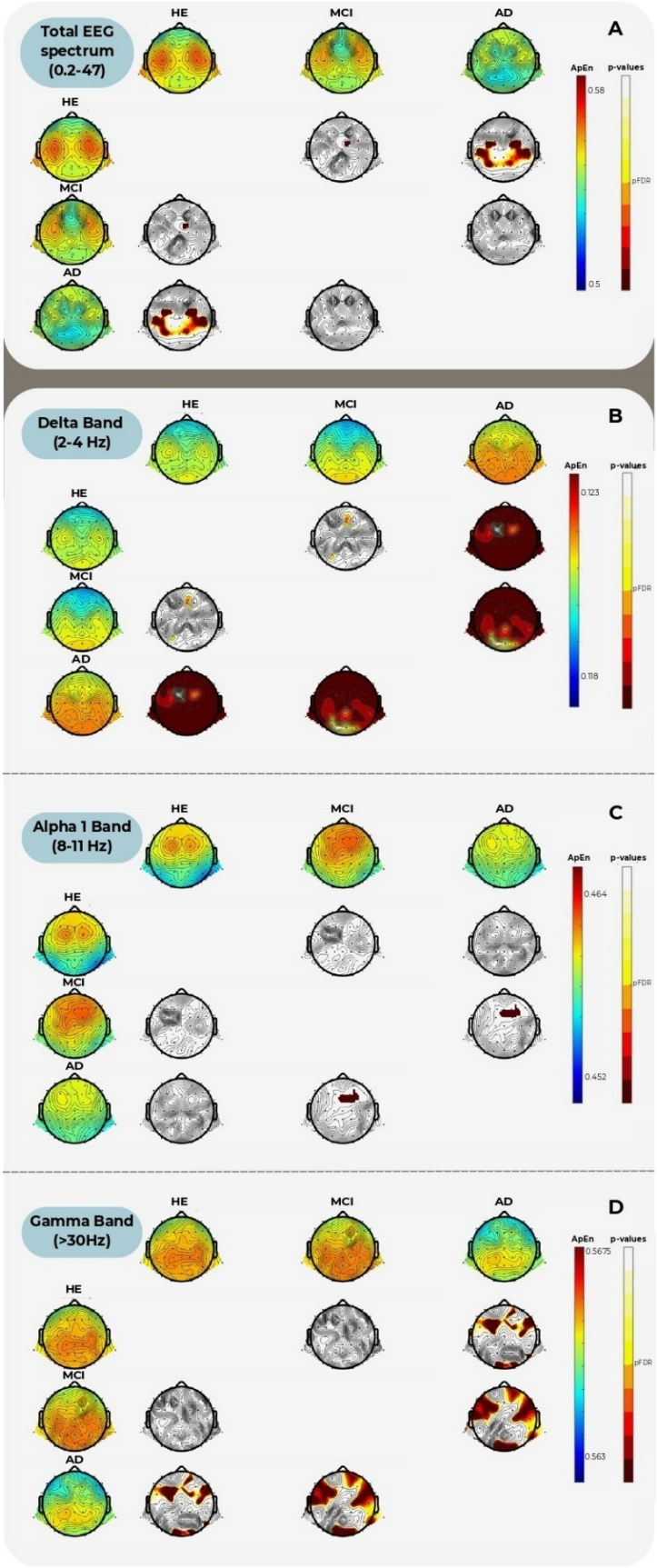

Figure 19. *Topographical maps display the distribution of Approximate Entropy (ApEn) values across the scalp in the three groups (Healthy Elderly, MCI, and AD) for the entire EEG spectrum (0.2-47 Hz) (Figure 19A) and*

for each frequency band: Delta (2–4 Hz) (Figure 19B), Alpha1 (8–11 Hz) (Figure 19C), and Gamma (30–45 Hz) (Figure 19D). Entropy values are color-coded from blue (low entropy/complexity) to red (high entropy/complexity), indicating increasing signal irregularity and complexity. In the central panels of each frequency band section, pairwise group comparisons are shown using FDR-corrected p-values (Healthy vs MCI, Healthy vs AD, MCI vs AD). The p-value maps are color-coded from dark red to white, with the blue–orange scale representing statistically significant comparisons after FDR correction (thresholded at the corrected significance level). For each frequency band, the arrangement of the maps follows a matrix structure where the top row and the lateral column represent the distribution of ApEn values across the scalp in the three groups while each column indicates a different pairwise comparison.

	Healthy Elderly vs MCI	***Healthy Elderly vs AD***	***MCI vs AD***
Total EEG Spectrum	0	0.01209	0
Delta	0	0.04518	0.04590
Theta	0	0	0
Alpha 1	0	0	0.00126
Alpha 2	0	0	0
Beta 1	0	0	0
Beta 2	0	0	0
Gamma	0	0.01204	0.02497

Table 6. *Significance thresholds identified using the False Discovery Rate (FDR) correction for the statistical comparisons between groups (Healthy Elderly vs. MCI, Healthy Elderly vs. AD, and MCI vs. AD) across the different EEG frequency bands. Threshold values are expressed as adjusted p-values after FDR correction. A value of 0 indicates that no significant threshold was identified for that specific comparison and frequency band.*

Machine Learning

For the classification process, a Random Forest model was utilized, trained using a One-vs-One strategy combined with Recursive Feature Elimination (RFE). The selected features (n=18) were: P3_Total, TP10_Total, AF7_Total, Fp1_Delta, Fz_Delta, FC2_Delta, CP1_Delta, FC5_Delta, AF7_Delta, AF8_Delta, Fpz_Delta, P7_Alpha1, CP2_Alpha1, O2_Beta2, Cz_Beta2, FC6_Beta2, FC2_Gamma, FC6_Gamma. The classes were defined as follows: Class 0 comprised Healthy Elderly (N = 109), Class 1 included MCI subjects (N = 75), and Class 2 consisted of AD patients (N = 85). The model achieved class-specific performance metrics as follows: sensitivity (recall) was 80.73% for Healthy Elderly, 42.67% for MCI, and 70.59% for AD patients. Sensitivity was calculated as the ratio of true positives to the sum of true positives and false negatives, corresponding to 88 out of 109 correctly identified Healthy Elderly, 32 out of 75 MCI cases, and 60 out of 85 AD cases. Specificity, defined as the ratio of true negatives to the sum of true negatives and false positives, was approximately 79.12% for Healthy Elderly,

83.19% for MCI, and 85.26% for AD. Overall, the model achieved an accuracy of approximately 66.9%, with 180 correctly classified samples out of a total of 269. The confusion matrix of the classification process is represented in Figure 20.

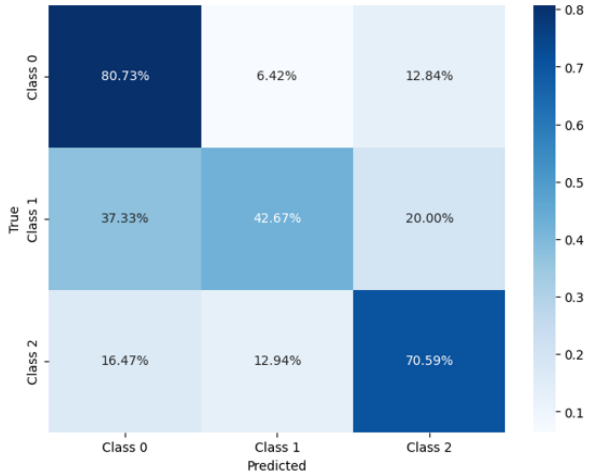

Figure 20. *The figure illustrates the classification performance of a Random Forest model trained using an OvR strategy and RFE-based feature selection on a three-class problem: Class 0 = Healthy Elderly (N = 109), Class 1 = Mild Cognitive Impairment (MCI, N = 75), Class 2 = Alzheimer's Disease (AD, N = 85). The values are presented as percentages of the total number of subjects in each true class (i.e., rows sum to 100%). Diagonal elements indicate correct classifications (true positives for each class), while off-diagonal values indicate misclassifications. Color intensity reflects the proportion of correctly or incorrectly classified instances, with darker shades representing higher percentages.*

Correlation Analysis

Correlational analyses between ApEn values and neuropsychological test scores were conducted within the predefined ROIs for those EEG frequency bands that previously demonstrated statistically significant group differences. The results of the correlation analysis are reported in Figure 21. For the total EEG spectrum ApEn (Figure 21A), significant positive correlations emerged especially between ApEn values in central, parietal, and occipital ROIs and both global cognitive measures (MMSE, ACE) and functional abilities (IADL, IADL-Q). Conversely, Delta ApEn exhibited negative correlations across most ROIs with global cognitive measures (Figure 21B), functional abilities, and several ACE subdomains, indicating that higher delta entropy is associated with poorer cognitive and functional performance. In the Alpha 1 band (Figure 21C), negative correlations were observed in more localized area, involving global cognitive measures, functional abilities, and attentional functions. Gamma ApEn showed widespread positive associations with global cognition and functional abilities (Figure 21D), particularly in frontal and parietal regions.

Overall, these findings suggest that increased total and gamma EEG complexity is associated with better cognitive and functional status, whereas higher delta and reduced alpha 1 entropy appear to reflect cognitive and functional decline.

Figure 21. *The figure illustrates the representation of statistically significant correlations between ApEn and neuropsychological test scores across all participants. Results are shown for the Entire EEG spectrum (Figure 21A), the Delta band (Figure 21B), the Alpha 1 band (Figure 21C), and the Gamma band (Figure 21D). For each*

statistically significant EEG frequency band and cognitive domain, bar plots display the correlation coefficients observed in predefined bilateral regions of interest, grouped by hemisphere (left and right). The representations of the ROIs are reported below, in the following order: frontal, central, parietal, temporal, and occipital, first for the left hemisphere and then for the right hemisphere. Positive correlations are shown in red, and negative correlations in blue, with colour intensity reflecting the strength of the correlation.

DISCUSSION AND CONCLUSION

This study explored alterations in EEG signal complexity, measured through Approximate Entropy (ApEn), across the spectrum from healthy aging to MCI and AD. Overall, ApEn revealed distinct spatial and frequency-specific changes along the continuum of cognitive decline. Total entropy progressively decreased from Healthy Elderly to MCI and AD, mainly over central regions, while frequency-specific analyses showed increased Delta and Alpha 1 entropy and reduced Gamma entropy in AD. By combining features from various frequency bands, the Random Forest classifier managed to reach an overall accuracy of 66.9%, being able to separate Healthy Elderly and AD effectively however, the identification of MCI was made with less accuracy. In the end, the correlational studies showed that the increase in Total and Gamma entropy was linked to improved cognitive and functional scores, whereas the increase in Delta and decrease in Alpha 1 entropy were related to worse performance.

On their own, the findings from this study indicate that brain signal complexity is frequency-dependent and changes drastically during the pathological aging process. The decrease of entropy from the Healthy Elderly to the AD group probably is the global signal of the loss of functional differentiation and neural flexibility. At the same time, the huge increase in Delta entropy all over the brain of the AD group may be interpreted as an indication of abnormal slow-wave activity and loss of inhibitory control, typical for cortical disconnection and compensatory desynchronization mechanisms. The Alpha 1 changes—marked by the decrease in the frontal and the increase in the posterior regions—are in line with the idea of a shift in top-down processing. This shift reflects the transition from efficient, frontally mediated control to less efficient activity that is posteriorly driven. Concerning the Gamma band, there is a very strong reduction of Gamma entropy in AD that spreads from the center to the back of the brain. Since Gamma activity is one of the major brain mechanisms involved in cognitive integration, attention, and memory binding, its reduction may be related to an alteration of fast-scale coordination of neural assemblies and synaptic dysfunction, which ultimately lead to AD. Moreover, the intermediate pattern in MCI, especially the partial preservation of Gamma entropy, might be a reflection of leftover compensatory mechanisms that work to maintain

cognitive performance in the early stages of the disease.
Additionally, machine learning and correlation analysis results highlighted that entropy can be used as electrophysiological biomarkers of cognitive decline. The lower sensitivity concerning MCI class most probably mirrors the clinical and biological heterogeneity of this transitional group, where compensatory and degenerative processes are present simultaneously. However, the high accuracy with which the classifier distinguishes between Healthy Elderly and AD is a clear indication of the high discriminative power of EEG complexity measures.

In conclusion, the current findings showed that EEG entropy constitutes a measure of the ongoing neurophysiological reorganization of the brain that accompanies aging and dementia. Neural frequency-specific patterns—most notably the increase in Delta and decrease in Gamma entropy—reflect two sides of the same coin of the diseased brain: loss of neural capacities and compensatory uptake. These results reinforce the idea of ApEn as a very sensitive, non-invasive marker of the brain's network integrity and point to its possible use for early diagnosis and clinical stratification in neurodegenerative disorders such as Alzheimer’s disease.

CORE PROJECT

INNOVATIVE EEG BIOMARKERS AND AI ALGORITHMS FOR THE EVALUATION OF PHYSIOLOGICAL AND PATHOLOGICAL AGING

ABSTRACT

Both physiological and pathological aging notably lead to functional brain reorganization, which is a natural progress over time. These changes can also be noticed in EEG-based measures such as connectivity, complexity, and network topology. The current study focused on the exploration of the age-related and disease-related variations in the brain physiology of adults across the lifespan and also the continuation of healthy aging to Alzheimer's disease (AD) by advanced signal processing, graph-theoretical metrics, and machine learning approaches.

In the case of normal aging, the neuronal synchronization between various brain regions lowered with age as shown by the frequency-dependent analyses of magnitude-squared coherence (MsCoh) while thinning out the delta, theta, and alpha 2 bands of the EEG spectrum. The decrease in the synchronicity of these bands means that the neural coupling efficiency is less with age. However, the rise in the coherence of the beta band in the senior population suggests that they are also using the compensatory mechanisms to keep the cognitive functions going. Graph-theoretical metrics revealed that the level of small-worldness was enhanced in the higher-frequency bands, thus indicating that the local network can continue with rearrangement to keep up with functional integration. Entropy analyses supported this view of the brain by revealing that the EEG signal complexity reductions in slow and alpha rhythms occurred in most of the brain regions while the increases in theta-band entropy became apparent from the posterior areas—another factor that underscores the brain activity that is compensatory in nature. The machine learning technique that utilized coherence, small-world, and entropy features could tell apart young adults, mature adults, and elderly groups with classification accuracy up to 65% facilitating identification of the electrophysiological signatures of the aging brain.

The results from the study on pathological aging showed that Alzheimer’s Disease (AD)

patients exhibited elevated functional connectivity in the frontal region as a result of hyper-synchronization with hypo-connectivity in the posterior areas across the frequency bands. At the same time, entropy parameters indicated lowered levels of complexity across the most extensive areas of the brain, especially the central and frontal cortices. Mild cognitive impairment (MCI) was characterized by the presence of intermediate and heterogeneous patterns, that is, consistent with the idea of a transitional stage. Correlation analyses showed that synchronization at low frequency (delta/theta) and reduction in entropy were associated with cognitive and functional performance deteriorations, whereas high frequency (gamma) activity and entropy were positively linked with the maintenance of cognition. Integrated machine learning models that utilized features of connectivity, entropy, and network could differentiate Healthy Elderly, MCI, and AD groups with an accuracy of up to 75%, hence local and global EEG markers complementarily contribute to the identification of stages of cognitive decline.

To sum up, these results offer a detailed electrophysiological account of brain aging, thereby reinforcing the idea that physiological and pathological aging entail separate, yet network reorganization processes that interact with each other. The advent of machine learning is instrumental in opening the road towards the use of EEG-based measurements of functional, topological, and complexity domains as biomarkers of cognitive decline.

INTRODUCTION

Brain aging is associated with deep structural and functional changes impinging on neural plasticity, connectivity, and overall activity. These changes reflect not only the physical but also cognitive transformations with time. Among more consistent structural findings, there is a gradual decrease in brain volume, which is due more to neuronal shrinkage than neuronal loss, along with changes in dendritic arborization and synaptic density [27, 31]. Decreased white matter integrity shows up as increased white matter lesions, especially within the frontal lobe, indicating microvascular and myelin changes [234]. These changes do not appear to distribute uniformly throughout the brain: the prefrontal cortex and hippocampus are particularly vulnerable, whereas occipital areas tend to be relative spares [28]. The topography of these changes echoes the cognitive profile of aging, wherein executive functions, memory, and learning abilities are affected more than perceptual or sensory processes.

On a functional level, the aging brain shows several mechanisms of adaptive reorganization in order to maintain performance in response to structural decline. A well-documented finding is the Hemispheric Asymmetry Reduction in Older Adults model, a conceptualization of the tendency of older adults to activate both hemispheres during tasks that are lateralized in younger individuals [48]. It has been debated whether this pattern represents compensatory activation in order to preserve cognitive efficiency or dedifferentiation reflecting reduced neural specificity. None of these functional reorganizations are more representative of how the brain struggles for equilibrium and cognitive reserve-the set of neural resources and compensatory mechanisms that buffer the effects of aging and pathology-on a daily basis [50]. Understanding these processes is essential not only for understanding the biological underpinnings of normal aging but also for differentiating physiological aging from pathological trajectories, such as those leading to neurodegenerative diseases.

Among these conditions, Alzheimer's disease (AD) is the most common cause of dementia among the elderly. It involves a continuous development of loss of memory, a decline in cognition on multiple domains, and daily functioning impairment. Most importantly, neuropathological changes in AD begin many years before the onset of symptoms, and thus, early identification of pre-dementia stages has become a central objective of current research [235]. In this sense, Mild Cognitive Impairment (MCI) reflects a transitional state between normal aging and dementia. Individuals with MCI have objective cognitive deficits-most often in episodic memory-but relatively preserved daily functioning. Longitudinal studies have shown that MCI very often deteriorates to AD, at an annual rate between 10% and 15% [101].

As a consequence, the early detection of MCI will be of basic importance in order to program preventive and rehabilitative strategies, maximize treatment intervention, and reduce health and social costs related to the care of dementia.

A wide range of neuroimaging and electrophysiological techniques—including fMRI, PET, fNIRS, MEG, and EEG—have all been utilized in the research of both physiological and pathological aging. Whereas imaging techniques like fMRI and PET offer very good spatial resolution, they are usually expensive, invasive, and thus unsuitable for large-scale population screening. Conversely, EEG is a low-cost, non-invasive technique with wide availability that measures neural electrical activity directly with high temporal precision. This ability to monitor rapid neural dynamics makes EEG particularly valuable for the study of brain network reorganization and cognitive processing throughout the lifespan. The aging process influences the amplitude and frequency of EEG signals, the synchronization of EEG signals, and the functional connectivity between EEG sources, thus providing measurable indexes of neural efficiency and integrity [205, 236].

Recent advances in computational neuroscience have made it possible to quantify brain connectivity using graph theory as a powerful mathematical framework. In this model, the brain is schematized as a complex network of nodes representing brain regions or electrodes, connected by edges that symbolize functional links between them. Graph theoretical measures such as clustering coefficient, path length, and small-worldness are metrics used to investigate how efficiently the brain integrates and segregates information. EEG-based graph analytical studies have indicated that aging operates on the modulation of brain network organization by shifting the topology toward a less integrated and more segregated one. For instance, Vecchio and colleagues (2014 [237]) showed a greater small-worldness in the alpha band and higher path length in lower frequency bands in old age, indicating a less integrated and more modular architecture. Pathological aging, as in the case of AD, has been associated with a breakdown of the network architecture characterized by reduced clustering coefficients and reduced small-worldness in alpha and beta bands, and its compensatory increase in low-frequency connectivity, such as delta and theta [238]. Such findings point to the progressive disorganization of the brain's communicational system that runs parallel to the course of cognitive decline and loss of neural integration.

Complementary approaches for studying neural dynamics include those that are based on entropy analyses, aimed at quantifying the complexity or regularity of EEG signals. Entropy reflects a measure of brain activity unpredictability and has been suggested as an index of neural

adaptability and cognitive flexibility. According to the Entropic Brain Hypothesis, higher entropy corresponds to the richness of mental states and higher dynamical variability within neural networks [239]. Measures such as Approximate Entropy, Sample Entropy, and Multiscale Entropy have been used on EEG data with the aim of evaluating how brain complexity has to change with age. Indeed, physiological aging tends to be accompanied by higher values of entropy in central and posterior regions of the scalp, reflecting a reduced synchrony of neural activity, with more chaotic characteristics due to synaptic loss and decreased connectivity [216]. However, in pathological aging, such as AD, entropy findings are related to lower complexity and rigidity in neural dynamical behaviour, pointing toward a correlation with the inability of information processing and network dysfunction [240, 241]. Although results are sometimes inconsistent, these measures provide extremely valuable insights into the nonlinear nature of the aging process of the brain and into the identification of physiological and pathological features.

All these neurophysiological markers are integrated with Artificial Intelligence (AI) and have opened new ways of understanding and predicting brain aging. AI, and particularly Machine Learning (ML), enables complex, nonlinear pattern identification within large and multidimensional datasets, which can be used in developing predictive models for brain health. One of the most important and relevant applications of such an approach is the so-called "brain age prediction," which tries to estimate an individual's biological brain age based on neuroimaging or EEG features [242]. Deviations between predicted brain age and chronological age-the brain age gap-can signal accelerated or delayed brain aging and may work as early biomarkers of cognitive decline. Connectivity and entropy parameters could be combined in an EEG-based model of brain age that enables the identification of individuals at risk of developing MCI or AD, aids clinical decision-making, and monitors the efficacy of interventions [243] Clemente et al., 2021; Engemann et al., 2020. These approaches also contribute to a broader understanding of brain reserve and resilience, emphasizing individual variability in neural aging trajectories.

Following this rationale, the project intended to provide a clear picture of the next-generation EEG biomarkers that can decisively delineate physiological aging from a pathological one. To exemplify, this study focused on the extraction of quantitative features from EEG signals. It involved the usage of graph theoretical indices and entropy measures, which were further linked with clinical parameters for creating predictive models of brain aging with the help of artificial intelligence algorithms. These models served as a basis for individual brain age estimation and

facilitated subject classification into healthy, MCI, and AD categories. Consequently, the research's final objective was the identification of the earliest changes before the onset of obvious symptoms, thus enabling the personalization of therapeutic and prognostic strategies.

In order to achieve the above objectives, 200 participants were enrolled in the study and assigned to five experimental groups as follows: 40 young adults (Young), 40 middle-aged adults (Adult), 40 healthy elderly individuals (Healthy Elderly), 40 subjects suffering from Mild Cognitive Impairment (MCI), and 40 patients diagnosed with Alzheimer's disease (AD). e. Furthermore, additional data from existing databases were included, leading to a total of 109 healthy elderly individuals, 75 MCI patients, and 85 AD patients. All participants underwent resting-state EEG recording with eyes closed. Besides, the neuropsychological assessment involved such tests as Mini-Mental State Examination (MMSE), Addenbrooke's Cognitive Examination (ACE-R), Instrumental Activities of Daily Living (IADL), and Digit Symbol Substitution Test (DSST) for elderly, MCI, and AD groups.

Connectivity, graph theory and entropy indexes from EEG data were computed and then used as features in the implementation of two machine learning models that aimed at estimating brain age in healthy participants and distinguishing between physiological and pathological aging. The accuracy of the models and the leading features used were detected, and finally, these features were evaluated for their potential to serve as biomarkers. Thus, the project deepened the understanding of aging's neurophysiological mechanisms and paved the way to the creation of easy-to-use methods that could revolutionize early-stage identification and timely intervention in neurodegenerative diseases.

METHODS

Participants

The sample comprised 349 participants. Of these, 200 participants were newly enrolled and assigned to five experimental groups as follows: 40 young adults (Young), 40 middle-aged adults (Adult), 40 healthy elderly individuals (Healthy Elderly), 40 subjects suffering from Mild Cognitive Impairment (MCI), and 40 patients diagnosed with Alzheimer's disease (AD). Additional data from existing databases were included, leading to a final total of 109 healthy elderly individuals, 75 MCI patients, and 85 AD patients. Participants were selected by applying both specific inclusion and exclusion criteria in order to make the sample as homogeneous as possible, thereby reducing most of the potentially confounding factors. After signing the informed consent forms, all subjects were allowed to take part in this research, which was

performed according to the Declaration of Helsinki and approved by the local Ethics Committee.

Control participants' inclusion criteria were having an age between 18 and 90 years, with the ability to give informed consent and adequate understanding of the instructions of tasks. Findings from neurological and psychiatric diseases and all other major comorbid medical conditions were part of the exclusion criteria.

Inclusion criteria for the MCI group consisted of objectively verified memory impairment, as determined by standardized neuropsychological assessment; preservation of activities of daily living and independent functioning, as evaluated by the Instrumental Activities of Daily Living (IADL) questionnaire; and CDR score equal to 0.5. These patients were excluded in the presence of unmeasurable deficits in memory, when extrapyramidal symptoms were present, other forms of dementia existed (such as frontotemporal, vascular, or reversible dementias), psychiatric disorders, intake of medications known to interfere with cognitive functions could be evidenced, and current and previous systemic diseases that were or remained uncontrolled, as well as those suffering a traumatic brain injury.

For the AD group, Inclusion criteria included a clinical diagnosis of AD based on NIA–AA workgroups and DSM-IV-TR. Exclusion criteria include other dementia syndromes, such as frontotemporal dementia, behavioural variants of frontotemporal dementia, vascular dementia, extrapyramidal syndromes, reversible dementias (including pseudodementia of depression), and Lewy body dementia.

This was done to control for demographic effects, matching all groups as far as possible by gender and education. Table 7 summarises the demographic details of the participants expressed as mean values and standard errors.

	n	***Gender (M/F)***	***Age***	***Education***
Young	40	16/24	29.3±0.7	17.8±0.4
Adult	40	23/17	53±0.9	15.7±0.6
Healthy Elderly	109	19/21	73.3±0.42	10.1±1.5
MCI	75	18/22	74.4±1.04	11.6±1.4
AD	85	21/19	75.9±1.1	10.9±1.2

Table 7. Demographic details expressed as *mean ± standard error across the five groups: Young, Adult, Healthy, Mild Cognitive Impairment (MCI), and Alzheimer's Disease (AD).*

All participants were righthanded, as determined by the Handedness Questionnaire [227]. The

study protocol adhered to the Declaration of Helsinki and the World Medical Association's ethical guidelines (1997) and it was approved by the Local Ethical Committee (IRCCS San Raffaele Roma). All individuals provided written informed consent prior to participation.

The healthy elderly participants, MCI subjects, and AD patients underwent a neuropsychological assessment aimed at evaluating both global cognitive functioning and specific cognitive domains. This comprehensive evaluation allowed for a detailed characterization of each individual's cognitive profile. In particular, to assess general cognitive functioning, participants were administered standard screening tools such as Mini-Mental State Examination (MMSE) [97] and the Addenbrooke's Cognitive Examination (ACE) [244]. The MMSE provided a quick overview of overall cognitive status, including orientation, attention, memory, and language abilities. The ACE offered a more in-depth cognitive profile, covering attention, memory, verbal fluency, language, and visuospatial processing. In addition, the Instrumental Activities of Daily Living (IADL) and its quantitative version (IADL-Q) were administered to assess functional autonomy in daily life. These tools evaluate the ability to perform complex everyday tasks providing an objective measure of functional independence and its potential relationship with cognitive decline. Executive functions and attention were explored using a range the Digit Symbol Substitution Test (DSST) [99] assessed processing speed, sustained attention, and visual-motor coordination.

The mean (± standard error) scores for each cognitive and functional assessment across the three groups (Healthy Elderly, MCI, and AD) are reported in Table 8.

	MMSE	ACE_R	ADL	A-IADL-Q	DSST	ACER_AO	ACER_ME	ACER_FL	ACER_LIN	ACER_VS
Healthy Elderly	29.4±0.1	92.9±0.5	5.9±0.0	8.0±0.0	42.8±1.0	17.9±0.0	22.4±0.3	11.5±0.2	25.8±0.1	15.1±0.1
MCI	27.7±0.4	83.1±1.6	5.8±0.2	7.6±0.3	29.3±1.7	17.1±0.2	17.8±0.9	9.9±0.4	24.1±0.5	14.2±0.4
AD	19.4±1.0	59.5±2.4	4.6±0.3	1.9±0.5	11.9±1.9	13.8±0.7	9.6±0.9	5.3±0.6	20.2±1.2	10.4±0.6

Table 8. *Mean (± standard error) scores for each cognitive and functional assessment across the three groups: Healthy, Mild Cognitive Impairment (MCI), and Alzheimer's Disease (AD). MMSE refers to the Mini-Mental State Examination, a global measure of cognitive functioning. ACE-R is the Addenbrooke's Cognitive Examination – Revised, a multidomain cognitive screening test, with the following subtests: AO (Attention and Orientation), ME (Memory), FL (Fluency), LIN (Language), and VS (Visuospatial). ADL indicates Activities of Daily Living, assessing basic functional abilities, while A-IADL-Q is the Amsterdam Instrumental Activities of Daily Living Questionnaire, which evaluates complex daily functioning. DSST corresponds to the Digit Symbol Substitution Test, measuring processing speed and attention.*

EEG Recording and Preprocessing

Continuous EEG was recorded using a 61electrode cap (EasyCap GmbH, Brain Products) configured according to the international 10–20 system, with Fpz serving as the reference. Vertical and horizontal electrooculogram (EOG) channels monitored eye movements and blinks. Electrode impedances were maintained below 5 kΩ, and signals were digitized at 1000 Hz. Each subject underwent a 6 minutes eyes-closed resting state session while seated comfortably in an electrically shielded, sound attenuated, dimly lit chamber. Raw data were imported into a custom MATLAB pipeline utilizing EEGLAB toolbox [228]. The recordings were down-sampled to 512 Hz and bandpass filtered between 0.2 and 47 Hz using a finite impulse response (FIR) filter. Continuous data were then segmented into nonoverlapping 2second epochs. Artefactual epochs contaminated by muscle noise, cardiac signals, or other abnormalities were first discarded through expert visual inspection. Subsequent artifact correction and removal were performed via Infomax independent component analysis (ICA), which isolates and eliminates components associated with nonneural artifacts [210]. Following these cleaning steps, at least 3 minutes of artifact free EEG data remained per participant for further analysis.

Magnitude Squared Coherence

EEG functional connectivity was assessed through the computation of magnitude-squared coherence (MsCoh), which quantifies the degree of synchronization between pairs of EEG signals across different frequency bands. This parameter provides a value ranging from 0 (no coherence) to 1 (maximum coherence), indicating the strength of the functional coupling between two signals. Connectivity analysis was performed using custom MATLAB scripts developed in-house [245]. The magnitude-squared coherence values were then used as weights to construct the hemispheric brain networks. MSCoh values were computed in the main EEG frequency bands, i.e., Delta (2–4 Hz), Theta (4–8 Hz), Alpha 1 (8–11 Hz), Alpha 2 (11–13 Hz), Beta 1 (13–20 Hz), Beta 2 (20–30 Hz), and Gamma (30–45 Hz) [246].

Total Coherence

To characterize the global functional connectivity, the Total Coherence (TotCoh) index was computed for each hemisphere and frequency band, following established procedures. Specifically, for each frequency band—Delta (2–4 Hz), Theta (4–8 Hz), Alpha 1 (8–11 Hz), Alpha 2 (11–13 Hz), Beta 1 (13–20 Hz), Beta 2 (20–30 Hz), and Gamma (30–45 Hz)—the coherence of each electrode was calculated as the average of its coherence values with all other electrodes. These electrode-specific coherence values were then averaged across all nodes of a hemisphere to obtain the TotCoh, which represents a global measure of hemispheric functional

coupling [247]. Higher TotCoh values indicate a greater degree of synchronization within the hemispheric network, while lower values reflect reduced functional integration.

Graph theory analysis

Subsequently, graph theory analysis was applied to describe the topological organization of EEG-derived functional networks. Electrodes were considered as nodes of a network in this framework, and edges weighted in accordance with the MsCoh values represented the interconnections of the nodes. The obtained networks were the representation of undirected and weighted graphs that made it possible to assess not only the local but also the global properties of brain connectivity [245].

Besides that, it was possible to derive from the graphs two main parameters: the weighted clustering coefficient (C_w), expressing network segregation or local connectedness, and the weighted path length (L_w), indicating network integration or the network's global information transfer capability. These indices were estimated for each hemisphere and frequency band separately. In every frequency band, for each individual, C_w and L_w values were divided by the average of these parameters obtained across all bands in order to reduce inter-band variability. After that, the Small-World (SW) coefficient was calculated as the proportion between the normalized C_w and L_w values in each frequency band [248]. SW is a parameter that reflects the trade-off between the local specialization and global integration and thus characterizes the efficiency and the organization of brain functional networks. SW values were computed in the main EEG frequency bands, i.e., Delta (2–4 Hz), Theta (4–8 Hz), Alpha 1 (8–11 Hz), Alpha 2 (11–13 Hz), Beta 1 (13–20 Hz), Beta 2 (20–30 Hz), and Gamma (30–45 Hz) [210].

Entropy analysis

To quantify the complexity of the EEG signals, Approximate Entropy (ApEn) was computed for each participant, electrode, and frequency band using a MATLAB routine. EEG data were first filtered into seven canonical frequency bands: Delta (2–4 Hz), Theta (4–8 Hz), Alpha 1 (8–11 Hz), Alpha 2 (11–13 Hz), Beta 1 (13–20 Hz), Beta 2 (20–30 Hz), and Gamma (30–45 Hz) [229]. For each 2-second epoch and for every channel, ApEn was calculated, generating a time-resolved series of entropy estimates for each frequency range. These per-epoch values were then averaged to obtain a single ApEn value for each electrode within each frequency band.

To ensure comparability with previous studies, the same procedure was also applied to the broadband EEG signal (0.2–47 Hz), yielding Total-band ApEn values that reflect the overall complexity of the entire signal. In this framework, ApEn provides a dimensionless score

ranging from 0 (highly regular, predictable signal) to 2 (maximally irregular, unpredictable signal), with higher values indicating greater signal complexity and reduced synchronization [230]. The algorithm was governed by two key parameters: the embedding dimension (m) and the tolerance (r). MATLAB's default parameters were adopted, applying the computation to each 2-second epoch under analysis.

AI Algorithms

To investigate the potential of EEG-derived features in distinguishing between different stages of physiological and pathological aging, two supervised machine learning classification problems were addressed. The first aimed to discriminate between physiological aging groups (Young, Adult, and Healthy Elderly), while the second focused on pathological aging (Healthy Elderly, MCI, and AD).

For each classification task, several sets of features were extracted and analysed independently to evaluate their discriminative power. Specifically, the following feature sets were considered:

1. Total Coherence (TotCoh) values computed within ten regions of interest (ROIs)—central, frontal, parietal, temporal, and occipital areas of both hemispheres;
2. Small-World (SW) coefficients derived from graph theory analysis;
3. Approximate Entropy (ApEn) values computed channel-by-channel as an index of neural complexity; and
4. A combined feature set, integrating all of the above measures (TotCoh, SW, and ApEn) to capture complementary aspects of functional connectivity, network topology, and signal complexity.

The classifier pipeline was implemented in Python with scikit-learn libraries. The data preprocessing included the removal of empty columns, the transformation of categorical variables into numeric codes, and the imputation of missing values using the KNN Imputer with five neighbors. Then, feature matrix X and class labels y were standardized by StandardScaler and MinMaxScaler to compare different features in a comparable way for different numerical ranges [249].

A range of supervised classifiers was trained and compared: Support Vector Machines with linear, polynomial (quadratic), and radial basis function kernels, Logistic Regression, ensemble learning methods like Random Forest, AdaBoost, and Gradient Boosting. Multiclass classification has been carried out adopting both One-vs-Rest and One-vs-One strategies [250]. In this respect, in order to maximize the number and quality of features, several feature selection techniques were tried: SelectKBest with ANOVA F-test and chi-square scoring function, and

RFE with Linear SVM and Random Forest estimators. The performed feature selection tested, in an iterative process, different subsets of features in a k range from 2 to 20 [251].

Performances were estimated with the 5-fold Stratified Cross-Validation scheme to ensure class balance across folds and robust generalization performance. For each setup-classifier, selection method, and feature set-the following three main performance metrics were computed: accuracy, sensitivity (recall), and specificity, using custom scoring functions. Additionally, confusion matrices are created for a visual assessment of class-wise classification performance. After exhaustive comparison of all the tested models and feature selection strategies, the classifier that reached the best overall performance-in terms of balanced accuracy, sensitivity, and specificity-was selected as an optimal model for each classification task. This systematic approach allowed them to get the most informative EEG features and machine learning configurations best suited to the characterization and differentiation of both physiological and pathological brain aging trajectories.

Statistical Analyses

The coherence analysis was performed by pairs, among the groups representing physiological aging: Young versus Adult, Adult versus Healthy Elderly, and Young vs Healthy Elderly and among those that represent pathological aging: Healthy Elderly versus MCI, Healthy Elderly vs AD, and MCI versus AD. Besides, these analyses were separately done for each frequency band: Total, Delta (2–4 Hz), Theta (4–8 Hz), Alpha 1 (8–11 Hz), Alpha 2 (11–13 Hz), Beta 1 (13–20 Hz), Beta 2 (20–30 Hz), and Gamma (30–45 Hz). For every electrode pair and frequency band, statistical differences between groups were assessed by two-tailed unpaired Student's t-tests. A preliminary threshold of statistical significance was considered as $p < 0.05$. In order to correct for multiple comparisons among electrodes and frequency bands, a Bonferroni correction was performed, and only results with adjusted p-values below the corrected threshold were considered statistically significant.

In order to aid result interpretation, visual representations of magnitude-squared coherence (MsCoh) were derived for each of the six bands of frequency and every experimental group. Topographical presentations displayed the information in the form of a matrix, which allowed for quick visual comparison of the three physiological aging groups and the three pathological aging groups. MsCoh values vary between 0 and 1 and are represented on a continuous color scale, extending from white (0, no coherence) to red (1, maximum coherence). In addition, to establish the direction and extent of the differences between the groups, pairwise difference maps (e.g., Young - Healthy Elderly) were generated for each frequency band. These were

color-coded from blue (reduced coherence) via red (increased coherence), with the statistically significant effects colored from orange via dark red.

The entropy analysis included similar pairwise comparisons between the same groups (i.e., Young, Adult, and Healthy Elderly, or Healthy Elderly, MCI, and AD), done separately for each frequency band: Total, Delta, Theta, Alpha 1, Alpha 2, Beta 1, Beta 2, and Gamma. Group differences for all electrodes and frequency bands were determined by two-tailed unpaired Student's t-tests. The significance level was set at $p < 0.05$, while controlling for the false discovery rate (FDR) in multiple comparisons. Only those results for which p-values were below the adjusted FDR threshold were considered statistically significant. To evaluate the spatial organization of EEG complexity, ApEn scalp topographies were generated by interpolating the entropy values between electrodes to create continuous spatial maps. This makes it possible to locate regional modulations of EEG complexity due to both physiological and pathological aging, thus providing a supplementary view to functional connectivity and an in-depth understanding of the neural dynamics underlying cognitive decline.

For the SW metrics, a mixed-model ANOVA was conducted with group (Young, Adult, Healthy Elderly, or Healthy Elderly, MCI, and AD) as a between-subject factor and frequency band (Delta, Theta, Alpha 1, Alpha 2, Beta 1, Beta 2, Gamma) as a within-subject factor. Post hoc tests were compared by Duncan's multiple comparisons if significant main effects or interactions were detected. Thus, the modeling approach employed here made it possible to first of all specify frequency and secondly to pinpoint certain groups for which the small-world network organization modulations associated with aging and neurodegeneration were evident.

Correlation Analysis

In addition to the group-level comparisons, a correlation analysis was performed to investigate the relationship between EEG-derived measures and neuropsychological performance in the pathological aging groups (Healthy Elderly, MCI, and AD). This analysis was not conducted in healthy young and adult participants, as the full neuropsychological assessment was only available for the clinical population. Correlations were computed using both Total Coherence (TotCoh) and Approximate Entropy (ApEn) values, each averaged across ten predefined regions of interest (ROIs). These ROIs included five anatomically defined cortical areas in each hemisphere—frontal, central, parietal, temporal, and occipital—for both the left and right sides of the brain. The analyses were done independently for the Total EEG spectrum as well as for each canonical frequency band (Delta, Theta, Alpha 1, Alpha 2, Beta 1, Beta 2, and Gamma).

The decision to carry out the correlation analysis at the ROI level instead of single electrodes

was influenced by both methodological and interpretative reasons. Since the aim was to investigate the correlations between electrophysiological measures and cognitive domains, it was deemed more significant to look at the combined activity of functionally and anatomically coherent cortical regions rather than the variability of individual electrodes. In each ROI, ApEn and TotCoh values were obtained by averaging the corresponding measures across all electrodes belonging to that region.

In order to make the interpretation easier and to emphasize the spatial patterns, the representations of the correlations in matrix form were created. For each frequency band, a correlation matrix was constructed with a continuous color scale going from blue (–1) to red (+1), denoting the direction and strength of the correlation between EEG metrics (TotCoh or ApEn) and neuropsychological scores. Only statistically significant correlations were shown. The intensity of the color represented the level of the statistical significance, with the lighter shades indicating stronger correlations. This method offered a straightforward way of visualizing the spatial distribution of brain–behaviour relationships. It helped to understand regional functional connectivity and signal complexity relation with cognitive performance across the pathological aging continuum.

RESULTS

PHYSIOLOGICAL AGING

1. Functional connectivity analysis

Topographical maps of magnitude-squared coherence (MsCoh) across frequency bands revealed distinct patterns of age-related modulation in functional connectivity (Figure 22, Figure 23). Only connections with a statistical *Bonferroni corrected p-values<0.05* were reported. No significant differences emerged when comparing the Young and Adult groups, indicating stable coherence values during early and middle adulthood. Nevertheless, significant changes based on statistics were found between younger and elderly people in many frequency bands, such as delta (2–4 Hz), theta (4–8 Hz), alpha 2 (11–13 Hz), beta 1 (13–20 Hz), and beta 2 (20–30 Hz).

The elderly group, in the delta and theta frequency bands, showed significantly lower coherence levels than the young group, especially in the rear cortical areas, which might reflect less large-scale synchronization of slow oscillatory activity in the brain of aged individuals. The decrease in functional connectivity also moved to the frontal areas in the alpha 2 band, revealing that the elderly had disrupted integrative processes normally facilitated by higher-frequency alpha

rhythms.

Overall, the observed pattern suggests a frequency-dependent decrease in inter-regional coherence with advancing age, predominantly involving posterior and frontal areas. These findings support the hypothesis of a progressive decline in neural coupling efficiency during physiological aging, consistent with previous evidence of reduced large-scale functional integration in elderly brains.

In the higher frequency ranges, corresponding to the Beta 1 (13–20 Hz) and Beta 2 (20–30 Hz) bands, no significant differences were observed between the Young and Adult groups, confirming that functional connectivity remains relatively stable through middle adulthood. However, when comparing the Elderly to the Young group, a distinct pattern of increased long-range coherence emerged. Specifically, the Elderly group exhibited stronger connectivity between frontal and posterior cortical regions, suggesting compensatory recruitment mechanisms aimed at maintaining cognitive efficiency despite age-related neural decline.

This enhancement of beta-band coherence may reflect greater reliance on higher-frequency oscillatory synchronization to preserve global communication efficiency within distributed brain networks. Such findings align with the notion of functional reorganization in the aging brain, whereby increased beta connectivity compensates for the loss of lower-frequency coupling observed in slower oscillatory bands.

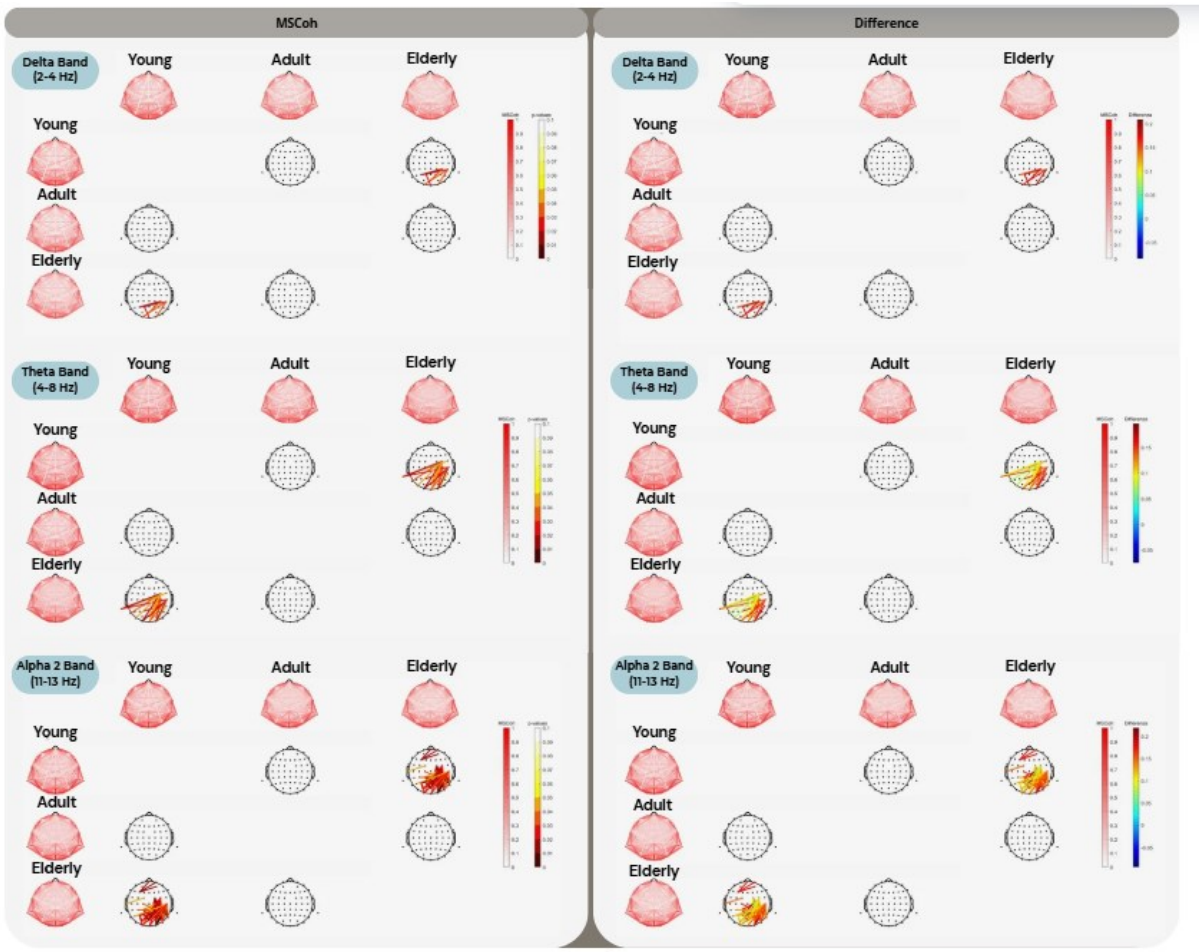

Figure 22. *Topographical representation of magnitude-squared coherence (MsCoh) across frequency bands and experimental groups. Topographical maps display the spatial distribution of MsCoh values for each EEG frequency band (Delta: 2–4 Hz; Theta: 4–8 Hz; Alpha 1: 8–11 Hz) and for each group, allowing visual comparison across the physiological aging continuum (Young, Adult, and Healthy Elderly).*

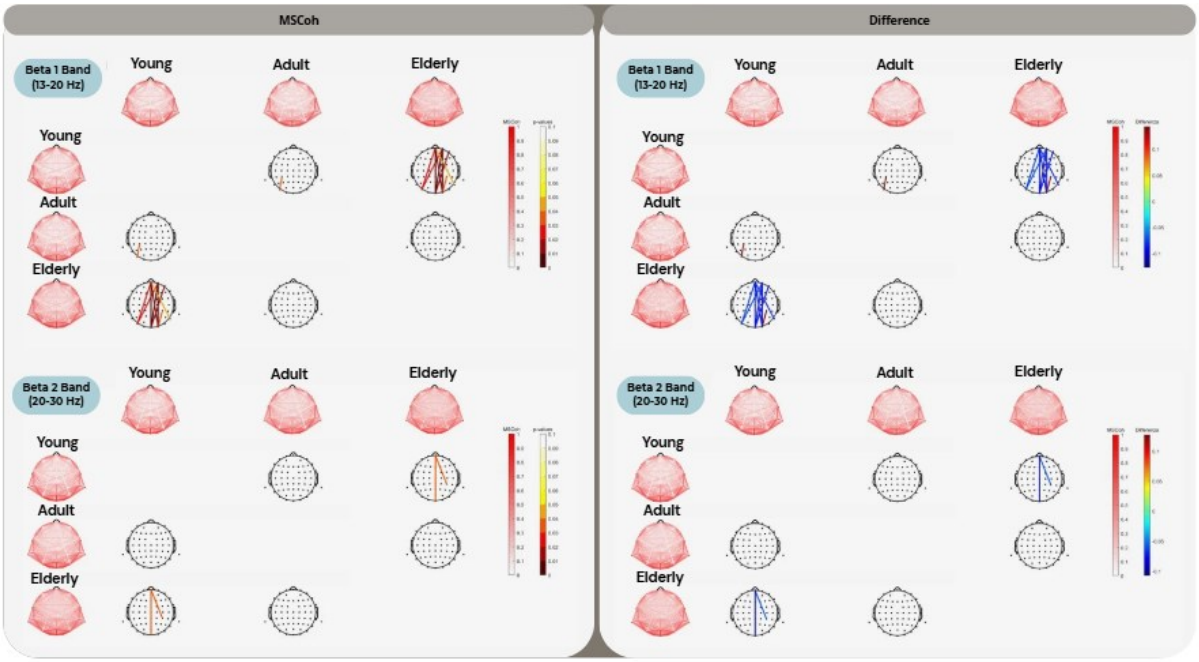

Figure 23. *Topographical representation of magnitude-squared coherence (MsCoh) across frequency bands and experimental groups. Topographical maps display the spatial distribution of MsCoh values for each EEG frequency band (Beta 1: 13–20 Hz; Beta 2: 20–30 Hz) and for each group, allowing visual comparison across the physiological aging continuum (Young, Adult, and Healthy Elderly).*

1.1. Machine learning algorithm

For the classification of physiological aging, the Total Coherence (TotCoh) values across seven EEG frequency bands (Delta, Theta, Alpha 1, Alpha 2, Beta 1, Beta 2, and Gamma) and ten regions of interest (ROIs: frontal, central, parietal, temporal, and occipital areas in both hemispheres) were used as input features. A Support Vector Machine (SVM) model with a Radial Basis Function (RBF) kernel was selected as the optimal classifier. The model was trained using a One-vs-Rest (OvR) strategy and combined with Recursive Feature Elimination (RFE) for feature selection to identify the most informative variables contributing to group discrimination.

The classification task included three classes: Class 0 (Young), Class 1 (Adult), and Class 2 (Elderly). The RFE procedure identified nine features as the most discriminative across groups: Alpha 2 Left Frontal, Theta Left Central, Alpha 1 Left Central, Beta 1 Left Central, Alpha 1 Right Parietal, Alpha 2 Right Parietal, Delta Left Occipital, Alpha 2 Left Occipital, and Beta 1 Left Temporal. These features reflect both low- and high-frequency functional connectivity modulations across anterior and posterior brain regions, consistent with the known reorganization of neural communication with aging.

The model reached good performances (Figure 24). Specifically, it achieved an overall

classification accuracy of 63.33%, with Class 0 (Young) showing the highest sensitivity (90.70%) and specificity (84.66%), indicating that the model was particularly effective in identifying younger participants. Class 2 (Elderly) was recognized with moderate sensitivity (66.67%) and high specificity (84.89%), whereas Class 1 (Adult) demonstrated lower sensitivity (29.41%) but comparable specificity (84.95%). These results suggest that the classifier effectively distinguishes young and elderly participants, while the adult group—representing an intermediate stage of physiological aging—exhibits overlapping functional features that reduce classification separability.

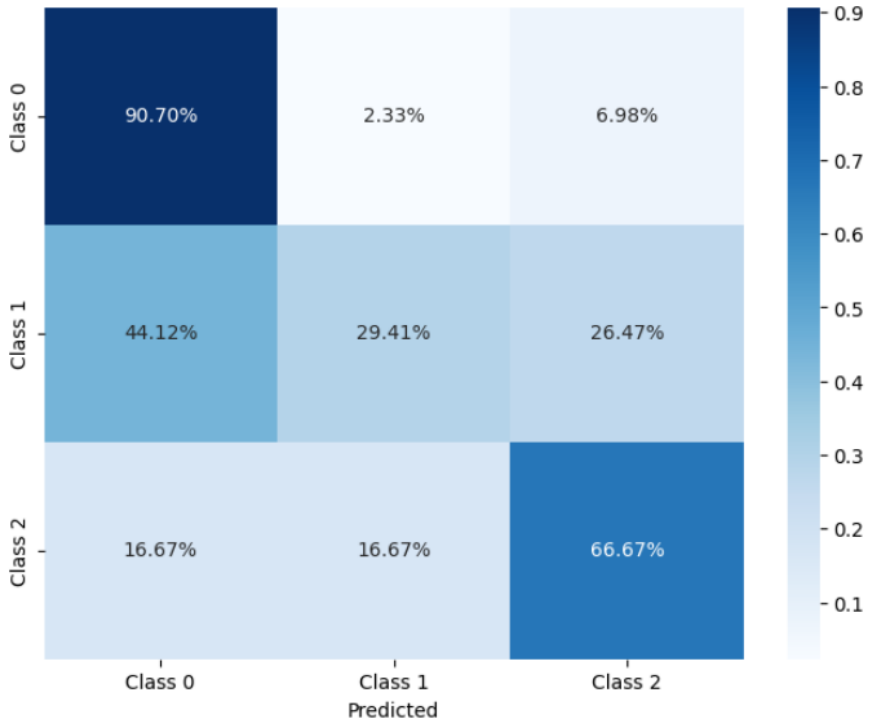

Figure 24. *Confusion matrix of the RBF SVM classifier based on Total Coherence (TotCoh) features across frequency bands and cortical regions.*

2. Graph theory analysis

Concerning the graph theory analysis, ANOVA results revealed a significant interaction (Figure 25) between the factors Group (Young, Adult, Healthy Elderly) and Frequency Band (Delta, Theta, Alpha 1, Alpha 2, Beta 1, Beta 2, and Gamma) ($F(12,624) = 2.54$, $p = 0.0027$). Post hoc analyses indicated that, when comparing the Young and Healthy Elderly groups (Figure 26), the latter exhibited significantly higher Small-World (SW) values in the Beta 1 ($p = 0.0003$) and Beta 2 ($p = 0.0023$) bands. Similarly, when comparing the Adult and Healthy Elderly groups (Figure 27), higher SW values were observed in the Healthy Elderly group within the

Beta 1 band (p = 0.0299).

These findings suggest an age-related increase in network clustering and local efficiency at higher frequencies, which may reflect compensatory reorganization processes aimed at maintaining functional integration and cognitive performance during healthy aging.

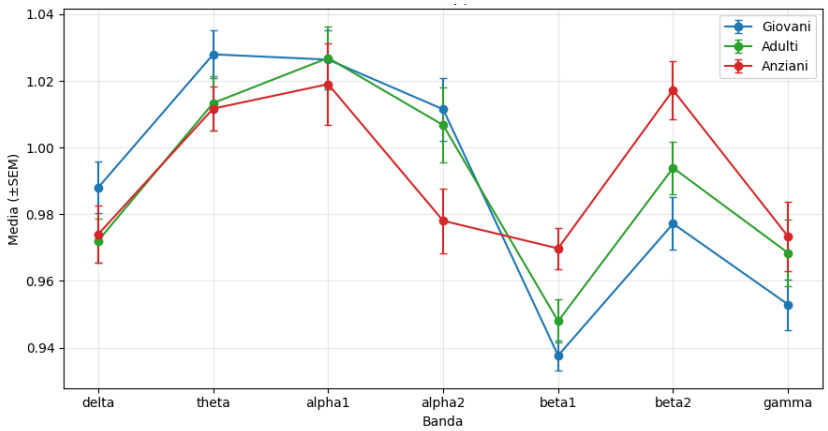

Figure 25. *Small-World (SW) index across EEG frequency bands for the Young, Adult, and Elderly groups. Mean SW values (± standard error) are plotted for each frequency band—Delta (2–4 Hz), Theta (4–8 Hz), Alpha 1 (8–11 Hz), Alpha 2 (11–13 Hz), Beta 1 (13–20 Hz), Beta 2 (20–30 Hz), and Gamma (30–45 Hz)—in the three physiological aging groups.*

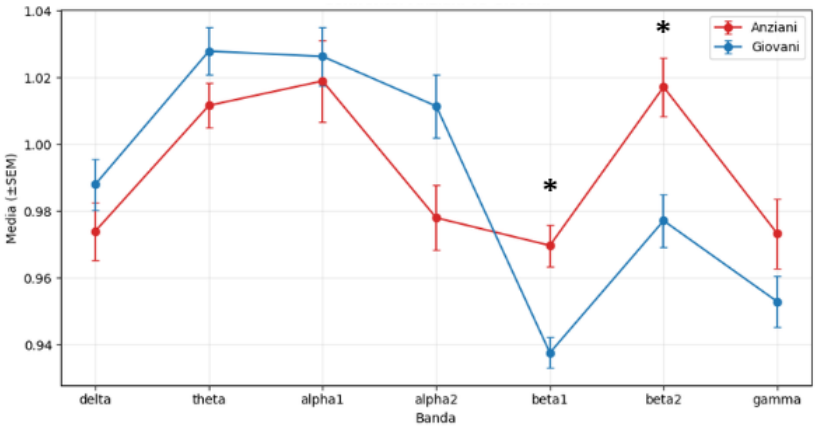

Figure 26. *Small-World (SW) index across EEG frequency bands for the Young and Elderly groups. Mean SW values (± standard error) are plotted for each frequency band—Delta (2–4 Hz), Theta (4–8 Hz), Alpha 1 (8–11 Hz), Alpha 2 (11–13 Hz), Beta 1 (13–20 Hz), Beta 2 (20–30 Hz), and Gamma (30–45 Hz)—in the Young and Elderly groups. Asterisks indicate the statistically significant different bands based on the post hoc analysis.*

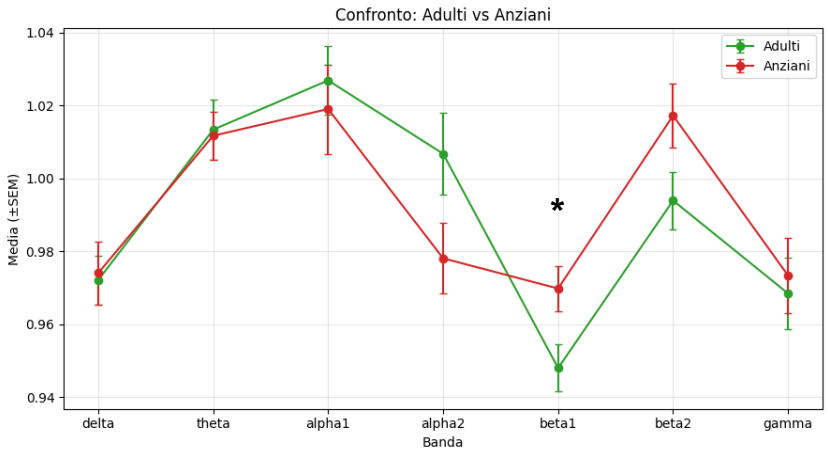

Figure 27. *Small-World (SW) index across EEG frequency bands for the Adult and Elderly groups. Mean SW values (± standard error) are plotted for each frequency band—Delta (2–4 Hz), Theta (4–8 Hz), Alpha 1 (8–11 Hz), Alpha 2 (11–13 Hz), Beta 1 (13–20 Hz), Beta 2 (20–30 Hz), and Gamma (30–45 Hz)—in the Young and Elderly groups. Asterisks indicate the statistically significant different bands based on the post hoc analysis.*

2.1. Machine learning algorithm

For the classification of physiological aging, the Small World (SW) values across seven EEG frequency bands (Delta, Theta, Alpha 1, Alpha 2, Beta 1, Beta 2, and Gamma) were used as input features. A linear Support Vector Machine (SVM) model was selected as the optimal classifier. The model was trained using a One-vs-One (OvO) strategy and combined with Recursive Feature Elimination (RFE) for feature selection to identify the most informative variables contributing to group discrimination.

The classification task included three classes: Class 0 (Young), Class 1 (Adult), and Class 2 (Elderly). The RFE procedure identified nine features as the most discriminative across groups: Theta SW and Alpha 2 SW.

The model reached good performances (Figure 28). Specifically, it achieved an overall classification accuracy of 52.27%, with Class 0 (Young) showing a sensitivity of 79.07% and specificity of 51.56%. Class 2 (Elderly) was recognized with moderate sensitivity (63.33%) and high specificity (77.92%), whereas Class 1 (Adult) demonstrated lower sensitivity (8.82%) but comparable specificity (77.92%). These results suggest that the classifier effectively distinguishes young and elderly participants, while the adult group—representing an intermediate stage of physiological aging—exhibits overlapping functional features that reduce classification separability.

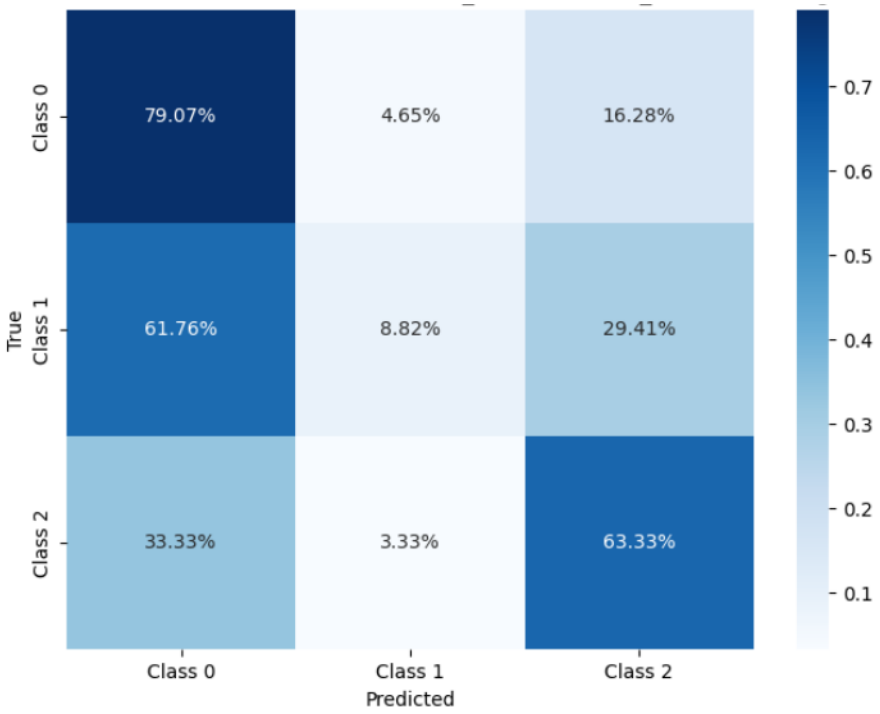

Figure 28. *Confusion matrix of the linear SVM classifier based on SW features across frequency bands.*

3. Entropy Analysis

Topographical maps of Approximate Entropy (ApEn) across frequency bands revealed clear, frequency-dependent changes in EEG signal complexity associated with physiological aging (Figure 29, Figure 30). Only statistically significant differences *pvalues* < *FDR_threshold* were reported.

In the Delta band (2–4 Hz), elderly participants exhibited significantly lower entropy values compared to both young and adult individuals, particularly in the frontal and temporal regions of both hemispheres. The observed lessening of slow-wave entropy across most of the brain regions points towards a decreased irregularity of the signals and thus indicates that there might be a reduction in neural variability and flexibility in front cortical areas of the brain as a result of aging.

Conversely, in the Theta band (4–8 Hz), the old age group presented a significant rise in entropy that was predominately directed towards the occipital regions. This backward increase in complexity might be indicative of the compensatory mechanisms in the visual and attentional processing systems that can allow counterbalancing of the reduced anterior neural variability in slower frequencies.

In the Alpha 1 band (8–11 Hz), entropy values in the elderly group were significantly lower than in both the young and adult groups of participants. The decrease of entropy spread over

the whole scalp when the comparison was made between the young and the elderly individuals, thereby implying that the aging process is associated with a global reduction of signal complexity. The differences that existed between adults and young participants were more localized, mainly implicating posterior regions and the left frontal cortex and thus suggesting that mid-adulthood may be the period when the dynamical richness in these brain areas starts to decline.

Moreover, there were no statistically significant differences between the young and the elderly participants as far as the Beta 2 band (20–30 Hz) is concerned. Nevertheless, compared to young individuals, adults had lower entropy values and the changes were predominantly centered on the right centro-parietal and left parietal regions. This spot-limited lowering may be indicative of temporary alterations in high-frequency neural dynamics during midlife, which do not continue into old age.

Collectively, these results reveal the intricate reorganization of EEG signal irregularity across different frequency bands and cortical areas that occurs during physiological aging. The decline in entropy in slow and alpha rhythms accompanied by the increased posterior entropy in theta frequencies may indicate that aging is characterized not only by losses of neural variability in some regions but also by the compensatory mechanisms leading to the rise of neural variability in other regions which, in turn, could serve as mechanisms for maintaining cognitive and functional stability in late adulthood.

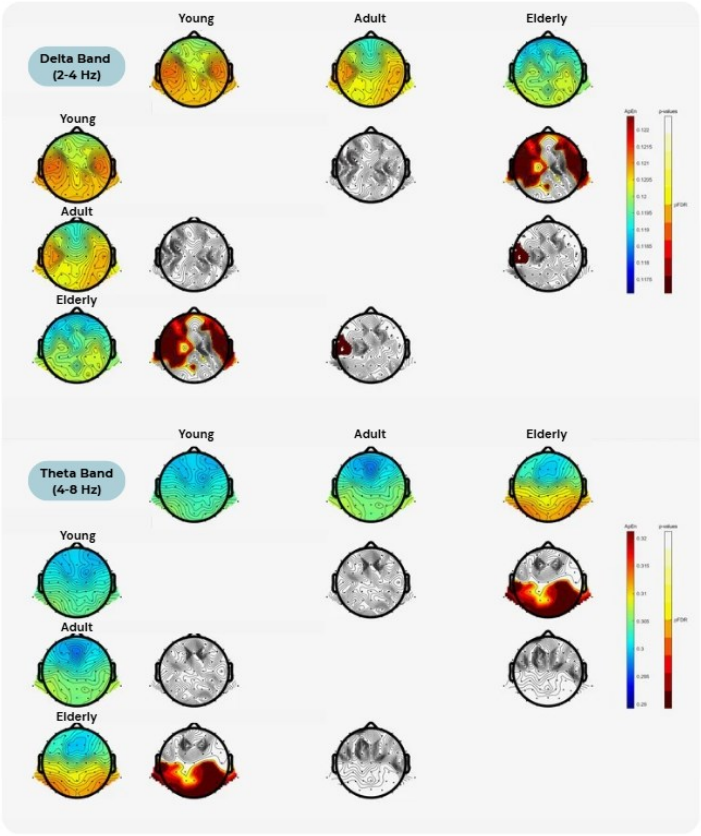

Figure 29. *Topographical maps display the distribution of Approximate Entropy (ApEn) values across the scalp in the three groups (Young, Adult, Healthy Elderly) for Delta (2–4 Hz) and Theta (4-8 Hz). Entropy values are color-coded from blue (low entropy/complexity) to red (high entropy/complexity), indicating increasing signal irregularity and complexity. In the central panels of each frequency band section, pairwise group comparisons are shown using FDR-corrected p-values (Healthy vs MCI, Healthy vs AD, MCI vs AD). The p-value maps are color-coded from dark red to white, with the blue–orange scale representing statistically significant comparisons after FDR correction (thresholded at the corrected significance level). For each frequency band, the arrangement of the maps follows a matrix structure where the top row and the lateral column represent the distribution of ApEn values across the scalp in the three groups while each column indicates a different pairwise comparison.*

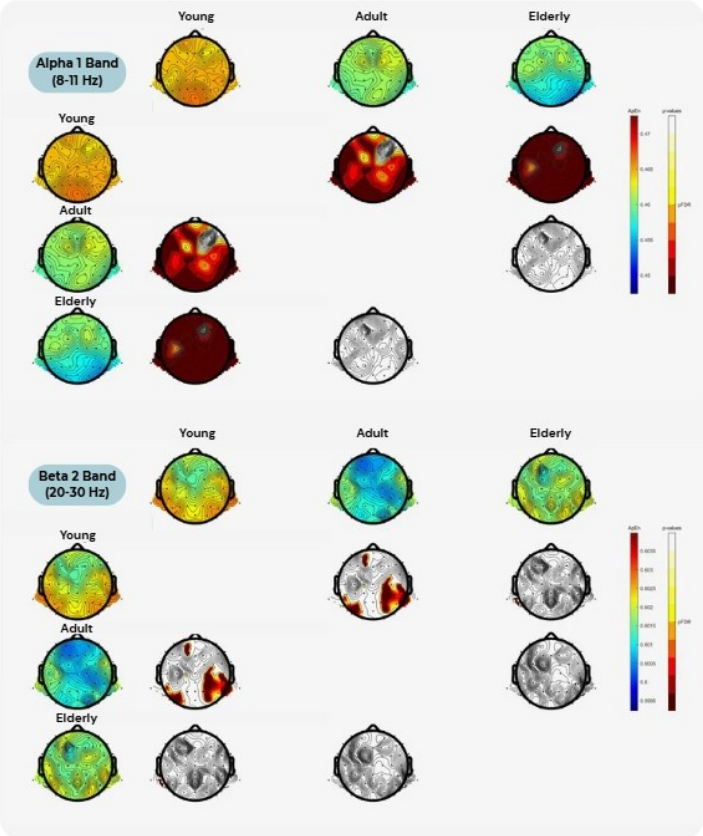

Figure 30. *Topographical maps display the distribution of Approximate Entropy (ApEn) values across the scalp in the three groups (Young, Adult, Healthy Elderly) for Alpha 1 (11–13 Hz) and Beta 2 (20-30 Hz). Entropy values are color-coded from blue (low entropy/complexity) to red (high entropy/complexity), indicating increasing signal irregularity and complexity. In the central panels of each frequency band section, pairwise group comparisons are shown using FDR-corrected p-values (Healthy vs MCI, Healthy vs AD, MCI vs AD). The p-value maps are color-coded from dark red to white, with the blue–orange scale representing statistically significant comparisons after FDR correction (thresholded at the corrected significance level). For each frequency band, the arrangement of the maps follows a matrix structure where the top row and the lateral column represent the distribution of ApEn values across the scalp in the three groups while each column indicates a different pairwise comparison.*

3.1. Machine Learning Algorithm

For the classification of physiological aging using EEG signal complexity, a Random Forest (RF) model was implemented. The model was trained using a One-vs-One (OvO) strategy and combined with Recursive Feature Elimination (RFE) for optimal feature selection. The classification task included three groups: Class 0 (Young), Class 1 (Adult), and Class 2 (Elderly). As input features, the Approximate Entropy (ApEn) values computed for each EEG channel and across all frequency bands (Delta, Theta, Alpha 1, Alpha 2, Beta 1, Beta 2, and Gamma) were used.

Among all features considered, the RFE method revealed a core of 17 variables that most

effectively differentiated the classes and thus contributed the most to the classification performance: F8_Total, F6_Total, P6_Total, FC5_Delta, C5_Delta, F7_Alpha1, P8_Alpha1, Fz_Alpha1, FC3_Alpha1, F5_Alpha1, F6_Alpha1, PO8_Alpha1, FC3_Beta1, PO8_Beta1, CP2_Beta2, PO4_Beta2 and P6_Beta2. These variables cover diverse frequency bands and cortical areas, including the front (frontal and fronto-central) and back (parietal and occipital) thus, they convey age-related changes in signal complexity, which are not localized but are spread all over the scalp.

The model had a total classification accuracy of 65.27% which was the highest for Class 0 (Young) in terms of both sensitivity (80.00%) and specificity (86.56%), thus the model was powerful in detecting younger subjects. Furthermore, Class 2 (Elderly) had a good sensitivity (70.97%) and a high specificity (85.54%) while Class 1 (Adult) was characterized by moderate sensitivity (44.44%) and specificity (80.39%) which implies a middle position of the adult group's electrophysiological characteristics between the young and elderly ones.

The confusion matrix (Figure 31) gives an account of the classification performance of each class, i.e., how well the model predicted each class; the number of correct predictions is shown on the diagonal and demonstrates that most of the young and elderly individuals were correctly identified while adults were mostly misclassified due to the transitional nature of their EEG complexity profiles.

These results reveal that physiologically aging stages may be distinguished by entropy-based features derived from multiband EEG activity, which, in turn, implies that such features have a significant discriminative power. The Random Forest model demonstrated strong generalization ability and effectively captured the nonlinear patterns underlying the evolution of brain signal irregularity across the adult lifespan.

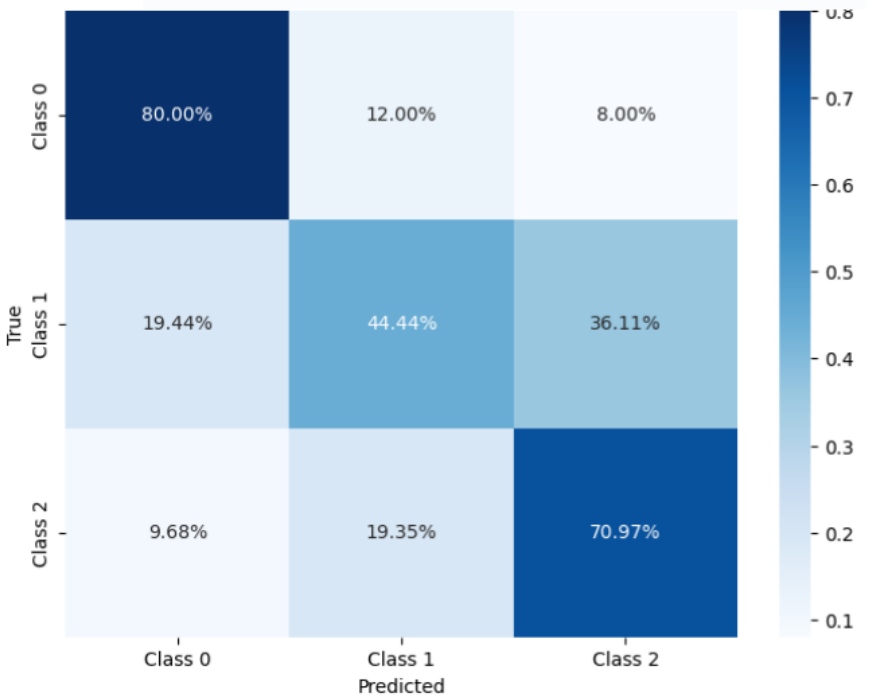

Figure 31. *Confusion matrix of the Random Forest classifier based on ApEn features across frequency bands and EEG channels.*

3.2. Machine Learning Algorithm with all features

For the classification of physiological aging, a Random Forest (RF) model was implemented, trained using a One-vs-Rest (OvR) strategy and combined with Recursive Feature Elimination (RFE) for feature selection. The classification included three groups: Class 0 (Young), Class 1 (Adult), and Class 2 (Elderly).

The model in this analysis combined a very broad range of EEG features derived from the brain signal. Various functional and complexity measures were considered. To be more specific, the researchers combined Small-World (SW) indices, Total Coherence (TotCoh) values computed from ten regions of interest (ROIs), and Approximate Entropy (ApEn) values calculated for each EEG channel and frequency band into one feature space that reflects both large-scale connectivity and local signal dynamics.

After RFE optimization, twelve features were singled out as the most discriminating of the groups: entropy values in C4_Total, F6_Total, AF3_Delta, C5_Delta, O2_Alpha1, P8_Alpha1, Fz_Alpha1, F5_Alpha1, F3_Alpha2, FC3_Beta1, PO8_Beta1; and the left Central Theta and left Occipital Alpha 2 bands connectivity features.

What is more, it appears that there are no Small-World (SW) parameters among the chosen features, which leads to the conclusion that, at least for this dataset, signal complexity locally

(ApEn) and functional coupling regionally (TotCoh) were able to provide more discriminative power than global topological network metrics for age stratification.

The overall accuracy of the model was 75.00% with the following sensitivity values: 93.02% for Young, 44.12% for Adult, and 80.00% for Elderly. Corresponding specificity values were 73.77%, 94.52%, and 91.89%, respectively. The confusion matrix (Figure 32) illustrates that the model accurately classified Young and Elderly individuals, whereas Adult subjects showed some overlap with other groups, which is indicative of their neurophysiological profile in transition.

In short, this work supports the view that the use of functional connectivity together with entropy-based measures has the power to increase the capability of the EEG in aging. It is quite telling that Small-World parameters were removed from the final model, which may mean that neural activity's regional and local features–instead of global network organization–could be the ones that mostly characterize the intermediate stages of adulthood.

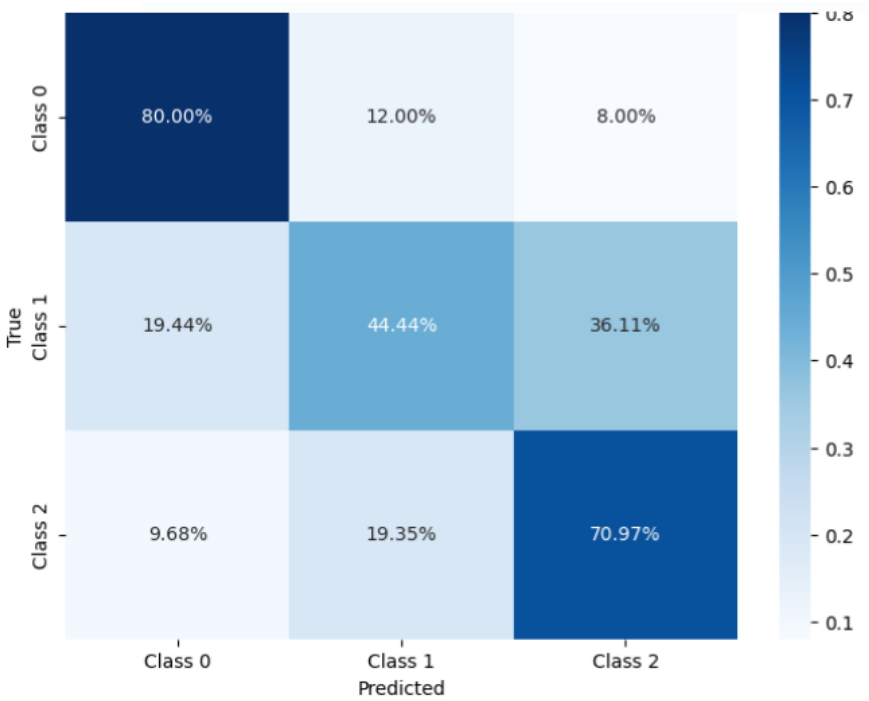

Figure 32. *Confusion matrix of the Random Forest classifier combining Total Coherence (TotCoh), and Approximate Entropy (ApEn) features.*

1. Functional connectivity analysis

Topographical maps of magnitude-squared coherence (MsCoh) across the analysed frequency bands revealed distinct patterns of age-related modulation in functional connectivity (Figure 33, Figure 34, Figure 35). Only statistically significant connections, corrected for multiple comparisons using the Bonferroni method ($p < 0.05$), were reported.

In the delta and theta frequency bands, Alzheimer's disease (AD) patients exhibited significantly higher coherence values within frontal regions compared to both mild cognitive impairment (MCI) patients and healthy elderly (HE) participants, accompanied by reduced connectivity in posterior regions.

A similar pattern was observed in the alpha 1 and alpha 2 bands, where AD patients showed enhanced frontal connectivity relative to the MCI and HE groups, paralleled by decreased posterior coherence. In the beta 1 and beta 2 bands, the same frontal–posterior dissociation emerged, with AD patients displaying increased functional coupling in frontal areas and diminished connectivity in posterior regions compared to the other groups

Finally, in the gamma band, AD patients demonstrated a generalized increase in coherence across the entire scalp, suggesting a diffuse enhancement of synchronization that was not spatially confined, distinguishing this frequency range from the more regionally specific modulations observed in the lower bands.

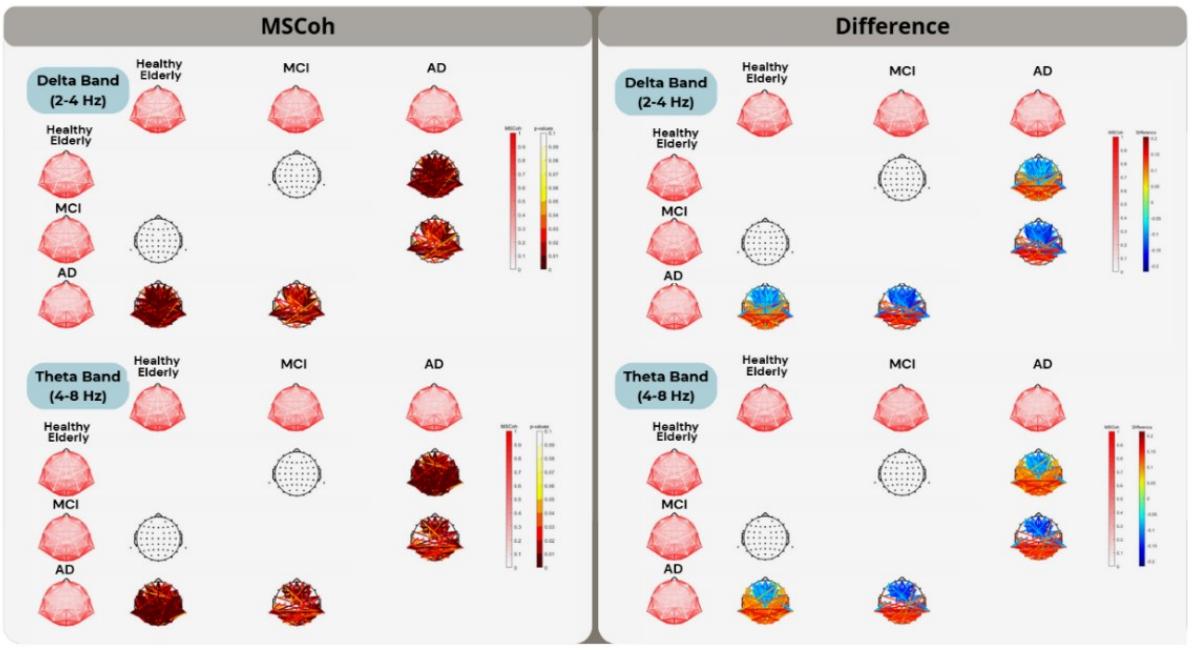

Figure 33. *Topographical representation of magnitude-squared coherence (MsCoh) across frequency bands and*

experimental groups. Topographical maps display the spatial distribution of MsCoh values for each EEG frequency band (Delta: 2-4 Hz; Theta: 4-8 Hz) and for each group, allowing visual comparison across the pathological aging continuum (Healthy Elderly, MCI, and AD).

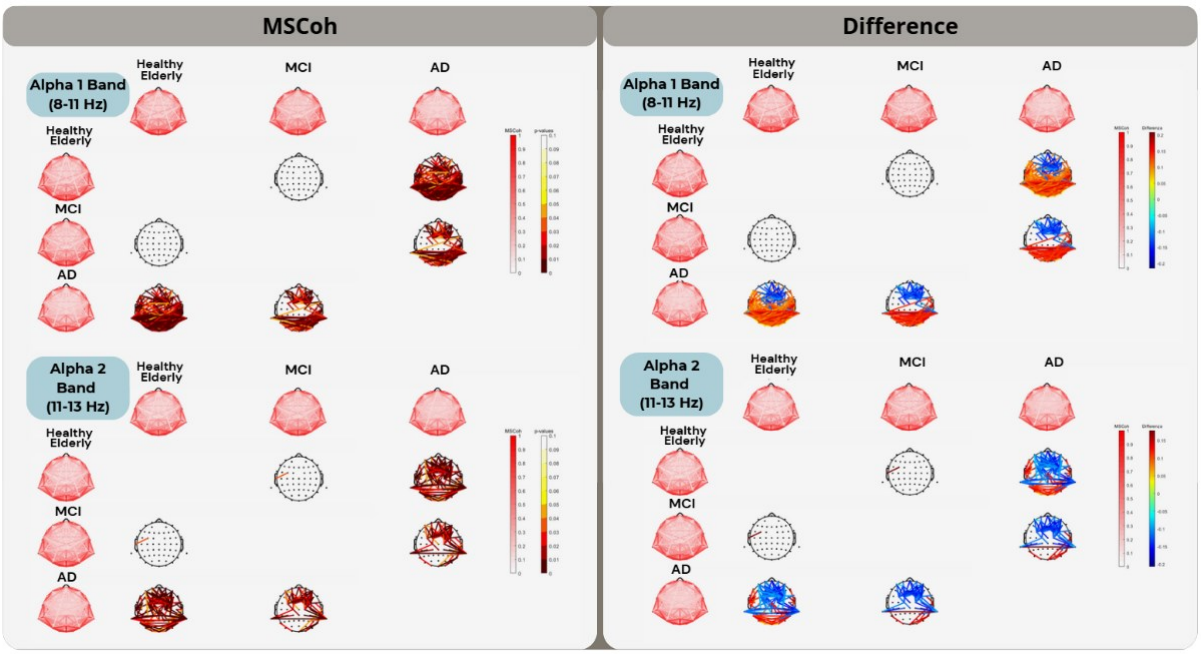

Figure 34. *Topographical representation of magnitude-squared coherence (MsCoh) across frequency bands and experimental groups. Topographical maps display the spatial distribution of MsCoh values for each EEG frequency band (Alpha 1: 8-11 Hz; Alpha 2: 11-13 Hz) and for each group, allowing visual comparison across the pathological aging continuum (Healthy Elderly, MCI, and AD).*

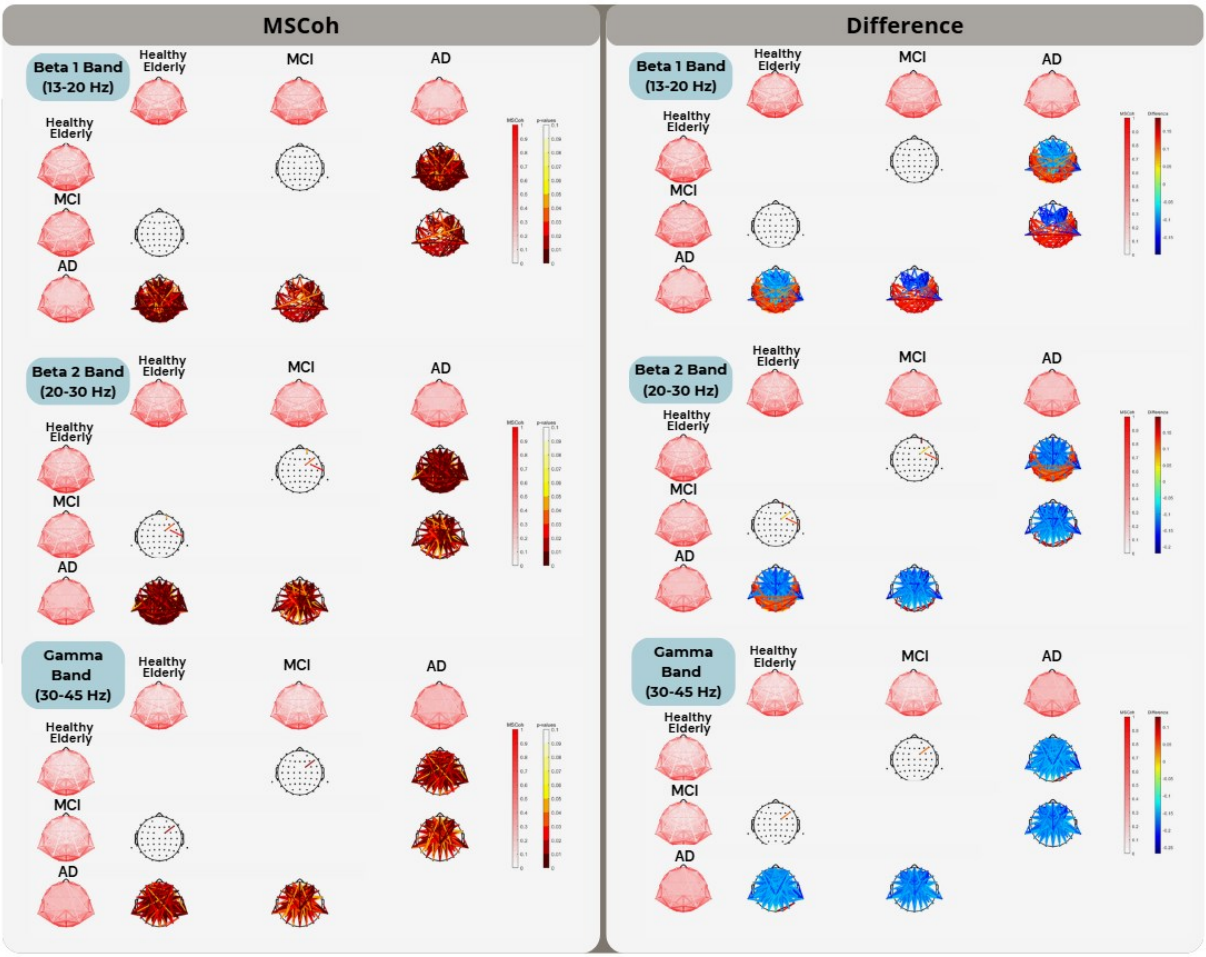

Figure 35. *Topographical representation of magnitude-squared coherence (MsCoh) across frequency bands and experimental groups. Topographical maps display the spatial distribution of MsCoh values for each EEG frequency band (Beta 1: 13-20 Hz; Beta 2: 20-30 Hz; Gamma: 30-45 Hz) and for each group, allowing visual comparison across the pathological aging continuum (Healthy Elderly, MCI, and AD).*

1.1. Machine learning algorithm

For the classification of pathological aging, Total Coherence (TotCoh) values across seven EEG frequency bands (Delta, Theta, Alpha 1, Alpha 2, Beta 1, Beta 2, and Gamma) were employed as input features. A Support Vector Machine (SVM) classifier with a Radial Basis Function (RBF) kernel was selected as the optimal model. The classifier was trained using a One-vs-One (OvO) strategy and integrated with Recursive Feature Elimination (RFE) to identify the most informative features contributing to the discrimination between groups.

The classification task included three diagnostic classes: Class 0 (Healthy Elderly, HE), Class 1 (Mild Cognitive Impairment, MCI), and Class 2 (Alzheimer's Disease, AD). The RFE procedure identified 19 features as the most discriminative across groups, primarily involving the frontal and central regions, with additional contributions from the parietal areas.

Specifically, relevant features were found in the frontal right (Delta, Theta, Alpha 1, Beta 1, Beta 2, Gamma), frontal left (Delta, Theta, Beta 1, Beta 2, Gamma), central right (Delta, Theta, Beta 2, Gamma), central left (Delta, Gamma), and parietal (Beta 2 in both hemispheres) regions. These features reflect widespread modulations of functional connectivity involving both low- and high-frequency bands, suggesting that alterations in frontal and central network synchronization play a crucial role in differentiating between stages of cognitive decline.

The model reached good performances (Figure 36). Specifically, it achieved an overall classification accuracy of 60.04%, with performance metrics varying across classes. Specifically, Healthy Elderly (Class 0) were identified with the highest sensitivity (80.73%), indicating strong model reliability in detecting normal aging patterns. The Alzheimer's Disease group (Class 2) also showed satisfactory sensitivity (64.71%) and very high specificity (94.62%), suggesting that AD-related connectivity alterations are distinct and consistently recognized by the classifier. Conversely, the MCI group (Class 1) exhibited lower sensitivity (34.67%), reflecting the intrinsic heterogeneity of this transitional stage between normal and pathological aging.

Overall, these findings indicate that the SVM model effectively distinguishes healthy and pathological aging profiles, particularly for AD, while intermediate cognitive impairment remains more challenging to classify due to overlapping functional connectivity features between MCI and the other groups.

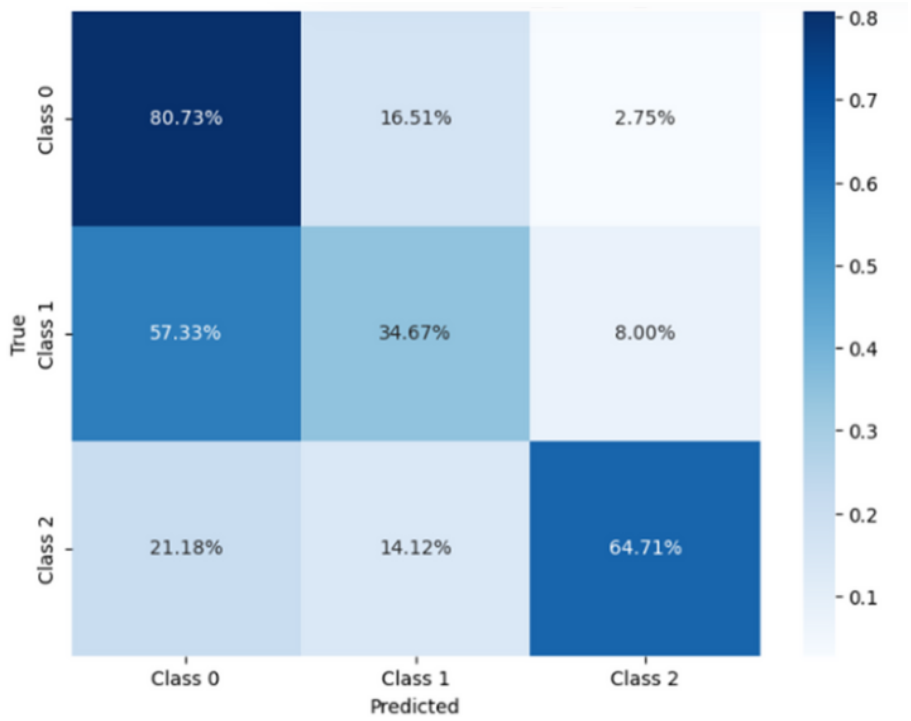

Figure 36. *Confusion matrix of the RBF SVM classifier based on Total Coherence (TotCoh) features across frequency bands and cortical regions.*

1.2. Correlation analysis

A correlation analysis was performed to investigate the relationship between clinical measures—grouped by cognitive domains (Global Cognition, Functional Abilities, Memory, Executive Function, and Language)—and Total Coherence (TotCoh) values computed over the full EEG frequency spectrum, as well as within individual frequency bands (Delta, Theta, Alpha 1, and Gamma). Coherence values were extracted from ten cortical regions of interest (ROIs), including frontal, central, parietal, temporal, and occipital areas, each analysed separately for the right and left hemispheres (Figure 37, Figure 38).

The findings showed different frequency-dependent patterns of associations between functional connectivity and cognitive performance. Correlations of delta and theta coherence with global cognition, executive, and attentional functions were positive, and the most strongly these correlations involved the frontal and temporal regions. It can be inferred from these results that the increased low-frequency synchronization may play a role in the retention of hierarchical cognitive functions, which might be a manifestation of compensatory processes directed at sustaining network integration in a situation of cognitive decline.

On the other hand, alpha-band connectivity was less and weaker associated with cognitive performance. Alpha 2 demonstrated some positive and negative correlations between regions,

thus indicating that the relationship between alpha activity and cognitive domains is more complex and less uniform.

It was only that the correlations they talked about within beta 1 and beta 2 frequency bands were limited in number but for the most part positive, especially those relationships involving executive (DSST), attentional (ACE AO), and language (ACE FL) functions. What this model implies is that the role of beta connectivity in the enhancement of higher cognitive processes is small yet quite specific.

Finally, the gamma band displayed widespread positive correlations across several cortical regions and cognitive domains, encompassing global cognition, executive, memory, and language functions. This consistent association between high-frequency coherence and cognitive performance suggests that enhanced gamma-band synchronization may reflect improved network integration and information processing efficiency.

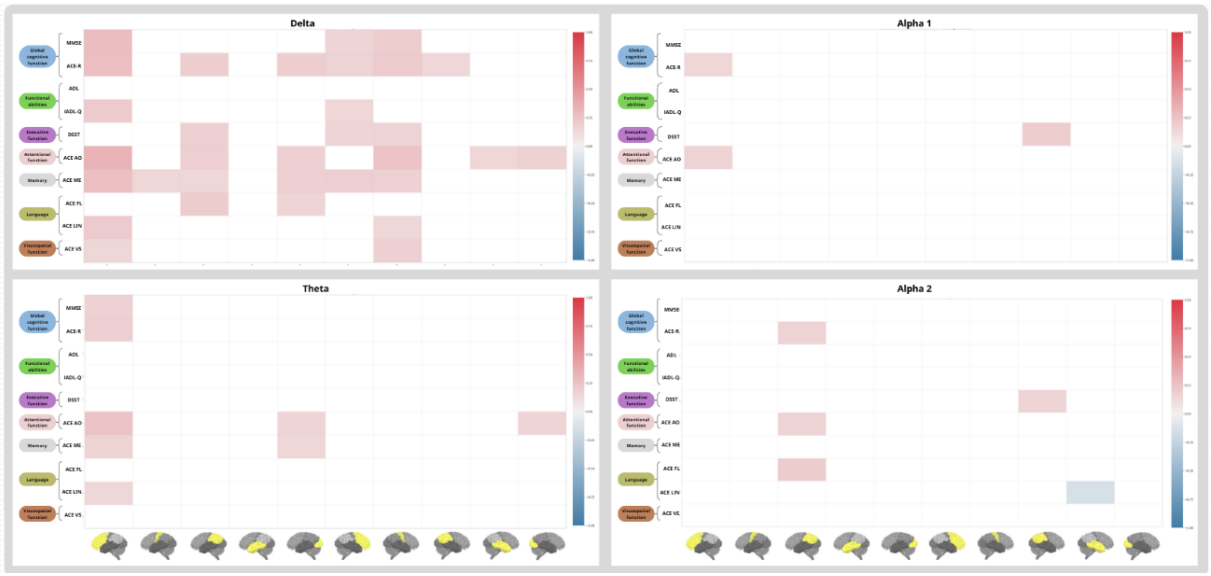

Figure 37. *The figure illustrates the representation of statistically significant correlations between TotCoh and neuropsychological test scores across all participants. Results are shown for the Delta, Theta, Alpha 1 and Alpha 2 bands. For each statistically significant EEG frequency band and cognitive domain, bar plots display the correlation coefficients observed in predefined bilateral regions of interest, grouped by hemisphere (left and right). The representations of the ROIs are reported below, in the following order: frontal, central, parietal, temporal, and occipital, first for the left hemisphere and then for the right hemisphere. Positive correlations are shown in red, and negative correlations in blue, with colour intensity reflecting the strength of the correlation.*

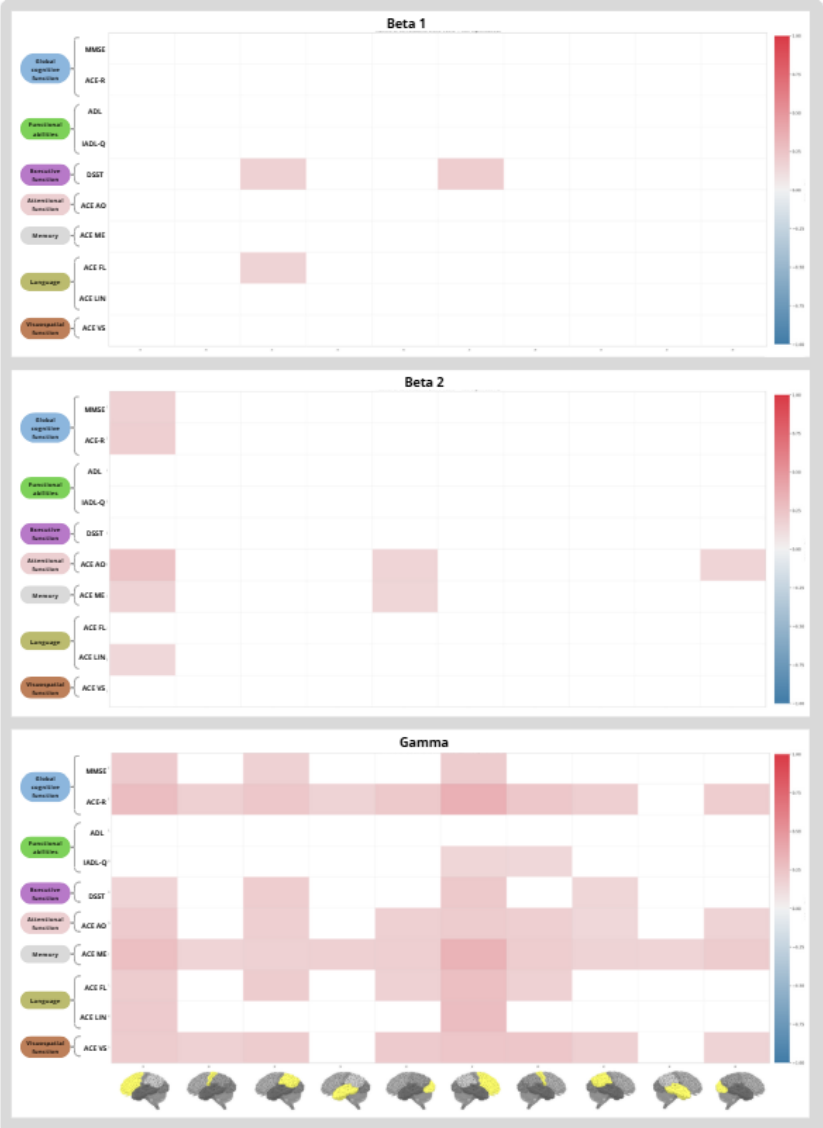

Figure 38. *The figure illustrates the representation of statistically significant correlations between TotCoh and neuropsychological test scores across all participants. Results are shown for the Beta 1, Beta 2 and Gamma bands. For each statistically significant EEG frequency band and cognitive domain, bar plots display the correlation coefficients observed in predefined bilateral regions of interest, grouped by hemisphere (left and right). The representations of the ROIs are reported below, in the following order: frontal, central, parietal, temporal, and occipital, first for the left hemisphere and then for the right hemisphere. Positive correlations are shown in red, and negative correlations in blue, with colour intensity reflecting the strength of the correlation.*

2. Graph theory analysis

Concerning the graph theory analysis, ANOVA results revealed no significant interaction (Figure 39) between the factors Group (Healthy Elderly, MCI and AD) and Frequency Band (Delta, Theta, Alpha 1, Alpha 2, Beta 1, Beta 2, and Gamma) ($F(12,1596)=1.7579$, $p=0.0501$).

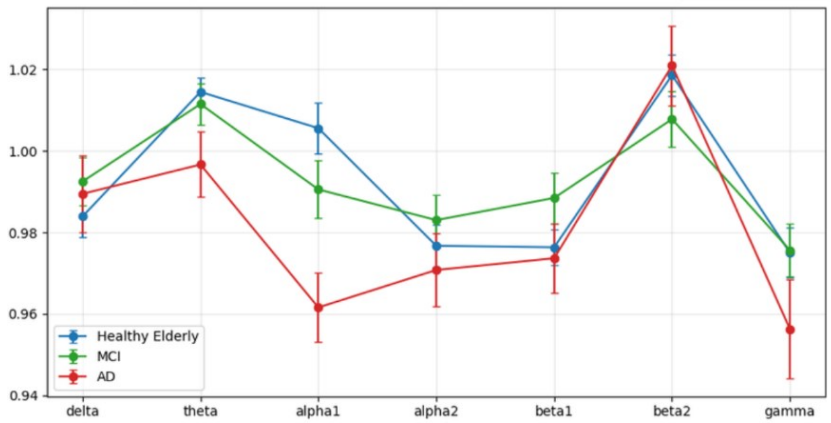

Figure 39. *Small-World (SW) index across EEG frequency bands for the Healthy Elderly, MCI, and AD groups. Mean SW values (± standard error) are plotted for each frequency band—Delta (2–4 Hz), Theta (4–8 Hz), Alpha 1 (8–11 Hz), Alpha 2 (11–13 Hz), Beta 1 (13–20 Hz), Beta 2 (20–30 Hz), and Gamma (30–45 Hz)—in the three groups.*

2.1. Machine learning algorithm

For the classification of pathological aging, the Small World (SW) values across seven EEG frequency bands (Delta, Theta, Alpha 1, Alpha 2, Beta 1, Beta 2, and Gamma) were used as input features. A Random Forest (RF) model was employed. The classifier was trained using a One-vs-Rest (OvR) strategy and combined with Recursive Feature Elimination (RFE) to identify the most relevant features contributing to group discrimination.

The classification task included three diagnostic categories: Class 0 (Healthy Elderly, HE), Class 1 (Mild Cognitive Impairment, MCI), and Class 2 (Alzheimer's Disease, AD). The RFE procedure identified five spectral features as the most informative for classification: Theta SW, Alpha 1 SW, Alpha 2 SW, Beta 2 SW, and Gamma SW. These features reflect frequency-specific alterations in signal complexity, potentially associated with disrupted neural synchronization and reduced information processing efficiency in pathological aging.

The model reached quite good performances (Figure 40). Specifically, it achieved an overall classification accuracy of 51.3%, with performance metrics varying across groups. Specifically, the Healthy Elderly (Class 0) group showed the highest sensitivity (70.64%), indicating good model reliability in identifying normal aging patterns. The Alzheimer's Disease (Class 2) group also exhibited moderate sensitivity (54.12%) and high specificity (82.6%), suggesting that entropy-based features effectively capture AD-related reductions in neural complexity. Conversely, the MCI group (Class 1) presented low sensitivity (20%), despite relatively high specificity (85.6%), reflecting the intrinsic variability and overlap of entropy patterns between normal and pathological aging.

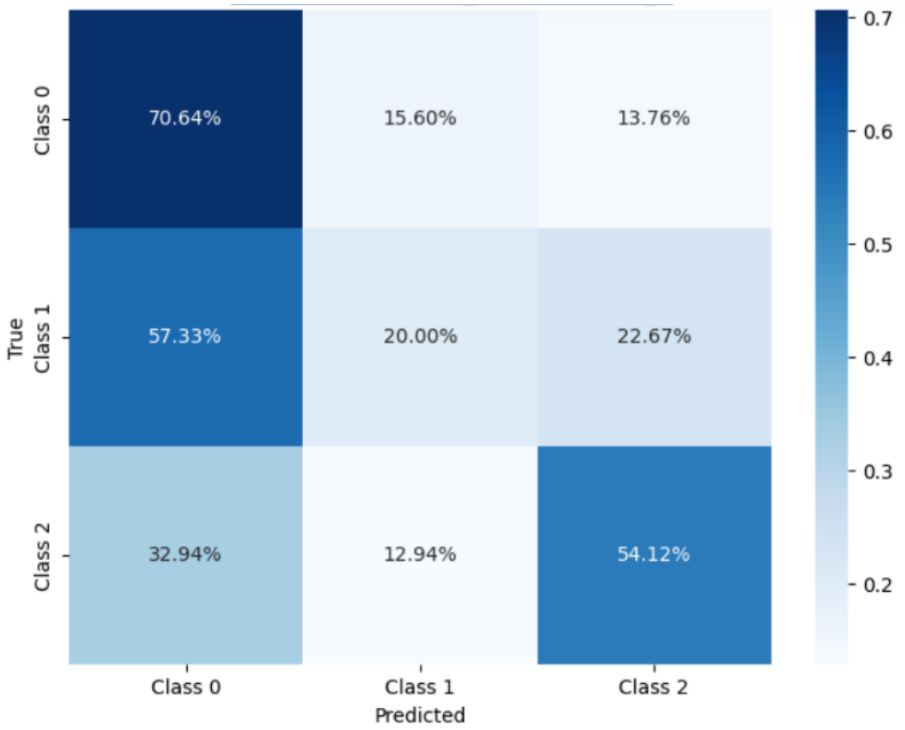

Figure 40. *Confusion matrix of the Random Forest classifier based on SW features across frequency bands.*

3. Entropy Analysis

Topographical maps of Approximate Entropy (ApEn) across frequency bands revealed clear, frequency-dependent changes in EEG signal complexity associated with pathological aging (Figure 41). Statistically significant differences in ApEn values among the three groups were identified in the Total EEG spectrum and were visualized using a symmetric matrix representation. In the comparison between Healthy Elderly and AD patients, the differences continued to predominantly affect the central region and additionally extended to the parietal area. Conversely, no statistically significant differences were found between the MCI and AD groups across any region. These findings likely reflect a progressive decrease in ApEn within the central region, as illustrated by scalp distribution patterns transitioning from Healthy Elderly to MCI subjects, and subsequently to AD patients, within the Total EEG spectrum.

When examining the distinct EEG frequency bands, statistically significant differences emerged specifically within the Delta, Alpha 1, and Gamma bands.

A highly statistically significant result was observed in the Delta frequency band. The difference in entropy distribution in AD patients is evident across the entire scalp, where an increase in ApEn values is observed compared to the other two groups. However, this increase is slightly less pronounced when comparing AD patients specifically to the MCI group. In contrast, this group exhibited a slight decrease in ApEn in the frontal regions compared to

Healthy Elderly, accompanied by a modest increase in the occipital areas. Consequently, statistical significance was reached only at two electrodes corresponding to these respective areas.

In the Alpha 1 band, AD patients consistently exhibited an increase in ApEn compared to Healthy Elderly, which, in this case, was confined exclusively to the occipital regions. Conversely, the frontal areas were characterized by a reduction in complexity. This pattern, however, was not observed in MCI subjects, who showed a marked increase in ApEn in the frontal regions relative to both Healthy Elderly and AD patients. Regarding the occipital distribution, MCI group displayed a pattern similar to that of AD patients, though with higher entropy levels compared to Healthy participants. These observed differences culminated in a statistically significant effect localized in the centro-frontal electrodes in the comparison between MCI subjects and AD patients. By contrast, no statistically significant differences were found between Healthy Elderly and MCI subjects in this frequency band.

The final observed difference was identified in the Gamma frequency band. Statistically significant differences within this band were evident in the comparisons between Healthy Elderly and AD groups, as well as between MCI and AD groups. Specifically, AD patients demonstrated a pronounced reduction in entropy across the entire scalp relative to both Healthy Elderly and MCI subjects. In the comparison between Healthy Elderly and AD subjects, these statistically significant differences were primarily localized to electrodes overlying the central and frontal cortices. Conversely, in the MCI versus AD comparison, significant alterations extended beyond the central and frontal regions to include occipital areas.

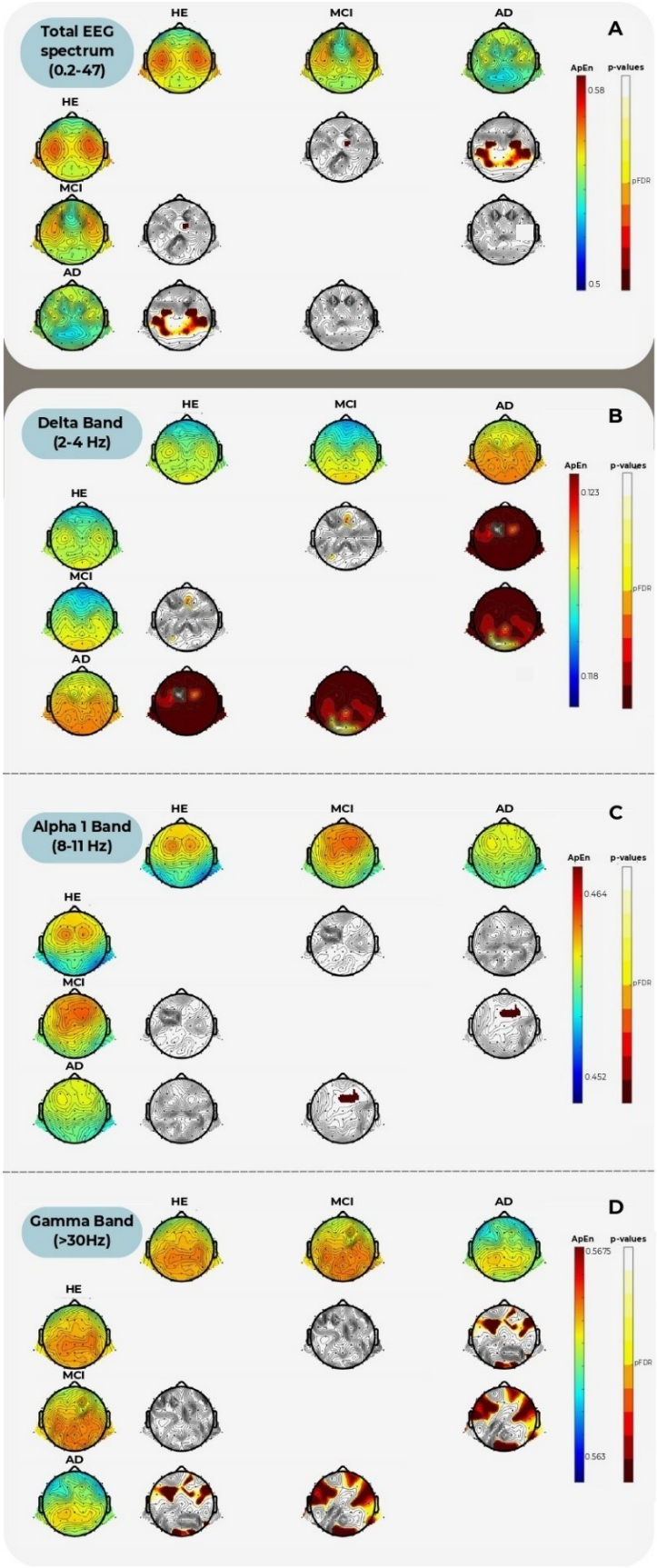

Figure 41. *Topographical maps display the distribution of Approximate Entropy (ApEn) values across the scalp in the three groups (Healthy Elderly, MCI and AD) for the entire EEG spectrum (0.2-47 Hz), Delta (2-4Hz), Alpha*

1 (11–13 Hz) and Gamma (30-45 Hz). Entropy values are color-coded from blue (low entropy/complexity) to red (high entropy/complexity), indicating increasing signal irregularity and complexity. In the central panels of each frequency band section, pairwise group comparisons are shown using FDR-corrected p-values (Healthy vs MCI, Healthy vs AD, MCI vs AD). The p-value maps are color-coded from dark red to white, with the blue–orange scale representing statistically significant comparisons after FDR correction (thresholded at the corrected significance level). For each frequency band, the arrangement of the maps follows a matrix structure where the top row and the lateral column represent the distribution of ApEn values across the scalp in the three groups while each column indicates a different pairwise comparison.

3.1. Machine Learning Algorithm

For the classification of pathological aging based on EEG signal complexity, a Random Forest (RF) model was employed. The classifier was trained using a One-vs-One (OvO) strategy and combined with Recursive Feature Elimination (RFE) to identify the most informative entropy features contributing to group discrimination. The analysis included three diagnostic classes: Class 0 (Healthy Elderly, HE), Class 1 (Mild Cognitive Impairment, MCI), and Class 2 (Alzheimer's Disease, AD). For the input variables, entropy values served as the basis for reconstructing signal complexity in a cortical ensemble. The values were obtained through the analysis of EEG channels for each condition over all frequency bands.

The RFE method used the 18-feature set to most effectively differentiate the groups, entailing the widespread changes in entropy over different cortical regions and frequency bands. In general, local features were found in both global (P3, TP10, AF7) and band-specific measurement, such as Delta (Fp1, Fz, FC2, CP1, FC5, AF7, AF8, Fpz), Alpha 1 (P7, CP2), Beta 2 (O2, Cz, FC6), and Gamma (FC2, FC6). The results demonstrate an extensively distributed pattern of entropy modulation that involves not only the frontal but also the posterior brain regions, thereby implying that neural complexity disruptions are extending beyond localized areas and reflecting a global reorganization of brain activity linked with cognitive decline.

The Random Forest tool had a total percentage of correct classifications of 66.9% (Figure 42), thus, it was judged to be a good classifier of three groups: healthy individuals, mildly impaired individuals, and demented participants. The recognition of the Healthy Elderly group (Class 0) was the most sensitive (80.73%), thus, the model was able to identify normal aging patterns with high accuracy. The Alzheimer's Disease group (Class 2) also had a reasonable sensitivity (70.59%) and a high specificity (85.26%), thus, it means that entropy features can be used to monitor the significant decrease of neural complexity, which is a typical characteristic of AD.

On the other hand, the MCI group (Class 1) had a lower sensitivity (42.67%) compared to a relatively high specificity (83.19%), thus, the intermediate and heterogeneous nature of this clinical stage which is a mixture of normal and pathological aging is reflected in the results.

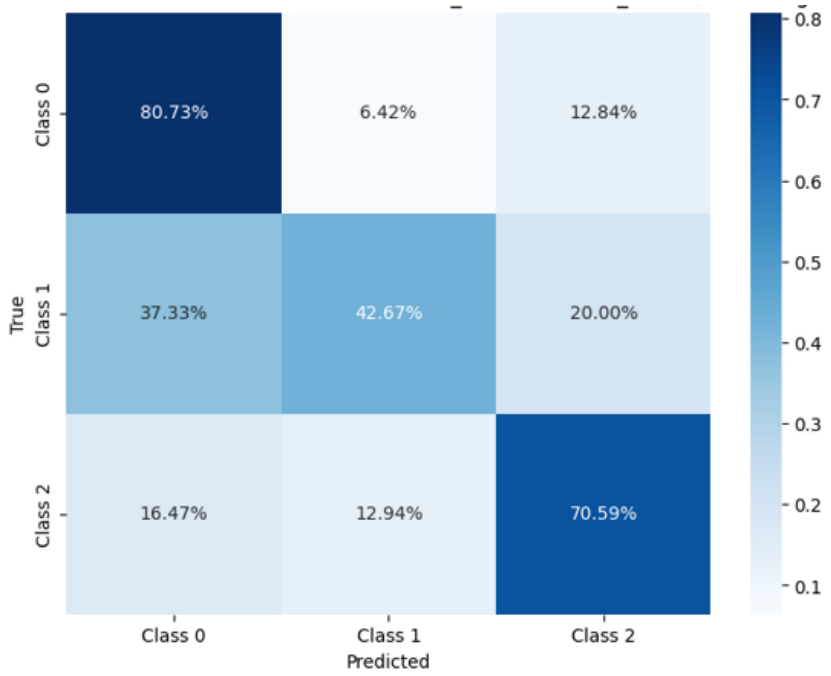

Figure 42. *Confusion matrix of the Random Forest classifier based on entropy features across frequency bands.*

3.2. Machine Learning Algorithm with all features

For the classification of pathological aging, a Random Forest (RF) model was implemented, trained using a One-vs-Rest (OvR) strategy and combined with Recursive Feature Elimination (RFE) for feature selection.

As input variables, all extracted EEG features—small-worldness (SW), entropy, and functional connectivity—were combined to represent different aspects of brain network organization for the final classification analysis. The AdaBoost model was chosen as the best performing classifier, it was trained with a One-vs-Rest (OvR) strategy and combined with Recursive Feature Elimination (RFE) to locate the features that guided the discrimination of groups most effectively.

Three diagnostic classes formed the classification problem: Class 0 (Healthy Elderly, HE), Class 1 (Mild Cognitive Impairment, MCI), and Class 2 (Alzheimer's Disease, AD).

RFE pointed to features that had the highest power of discrimination between groups, including both entropy-based (Fp1_Delta, P3_Delta, Fz_Delta, TP10_Delta, CP2_Alpha1, O2_Beta2, FC6_Beta2) and connectivity-based (Delta Frontal Right, Theta Frontal Right, Alpha1 Frontal

Right, Gamma Frontal Right, Delta Frontal Left, Theta Frontal Left, Gamma Frontal Left, Delta Central Right, Gamma Central Right, Beta2 Parietal Right, Gamma Parietal Left) terms.

These features reveal that not only the frontal but also the posterior regions of the brain are the main areas involved in the separation of normal and pathological aging with changes occurring in the low-frequency (delta, theta) as well as in the high-frequency (beta, gamma) bands. The joint play of entropy and connectivity terms shows that alterations in local signal complexity as well as in long-range neural coupling are the main signs of cognitive decline.

The AdaBoost model, as a whole, was able to classify correctly with a 67.29% accuracy (Figure 43), and was able to perform well for each class. More specifically, the Healthy Elderly group (Class 0) had the highest sensitivity (77.06%) as well as a good specificity (75.00%), showing that the patterns of normal aging were detected correctly. Similarly, the Alzheimer's Disease group (Class 2) showed a high sensitivity (71.76%) and a very high specificity (92.39%), thus, the classifier was successful in identifying the distinctive electrophysiological changes that characterize advanced neurodegeneration. The MCI group (Class 1), however, was able to show only a limited sensitivity (48.00%), alongside a good specificity (82.47%), thus, reflecting the intermediate and heterogeneous features of this clinical condition.

In essence, the present results demonstrate that EEG features from multiple sources—such as network topology, signal entropy, and functional connectivity—could be effectively combined within an AdaBoost model to distinguish healthy, mildly impaired, and demented individuals. The main idea conveyed by the findings is that a cognitive decline scenario is more compatible with a simultaneous disruption of local and global neural organization than with changes of a single electrophysiological dimension.

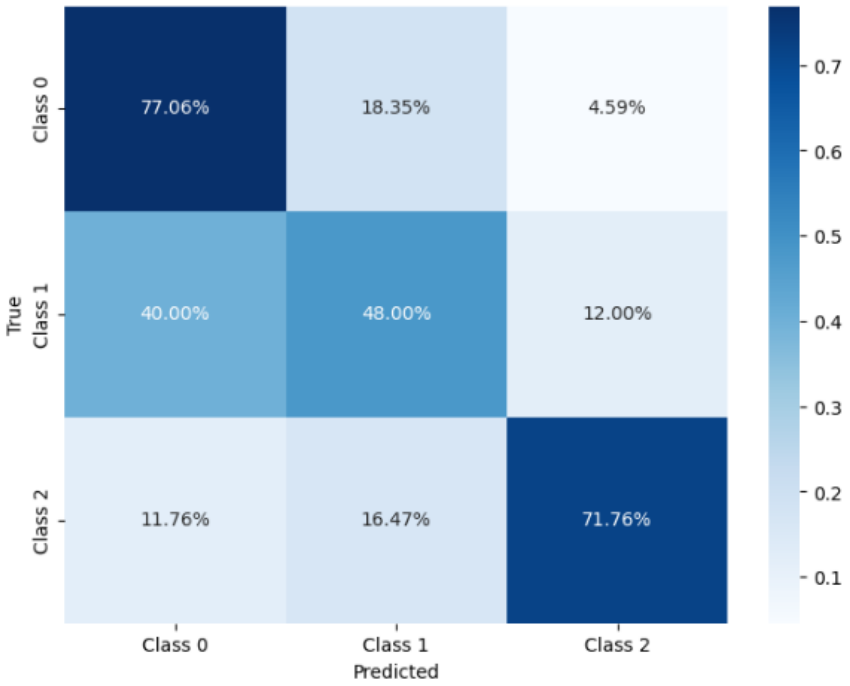

Figure 43. *Confusion matrix of the AdaBoost classifier combining Total Coherence (TotCoh), and Approximate Entropy (ApEn) features*

3.3. Correlation analysis

A correlation analysis was performed to explore the relationship between clinical measures—grouped into the cognitive domains of Global Cognition, Functional Abilities, Memory, Executive Function, and Language—and entropy values computed across the full EEG frequency spectrum, as well as within the delta, theta, alpha 1, and gamma bands (Figure 44). Entropy measures were determined for ten different cortical regions of interest (ROIs) that included the frontal, central, parietal, temporal, and occipital areas, separately for the right and left hemispheres.

Significant positive correlations were found between Approximate Entropy (ApEn) values in central, parietal, and occipital regions and global cognition (MMSE, ACE) as well as functional abilities (IADL, IADL-Q) when the full EEG spectrum was considered. These results indicate that higher overall entropy, a marker of higher neural complexity, is associated with better cognitive and functional performance.

Conversely, delta-band entropy showed negative correlations with global cognitive scores, functional abilities, and several ACE subdomains across most cortical regions. The pattern suggests that increased irregularity of low-frequency activity might be associated with worse cognitive and functional abilities, which could be the case if impaired neural efficiency and

disorganized large-scale network activity characterize the pathological aging process. Within the alpha 1 band, negative correlations were found in more localized cortical areas, involving measures of global cognition, functional performance, and attentional abilities, suggesting that reduced alpha-band regularity may be associated with attentional and integrative deficits.

Finally, gamma-band entropy showed widespread positive correlations across multiple cortical regions, particularly in the frontal and parietal areas. These associations involved global cognition, and functional abilities, indicating that higher gamma-band entropy—representing greater variability and flexibility of high-frequency neural activity—is linked to preserved cognitive efficiency and adaptive information processing.

Overall, these findings suggest that distinct frequency bands convey complementary information regarding cognitive functioning: while low-frequency (delta) irregularities are associated with cognitive decline, high-frequency (gamma) entropy appears to reflect preserved or compensatory neural dynamics supporting cognitive performance.

Figure 44. *The figure illustrates the representation of statistically significant correlations between ApEn and neuropsychological test scores across all participants. Results are shown for the Beta 1, Beta 2 and Gamma bands. For each statistically significant EEG frequency band and cognitive domain, bar plots display the correlation coefficients observed in predefined bilateral regions of interest, grouped by hemisphere (left and right). The representations of the ROIs are reported below, in the following order: frontal, central, parietal, temporal, and occipital, first for the left hemisphere and then for the right hemisphere. Positive correlations are shown in red, and negative correlations in blue, with colour intensity reflecting the strength of the correlation.*

DISCUSSION AND CONCLUSION

The present work investigated electrophysiological correlates of physiological and pathological aging through the combined analysis of EEG functional connectivity, signal complexity (entropy), and graph-theoretical network properties. Furthermore, a series of machine learning models were employed to assess the discriminative power of these features in classifying individuals along the continuum from healthy aging to cognitive impairment and dementia.

The findings revealed a series of unambiguous and frequency-dependent patterns of modulation across all EEG-derived measures. Aging physiologically brought about a decline in functional connectivity, which was general in nature and can be particularly attributed to interactions between posterior and frontal regions. The decrease was also associated with a shift to higher-frequency compensatory synchronization in beta bands. Investigating entropy, the researchers found a decrease in complexity of the signal in slow and alpha bands accompanied by the increase of local activity in the theta band in posterior region that could be interpreted as the signs of neural degeneration as well as adaptation. Graph theory metrics showed that the elderly demonstrated higher small-worldness, which is explained as supported functional compensation by increased local clustering.

Furthermore, machine learning models validated these patterns through good discriminative power for age groups brought by coherence and entropy features. The models were around 60–65% accurate, and the differences between young and elderly individuals were most pronounced, whereas adults had mixed features, which is indicative of the progressive nature of neural aging.

Within the pathological domain, patterns with intensified severity of symptoms were similarly observed. The patients with Alzheimer's disease (AD) rewired frontal connections and weakened posterior ones as they exhibited increased frontal and reduced posterior connectivity across all frequency bands. This reinforces the idea of the fragmenting of long-range neural communication resulting in the loss of frontal and posterior connectivity. Entropy studies pointed to a universal decline in the complexity of the neural signal, especially in the gamma band, while the local increase in delta and alpha 1 entropy indicated oscillatory regulation impairment.

Machine learning techniques were in line with the findings stating that entropy and connectivity features are reliable indicators of disease staging, thus, they have the potential of attaining the highest accuracies of over 65%. The combination of all EEG-derived metrics (connectivity, entropy, and network topology) by an AdaBoost classifier led to the overall highest

performance (67.29%) in distinguishing AD and healthy elderly subjects, while the MCI group was located in the middle between the both, i.e., consistent with its transitional neurophysiological status.

Finally, correlation analyses demonstrated that low-frequency irregularities (delta) were associated with poorer cognitive performance, while higher-frequency activity (gamma) correlated positively with global cognition, executive function, and functional abilities, supporting the view that preserved neural complexity at fast frequencies underlies adaptive compensation.

PHYSIOLOGICAL AGING: NEURAL REORGANIZATION AND COMPENSATORY DYNAMICS

The results obtained for physiological aging delineate a complex and dynamic process in which the aging brain undergoes progressive functional reorganization rather than a simple, linear decline. The reduction in inter-regional coherence within the delta, theta, and alpha 2 frequency bands observed in elderly participants highlights a weakening of long-range synchronization, particularly involving posterior cortical regions. This decrease may be seen as a reduction of large-scale integration, i.e. the lowering of the ability of widely spread cortical areas to conduct the same oscillatory communication. The fading of synchrony in the back of the brain, particularly in slow frequency ranges, could reflect less efficient sensory integration and attentional processing, which are functions classically attributed to occipital and parietal lobes. Curiously, the deficit in the low-frequency interaction was also associated with the increase of beta-band coherence, particularly between frontal and posterior areas. Beta oscillations are generally linked with top-down control, motor coordination, and cognitive set maintenance, thus suggesting that older adults might be utilizing these networks more intensively as a compensatory mechanism in order to keep their performance levels despite global efficiency decrement. Moving towards higher frequencies means that the brain of an elderly person is not simply fading away, it is actually reorganizing its oscillatory architecture and hence, redirecting the resources for the preservation of behavioural stability.

The entropy findings corroborate this compensatory argument. The widespread decrease of Approximate Entropy (ApEn) in delta and alpha bands for the aged group can be interpreted as less irregularity of the signal and a narrowing of the brain's dynamical repertoire, which is a neural flexibility marker. Reduced entropy indicates that the neural activity becomes more predictable and less complex, thus pointing towards the brain being less capable of flexibly

adapting to the environmental demands. The increase in posterior theta entropy, however, suggests that some cortical areas are able to retain or even increase their variability and thus, it may reflect local compensatory mechanisms implemented to stabilize sensory and attentional functions.

Graph theoretical analyses provide additional evidence for these conclusions and show that aging is associated with an increase in small-worldness in the higher frequency bands. A higher small-world index denotes stronger local clustering and network segregation, thus possibly promoting local processing capacity when the long-range communication is impaired. The brain's topological adjustment may represent an adaptive strategy, facilitating the maintenance of the balance between segregation and integration, which is a characteristic of efficient network functioning.

To a large extent, the electrophysiological findings sketch a dual-process model of physiological aging. The first aspect is a slow reduction of large-scale synchronization and neural plasticity that comes with age; the second aspect is an adaptive reorganization marked by local increases in coherence and clustering, mainly in the faster frequency domains. The results are consistent with the view of the aged brain reorganizing its functional architecture so as to compensate for structural decline and reduced metabolic efficiency.

Moreover, the classification models that utilized coherence, entropy, and small-world indices provide additional evidence for this continuum. Machine learning methods were best at distinguishing between young and elderly participants, but had less performance in differentiating adults, thus middle adulthood was identified as a transitional stage where both compensatory and degenerative mechanisms are at work. In sum, results point towards healthy aging not being a uniform phenomenon, but rather a neural recalibration process which is oscillatory and topological in nature, and by which cognitive stability is preserved.

PATHOLOGICAL AGING: BREAKDOWN OF INTEGRATION AND LOSS OF NEURAL COMPLEXITY

In contrast to the adaptive reorganization observed in physiological aging, pathological aging—as represented by Mild Cognitive Impairment (MCI) and Alzheimer's Disease (AD)—is characterized by a progressive breakdown of network integration and a loss of neural complexity. The functional connectivity analyses revealed a clear frontal–posterior dissociation across nearly all frequency bands: AD patients exhibited increased coherence in frontal regions and reduced connectivity in posterior areas compared to both MCI and healthy elderly

participants. This likely reflects functional disconnection of posterior associative networks, including parietal and occipital cortices, among the first regions to be affected by neurodegenerative processes.

The frontal hyperconnectivity observed in AD patients can be interpreted as a form of compensatory recruiting that is inefficient. While an initial increase in frontal synchronization indeed may reflect adaptive engagement of executive and attentional systems to counteract posterior disconnection, excessive frontal coherence can become maladaptive, leading to network rigidity and decreased flexibility in information transfer. This "over-synchronization" phenomenon might drive cognitive rigidity and slower information processing frequently found in dementia.

Entropy analyses from this same perspective give further support to the phenomena observed. In these, AD patients showed a significant decline in Approximate Entropy within central and parietal regions, reflecting the global loss of neural variability and reduced ability of the brain to generate complex, adaptive patterns of activity. With lower entropy, cortical signals are more regular and predictable; both these aspects reflect reduced richness in neural dynamics and reduced capacity for flexible adaptation-both hallmarks of cognitive impairment.

However, this general reduction in entropy was not quite uniform across frequencies or regions. In the delta band, AD patients showed an increase in entropy across the scalp, which may reflect disorganized or noisy rather than healthy low-frequency activity. Conversely, in the alpha 1 band, MCI subjects showed increased frontal entropy relative to both healthy elderly and AD patients, which might represent a transient compensatory phase during which neural systems try to counterbalance early deficits by enhanced variability and recruitment of additional regions. The gamma band showed the most distinct pattern, with AD patients displaying a pronounced reduction in entropy across frontal and central regions compared to both MCI and healthy individuals. Considering the role of gamma oscillations in high-level cognitive processes and neural binding, this finding is in line with the idea that loss of high-frequency complexity reflects the failure of the integrative processing mechanisms that underlie memory and executive functions.

Correlation analyses reveal negative associations between low-frequency entropy and cognitive performance, as well as positive associations between gamma entropy and executive and memory measures. The main message of these findings is that the high-frequency variability can be considered a marker of continued neural efficiency, while the increase of low-frequency irregularity is a sign of network activity that is disorganized and inefficient.

According to machine learning point of view, entropy and connectivity features-based models managed to depict these changes effectively, as reflected by classification accuracies close to 65-67%. The most effective model - AdaBoost merging all EEG-derived features - demonstrated the benefit of combining local complexity (entropy) and inter-regional synchronization (connectivity).

Compensatory changes are evident in the electrophysiological data of the disease progression presenting nonlinear trajectory: In the early stages, the MCI group consistently showed intermediate and overlapping patterns, underscoring its nature as a transitional state between compensation and decompensation.

Neural circuits try to maintain their capacity through compensatory augmentations in entropy and frontal connectivity; however, as the deterioration goes on (AD), these mechanisms fail, leading to global loss of complexity, over-synchronization, and functional isolation of posterior regions. This progressive collapse of network integration mirrors the clinical deterioration observed in cognitive and functional domains.

Eventually, the compromised neuronal network functioning as the groundwork of clinical symptoms seen in cognitive and functional domains reflects the gradual fatal generalization of the brain's integration capability, observed both electrophysiologically and behaviourally.

A brain aging from normal to pathological state can be illustrated as a transference of adaptive reorganization to maladaptive rigidity—a stage, where compensatory mechanisms of the brain are exhausted, and functional networks lose their dynamic capacity for reconfiguration.

The present findings reveal a seamless progression between physiological and pathological aging, characterized by such early adaptations that are eventually supplanted by neural disorganization and cognitive decline. Normal aging is associated with increased beta connectivity and enhanced local clustering that may be regarded as compensatory mechanisms balancing the reduced global efficiency. Nevertheless, when these mechanisms fail or become dysregulated as in the case of MCI and AD, the system moves towards decreased complexity and over-synchronization that hinders not only cognitive abilities but also flexibility.

Both entropy and coherence measures highlight that excessive regularity (low entropy) and excessive desynchronization are equally harmful, thus stressing the necessity o f maintaining an optimal balance between integration and variability. In this view, healthy aging corresponds to a dynamic equilibrium, whereas pathological aging reflects its breakdown

Machine learning outcomes are in line with the continuum model and demonstrate that EEG-based measures can be used for accurate classification of individuals along this trajectory, with

most informative biomarkers being entropy and connectivity.

Models that combine multiple EEG features thus explaining the present notion of constraints being of a multidimensional nature influencing local, regional, and global neural properties concurrently. This study demonstrates the potential of EEG connectivity measures and complexity to be highly sensitive markers of both adaptive and maladaptive neural dynamics over the aging spectrum. The findings shed light on the brain, amazing capacity to reorganize functional networks in response to aging, but at the same time, they identify the electrophysiological signatures of its inevitable decline. These findings provide a more comprehensive view of the effects of aging on brain functioning, which serves as a basis for the potential EEG biomarkers applications in early diagnosis, monitoring, and targeted interventions in neurodegenerative diseases.

BIBLIOGRAPHY

[1] D. Harman, "The aging process," (in eng), *Basic Life Sci,* vol. 49, pp. 1057-65, 1988, doi: 10.1007/978-1-4684-5568-7_175.

[2] A. Grimm and A. Eckert, "Brain aging and neurodegeneration: from a mitochondrial point of view," (in eng), *J Neurochem,* vol. 143, no. 4, pp. 418-431, 11 2017, doi: 10.1111/jnc.14037.

[3] P. M. Rossini, M. A. Ferilli, L. Rossini, and F. Ferreri, "Clinical neurophysiology of brain plasticity in aging brain," (in eng), *Curr Pharm Des,* vol. 19, no. 36, pp. 6426-39, 2013, doi: 10.2174/1381612811319360004.

[4] Y. Blinkouskaya, A. Caçoilo, T. Gollamudi, S. Jalalian, and J. Weickenmeier, "Brain aging mechanisms with mechanical manifestations," (in eng), *Mech Ageing Dev,* vol. 200, p. 111575, Dec 2021, doi: 10.1016/j.mad.2021.111575.

[5] G. E. Swan, A. LaRue, D. Carmelli, T. E. Reed, and R. R. Fabsitz, "Decline in cognitive performance in aging twins. Heritability and biobehavioral predictors from the National Heart, Lung, and Blood Institute Twin Study," (in eng), *Arch Neurol,* vol. 49, no. 5, pp. 476-81, May 1992, doi: 10.1001/archneur.1992.00530290058012.

[6] B. J. Morris, B. J. Willcox, and T. A. Donlon, "Genetic and epigenetic regulation of human aging and longevity," (in eng), *Biochim Biophys Acta Mol Basis Dis,* vol. 1865, no. 7, pp. 1718-1744, Jul 01 2019, doi: 10.1016/j.bbadis.2018.08.039.

[7] B. J. Willcox *et al.*, "FOXO3A genotype is strongly associated with human longevity," (in eng), *Proc Natl Acad Sci U S A,* vol. 105, no. 37, pp. 13987-92, Sep 16 2008, doi: 10.1073/pnas.0801030105.

[8] A. Z. Herskovits and L. Guarente, "SIRT1 in neurodevelopment and brain senescence," (in eng), *Neuron,* vol. 81, no. 3, pp. 471-83, Feb 05 2014, doi: 10.1016/j.neuron.2014.01.028.

[9] G. Donmez and T. F. Outeiro, "SIRT1 and SIRT2: emerging targets in neurodegeneration," (in eng), *EMBO Mol Med,* vol. 5, no. 3, pp. 344-52, Mar 2013, doi: 10.1002/emmm.201302451.

[10] E. M. Bertucci-Richter, E. P. Shealy, and B. B. Parrott, "Epigenetic drift underlies epigenetic clock signals, but displays distinct responses to lifespan interventions, development, and cellular dedifferentiation," (in eng), *Aging (Albany NY),* vol. 16, no. 2, pp. 1002-1020, Jan 26 2024, doi: 10.18632/aging.205503.

[11] T. M. Karrer, A. K. Josef, R. Mata, E. D. Morris, and G. R. Samanez-Larkin, "Reduced dopamine receptors and transporters but not synthesis capacity in normal aging adults: a meta-analysis," (in eng), *Neurobiol Aging,* vol. 57, pp. 36-46, Sep 2017, doi: 10.1016/j.neurobiolaging.2017.05.006.

[12] E. J. Juarez *et al.*, "Reproducibility of the correlative triad among aging, dopamine receptor availability, and cognition," (in eng), *Psychol Aging,* vol. 34, no. 7, pp. 921-932, Nov 2019, doi: 10.1037/pag0000403.

[13] G. Papenberg *et al.*, "Aging-related losses in dopamine D2/3 receptor availability are linked to working-memory decline across five years," (in eng), *Cereb Cortex,* vol. 35, no. 2, Feb 05 2025, doi: 10.1093/cercor/bhae481.

[14] J. Lee and H. J. Kim, "Normal Aging Induces Changes in the Brain and Neurodegeneration Progress: Review of the Structural, Biochemical, Metabolic, Cellular, and Molecular Changes," (in eng), *Front Aging Neurosci,* vol. 14, p. 931536, 2022, doi: 10.3389/fnagi.2022.931536.

[15] T. M. Karrer, C. L. McLaughlin, C. P. Guaglianone, and G. R. Samanez-Larkin, "Reduced serotonin receptors and transporters in normal aging adults: a meta-analysis of PET and SPECT imaging studies," (in eng), *Neurobiol Aging,* vol. 80, pp. 1-10, Aug 2019, doi: 10.1016/j.neurobiolaging.2019.03.021.

[16] E. Mariani, M. C. Polidori, A. Cherubini, and P. Mecocci, "Oxidative stress in brain aging, neurodegenerative and vascular diseases: an overview," (in eng), *J Chromatogr B Analyt Technol Biomed Life Sci,* vol. 827, no. 1, pp. 65-75, Nov 15 2005, doi: 10.1016/j.jchromb.2005.04.023.

[17] R. D. Brinton, "Estrogen-induced plasticity from cells to circuits: predictions for cognitive function," (in eng), *Trends Pharmacol Sci,* vol. 30, no. 4, pp. 212-22, Apr 2009, doi:

10.1016/j.tips.2008.12.006.
[18] R. O. Roberts, R. H. Cha, D. S. Knopman, R. C. Petersen, and W. A. Rocca, "Postmenopausal estrogen therapy and Alzheimer disease: overall negative findings," (in eng), *Alzheimer Dis Assoc Disord,* vol. 20, no. 3, pp. 141-6, 2006, doi: 10.1097/00002093-200607000-00004.
[19] P. M. Maki and V. W. Henderson, "Hormone therapy, dementia, and cognition: the Women's Health Initiative 10 years on," (in eng), *Climacteric,* vol. 15, no. 3, pp. 256-62, Jun 2012, doi: 10.3109/13697137.2012.660613.
[20] A. Salzmann *et al.*, "Investigating the Relationship Between IGF-I, IGF-II, and IGFBP-3 Concentrations and Later-Life Cognition and Brain Volume," (in eng), *J Clin Endocrinol Metab,* vol. 106, no. 6, pp. 1617-1629, May 13 2021, doi: 10.1210/clinem/dgab121.
[21] W. E. Sonntag, M. Ramsey, and C. S. Carter, "Growth hormone and insulin-like growth factor-1 (IGF-1) and their influence on cognitive aging," (in eng), *Ageing Res Rev,* vol. 4, no. 2, pp. 195-212, May 2005, doi: 10.1016/j.arr.2005.02.001.
[22] S. Gubbi, G. F. Quipildor, N. Barzilai, D. M. Huffman, and S. Milman, "40 YEARS of IGF1: IGF1: the Jekyll and Hyde of the aging brain," (in eng), *J Mol Endocrinol,* vol. 61, no. 1, pp. T171-T185, Jul 2018, doi: 10.1530/JME-18-0093.
[23] S. J. Lupien *et al.*, "Stress hormones and human memory function across the lifespan," (in eng), *Psychoneuroendocrinology,* vol. 30, no. 3, pp. 225-42, Apr 2005, doi: 10.1016/j.psyneuen.2004.08.003.
[24] R. I. Scahill, C. Frost, R. Jenkins, J. L. Whitwell, M. N. Rossor, and N. C. Fox, "A longitudinal study of brain volume changes in normal aging using serial registered magnetic resonance imaging," (in eng), *Arch Neurol,* vol. 60, no. 7, pp. 989-94, Jul 2003, doi: 10.1001/archneur.60.7.989.
[25] A. F. Fotenos, A. Z. Snyder, L. E. Girton, J. C. Morris, and R. L. Buckner, "Normative estimates of cross-sectional and longitudinal brain volume decline in aging and AD," (in eng), *Neurology,* vol. 64, no. 6, pp. 1032-9, Mar 22 2005, doi: 10.1212/01.WNL.0000154530.72969.11.
[26] S. Reix, N. Mechawar, S. A. Susin, R. Quirion, and S. Krantic, "Expression of cortical and hippocampal apoptosis-inducing factor (AIF) in aging and Alzheimer's disease," (in eng), *Neurobiol Aging,* vol. 28, no. 3, pp. 351-6, Mar 2007, doi: 10.1016/j.neurobiolaging.2006.01.003.
[27] J. H. Morrison and M. G. Baxter, "The ageing cortical synapse: hallmarks and implications for cognitive decline," (in eng), *Nat Rev Neurosci,* vol. 13, no. 4, pp. 240-50, Mar 2012, doi: 10.1038/nrn3200.
[28] N. Raz *et al.*, "Regional brain changes in aging healthy adults: general trends, individual differences and modifiers," (in eng), *Cereb Cortex,* vol. 15, no. 11, pp. 1676-89, Nov 2005, doi: 10.1093/cercor/bhi044.
[29] S. G. Mueller *et al.*, "Measurement of hippocampal subfields and age-related changes with high resolution MRI at 4T," (in eng), *Neurobiol Aging,* vol. 28, no. 5, pp. 719-26, May 2007, doi: 10.1016/j.neurobiolaging.2006.03.007.
[30] M. A. Yassa, L. T. Muftuler, and C. E. Stark, "Ultrahigh-resolution microstructural diffusion tensor imaging reveals perforant path degradation in aged humans in vivo," (in eng), *Proc Natl Acad Sci U S A,* vol. 107, no. 28, pp. 12687-91, Jul 13 2010, doi: 10.1073/pnas.1002113107.
[31] A. M. Fjell and K. B. Walhovd, "Structural brain changes in aging: courses, causes and cognitive consequences," (in eng), *Rev Neurosci,* vol. 21, no. 3, pp. 187-221, 2010, doi: 10.1515/revneuro.2010.21.3.187.
[32] D. H. Salat *et al.*, "Age-related alterations in white matter microstructure measured by diffusion tensor imaging," (in eng), *Neurobiol Aging,* vol. 26, no. 8, pp. 1215-27, 2005, doi: 10.1016/j.neurobiolaging.2004.09.017.
[33] S. R. Cox *et al.*, "Ageing and brain white matter structure in 3,513 UK Biobank participants," (in eng), *Nat Commun,* vol. 7, p. 13629, Dec 15 2016, doi: 10.1038/ncomms13629.
[34] D. Head *et al.*, "Differential vulnerability of anterior white matter in nondemented aging with minimal acceleration in dementia of the Alzheimer type: evidence from diffusion tensor imaging," (in eng), *Cereb Cortex,* vol. 14, no. 4, pp. 410-23, Apr 2004, doi: 10.1093/cercor/bhh003.

[35] S. Debette and H. S. Markus, "The clinical importance of white matter hyperintensities on brain magnetic resonance imaging: systematic review and meta-analysis," (in eng), *BMJ,* vol. 341, p. c3666, Jul 26 2010, doi: 10.1136/bmj.c3666.
[36] D. Dumitriu *et al.*, "Selective changes in thin spine density and morphology in monkey prefrontal cortex correlate with aging-related cognitive impairment," (in eng), *J Neurosci,* vol. 30, no. 22, pp. 7507-15, Jun 02 2010, doi: 10.1523/JNEUROSCI.6410-09.2010.
[37] G. Kempermann *et al.*, "Why and how physical activity promotes experience-induced brain plasticity," (in eng), *Front Neurosci,* vol. 4, p. 189, 2010, doi: 10.3389/fnins.2010.00189.
[38] K. I. Erickson *et al.*, "Exercise training increases size of hippocampus and improves memory," (in eng), *Proc Natl Acad Sci U S A,* vol. 108, no. 7, pp. 3017-22, Feb 15 2011, doi: 10.1073/pnas.1015950108.
[39] L. Nyberg, M. Lövdén, K. Riklund, U. Lindenberger, and L. Bäckman, "Memory aging and brain maintenance," (in eng), *Trends Cogn Sci,* vol. 16, no. 5, pp. 292-305, May 2012, doi: 10.1016/j.tics.2012.04.005.
[40] J. S. Damoiseaux *et al.*, "Reduced resting-state brain activity in the "default network" in normal aging," (in eng), *Cereb Cortex,* vol. 18, no. 8, pp. 1856-64, Aug 2008, doi: 10.1093/cercor/bhm207.
[41] N. A. Dennis and R. Cabeza, "Age-related dedifferentiation of learning systems: an fMRI study of implicit and explicit learning," (in eng), *Neurobiol Aging,* vol. 32, no. 12, pp. 2318.e17-30, Dec 2011, doi: 10.1016/j.neurobiolaging.2010.04.004.
[42] R. Cabeza *et al.*, "Maintenance, reserve and compensation: the cognitive neuroscience of healthy ageing," (in eng), *Nat Rev Neurosci,* vol. 19, no. 11, pp. 701-710, Nov 2018, doi: 10.1038/s41583-018-0068-2.
[43] T. A. Salthouse, "Selective review of cognitive aging," (in eng), *J Int Neuropsychol Soc,* vol. 16, no. 5, pp. 754-60, Sep 2010, doi: 10.1017/s1355617710000706.
[44] D. Finkel, C. A. Reynolds, J. J. McArdle, and N. L. Pedersen, "The longitudinal relationship between processing speed and cognitive ability: genetic and environmental influences," (in eng), *Behav Genet,* vol. 35, no. 5, pp. 535-49, Sep 2005, doi: 10.1007/s10519-005-3281-5.
[45] L. G. Nilsson, "Memory function in normal aging," (in eng), *Acta Neurol Scand Suppl,* vol. 179, pp. 7-13, 2003, doi: 10.1034/j.1600-0404.107.s179.5.x.
[46] D. C. Park and P. Reuter-Lorenz, "The adaptive brain: aging and neurocognitive scaffolding," (in eng), *Annu Rev Psychol,* vol. 60, pp. 173-96, 2009, doi: 10.1146/annurev.psych.59.103006.093656.
[47] P. A. Reuter-Lorenz and D. C. Park, "Human neuroscience and the aging mind: a new look at old problems," (in eng), *J Gerontol B Psychol Sci Soc Sci,* vol. 65, no. 4, pp. 405-15, Jul 2010, doi: 10.1093/geronb/gbq035.
[48] R. Cabeza, "Hemispheric asymmetry reduction in older adults: the HAROLD model," (in eng), *Psychol Aging,* vol. 17, no. 1, pp. 85-100, Mar 2002, doi: 10.1037//0882-7974.17.1.85.
[49] S. W. Davis, N. A. Dennis, S. M. Daselaar, M. S. Fleck, and R. Cabeza, "Que PASA? The posterior-anterior shift in aging," (in eng), *Cereb Cortex,* vol. 18, no. 5, pp. 1201-9, May 2008, doi: 10.1093/cercor/bhm155.
[50] P. A. Reuter-Lorenz and D. C. Park, "How does it STAC up? Revisiting the scaffolding theory of aging and cognition," (in eng), *Neuropsychol Rev,* vol. 24, no. 3, pp. 355-70, Sep 2014, doi: 10.1007/s11065-014-9270-9.
[51] Y. Stern, C. A. Barnes, C. Grady, R. N. Jones, and N. Raz, "Brain reserve, cognitive reserve, compensation, and maintenance: operationalization, validity, and mechanisms of cognitive resilience," (in eng), *Neurobiol Aging,* vol. 83, pp. 124-129, Nov 2019, doi: 10.1016/j.neurobiolaging.2019.03.022.
[52] C. N. Harada, M. C. Natelson Love, and K. L. Triebel, "Normal cognitive aging," (in eng), *Clin Geriatr Med,* vol. 29, no. 4, pp. 737-52, Nov 2013, doi: 10.1016/j.cger.2013.07.002.
[53] A. B. Storsve *et al.*, "Differential longitudinal changes in cortical thickness, surface area and volume across the adult life span: regions of accelerating and decelerating change," (in eng), *J Neurosci,* vol. 34, no. 25, pp. 8488-98, Jun 18 2014, doi: 10.1523/JNEUROSCI.0391-14.2014.
[54] J. R. Andrews-Hanna *et al.*, "Disruption of large-scale brain systems in advanced aging," (in

eng), *Neuron,* vol. 56, no. 5, pp. 924-35, Dec 06 2007, doi: 10.1016/j.neuron.2007.10.038.
[55] P. Verhaeghen, "Aging and vocabulary scores: a meta-analysis," (in eng), *Psychol Aging,* vol. 18, no. 2, pp. 332-9, Jun 2003, doi: 10.1037/0882-7974.18.2.332.
[56] L. L. Carstensen *et al.*, "Emotional experience improves with age: evidence based on over 10 years of experience sampling," (in eng), *Psychol Aging,* vol. 26, no. 1, pp. 21-33, Mar 2011, doi: 10.1037/a0021285.
[57] R. L. Buckner, "Memory and executive function in aging and AD: multiple factors that cause decline and reserve factors that compensate," (in eng), *Neuron,* vol. 44, no. 1, pp. 195-208, Sep 30 2004, doi: 10.1016/j.neuron.2004.09.006.
[58] D. Barulli and Y. Stern, "Efficiency, capacity, compensation, maintenance, plasticity: emerging concepts in cognitive reserve," (in eng), *Trends Cogn Sci,* vol. 17, no. 10, pp. 502-9, Oct 2013, doi: 10.1016/j.tics.2013.08.012.
[59] Y. Stern *et al.*, "Whitepaper: Defining and investigating cognitive reserve, brain reserve, and brain maintenance," (in eng), *Alzheimers Dement,* vol. 16, no. 9, pp. 1305-1311, Sep 2020, doi: 10.1016/j.jalz.2018.07.219.
[60] J. L. Price *et al.*, "Neuropathology of nondemented aging: presumptive evidence for preclinical Alzheimer disease," (in eng), *Neurobiol Aging,* vol. 30, no. 7, pp. 1026-36, Jul 2009, doi: 10.1016/j.neurobiolaging.2009.04.002.
[61] D. A. Bennett *et al.*, "Neuropathology of older persons without cognitive impairment from two community-based studies," (in eng), *Neurology,* vol. 66, no. 12, pp. 1837-44, Jun 27 2006, doi: 10.1212/01.wnl.0000219668.47116.e6.
[62] E. J. Rogalski *et al.*, "Youthful memory capacity in old brains: anatomic and genetic clues from the Northwestern SuperAging Project," (in eng), *J Cogn Neurosci,* vol. 25, no. 1, pp. 29-36, Jan 2013, doi: 10.1162/jocn_a_00300.
[63] C. Soto and S. Pritzkow, "Protein misfolding, aggregation, and conformational strains in neurodegenerative diseases," (in eng), *Nat Neurosci,* vol. 21, no. 10, pp. 1332-1340, Oct 2018, doi: 10.1038/s41593-018-0235-9.
[64] V. L. Feigin *et al.*, "The global burden of neurological disorders: translating evidence into policy," (in eng), *Lancet Neurol,* vol. 19, no. 3, pp. 255-265, Mar 2020, doi: 10.1016/S1474-4422(19)30411-9.
[65] "2023 Alzheimer's disease facts and figures," (in eng), *Alzheimers Dement,* vol. 19, no. 4, pp. 1598-1695, Apr 2023, doi: 10.1002/alz.13016.
[66] E. R. Dorsey *et al.*, "Global, regional, and national burden of Parkinson's disease, 1990–2016: a systematic analysis for the Global Burden of Disease Study 2016," *The Lancet Neurology,* vol. 17, no. 11, pp. 939-953, 2018, doi: 10.1016/S1474-4422(18)30295-3.
[67] J. Bang, S. Spina, and B. L. Miller, "Frontotemporal dementia," (in eng), *Lancet,* vol. 386, no. 10004, pp. 1672-82, Oct 24 2015, doi: 10.1016/s0140-6736(15)00461-4.
[68] A. Wimo *et al.*, "The worldwide costs of dementia in 2019," *Alzheimer's & Dementia,* vol. 19, no. 7, pp. 2865-2873, 2023/07/01 2023, doi: https://doi.org/10.1002/alz.12901.
[69] L. C. Walker and M. Jucker, "Neurodegenerative diseases: expanding the prion concept," (in eng), *Annu Rev Neurosci,* vol. 38, pp. 87-103, Jul 08 2015, doi: 10.1146/annurev-neuro-071714-033828.
[70] T. P. Knowles, M. Vendruscolo, and C. M. Dobson, "The amyloid state and its association with protein misfolding diseases," (in eng), *Nat Rev Mol Cell Biol,* vol. 15, no. 6, pp. 384-96, Jun 2014, doi: 10.1038/nrm3810.
[71] S. Gandhi and A. Y. Abramov, "Mechanism of oxidative stress in neurodegeneration," (in eng), *Oxid Med Cell Longev,* vol. 2012, p. 428010, 2012, doi: 10.1155/2012/428010.
[72] M. T. Heneka *et al.*, "Neuroinflammation in Alzheimer's disease," (in eng), *Lancet Neurol,* vol. 14, no. 4, pp. 388-405, Apr 2015, doi: 10.1016/s1474-4422(15)70016-5.
[73] R. Sims *et al.*, "Rare coding variants in PLCG2, ABI3, and TREM2 implicate microglial-mediated innate immunity in Alzheimer's disease," (in eng), *Nat Genet,* vol. 49, no. 9, pp. 1373-1384, Sep 2017, doi: 10.1038/ng.3916.
[74] A. Ciechanover and Y. T. Kwon, "Degradation of misfolded proteins in neurodegenerative diseases: therapeutic targets and strategies," (in eng), *Exp Mol Med,* vol. 47, no. 3, p. e147, Mar

13 2015, doi: 10.1038/emm.2014.117.
[75] M. Sheng, B. L. Sabatini, and T. C. Südhof, "Synapses and Alzheimer's disease," (in eng), *Cold Spring Harb Perspect Biol,* vol. 4, no. 5, May 1 2012, doi: 10.1101/cshperspect.a005777.
[76] M. Prince, A. Wimo, M. Guerchet, G.-C. Ali, Y.-T. Wu, and M. Prina, *World Alzheimer Report 2015. The Global Impact of Dementia. An Analysis of Prevalence, Incidence, Cost and Trends*. 2015.
[77] G. D. F. Collaborators, "Estimation of the global prevalence of dementia in 2019 and forecasted prevalence in 2050: an analysis for the Global Burden of Disease Study 2019," (in eng), *Lancet Public Health,* vol. 7, no. 2, pp. e105-e125, Feb 2022, doi: 10.1016/S2468-2667(21)00249-8.
[78] M. T. Ferretti *et al.*, "Sex differences in Alzheimer disease - the gateway to precision medicine," (in eng), *Nat Rev Neurol,* vol. 14, no. 8, pp. 457-469, Aug 2018, doi: 10.1038/s41582-018-0032-9.
[79] J. A. Hardy and G. A. Higgins, "Alzheimer's disease: the amyloid cascade hypothesis," (in eng), *Science,* vol. 256, no. 5054, pp. 184-5, Apr 10 1992, doi: 10.1126/science.1566067.
[80] D. J. Selkoe and J. Hardy, "The amyloid hypothesis of Alzheimer's disease at 25 years," (in eng), *EMBO Mol Med,* vol. 8, no. 6, pp. 595-608, Jun 2016, doi: 10.15252/emmm.201606210.
[81] D. M. Walsh and D. J. Selkoe, "A beta oligomers - a decade of discovery," (in eng), *J Neurochem,* vol. 101, no. 5, pp. 1172-84, Jun 2007, doi: 10.1111/j.1471-4159.2006.04426.x.
[82] G. M. Shepherd and S. D. Erulkar, "Centenary of the synapse: from Sherrington to the molecular biology of the synapse and beyond," (in eng), *Trends Neurosci,* vol. 20, no. 9, pp. 385-92, Sep 1997, doi: 10.1016/s0166-2236(97)01059-x.
[83] C. C. Liu, T. Kanekiyo, H. Xu, and G. Bu, "Apolipoprotein E and Alzheimer disease: risk, mechanisms and therapy," (in eng), *Nat Rev Neurol,* vol. 9, no. 2, pp. 106-18, Feb 2013, doi: 10.1038/nrneurol.2012.263.
[84] J. C. Lambert *et al.*, "Meta-analysis of 74,046 individuals identifies 11 new susceptibility loci for Alzheimer's disease," (in eng), *Nat Genet,* vol. 45, no. 12, pp. 1452-8, Dec 2013, doi: 10.1038/ng.2802.
[85] H. Braak and E. Braak, "Neuropathological stageing of Alzheimer-related changes," (in eng), *Acta Neuropathol,* vol. 82, no. 4, pp. 239-59, 1991, doi: 10.1007/bf00308809.
[86] H. Braak and K. Del Tredici, "The preclinical phase of the pathological process underlying sporadic Alzheimer's disease," (in eng), *Brain,* vol. 138, no. Pt 10, pp. 2814-33, Oct 2015, doi: 10.1093/brain/awv236.
[87] P. T. Nelson *et al.*, "Correlation of Alzheimer disease neuropathologic changes with cognitive status: a review of the literature," (in eng), *J Neuropathol Exp Neurol,* vol. 71, no. 5, pp. 362-81, May 2012, doi: 10.1097/NEN.0b013e31825018f7.
[88] S. W. Scheff, D. A. Price, F. A. Schmitt, and E. J. Mufson, "Hippocampal synaptic loss in early Alzheimer's disease and mild cognitive impairment," (in eng), *Neurobiol Aging,* vol. 27, no. 10, pp. 1372-84, Oct 2006, doi: 10.1016/j.neurobiolaging.2005.09.012.
[89] R. Guerreiro *et al.*, "TREM2 variants in Alzheimer's disease," (in eng), *N Engl J Med,* vol. 368, no. 2, pp. 117-27, Jan 10 2013, doi: 10.1056/NEJMoa1211851.
[90] R. H. Swerdlow, J. M. Burns, and S. M. Khan, "The Alzheimer's disease mitochondrial cascade hypothesis: progress and perspectives," (in eng), *Biochim Biophys Acta,* vol. 1842, no. 8, pp. 1219-31, Aug 2014, doi: 10.1016/j.bbadis.2013.09.010.
[91] A. Montagne, Z. Zhao, and B. V. Zlokovic, "Alzheimer's disease: A matter of blood-brain barrier dysfunction?," (in eng), *J Exp Med,* vol. 214, no. 11, pp. 3151-3169, Nov 6 2017, doi: 10.1084/jem.20171406.
[92] C. R. Jack *et al.*, "NIA-AA Research Framework: Toward a biological definition of Alzheimer's disease," (in eng), *Alzheimers Dement,* vol. 14, no. 4, pp. 535-562, Apr 2018, doi: 10.1016/j.jalz.2018.02.018.
[93] G. McKhann, D. Drachman, M. Folstein, R. Katzman, D. Price, and E. M. Stadlan, "Clinical diagnosis of Alzheimer's disease," *Report of the NINCDS-ADRDA Work Group* under the auspices of Department of Health and Human Services Task Force on Alzheimer's Disease,* vol. 34, no. 7, pp. 939-939, 1984, doi: 10.1212/wnl.34.7.939.
[94] B. Dubois *et al.*, "[Toward a preventive management Alzheimer's disease]," (in fre), *Bull Acad*

Natl Med, vol. 204, no. 6, pp. 583-588, Jun 2020, doi: 10.1016/j.banm.2020.04.012. Pour une prise en charge préventive de la maladie d'Alzheimer.

[95] D. S. Knopman *et al.*, "Practice parameter: diagnosis of dementia (an evidence-based review). Report of the Quality Standards Subcommittee of the American Academy of Neurology," (in eng), *Neurology,* vol. 56, no. 9, pp. 1143-53, May 8 2001, doi: 10.1212/wnl.56.9.1143.

[96] *Diagnostic and statistical manual of mental disorders: DSM-5™, 5th ed* (Diagnostic and statistical manual of mental disorders: DSM-5™, 5th ed.). Arlington, VA, US: American Psychiatric Publishing, Inc., 2013, pp. xliv, 947-xliv, 947.

[97] M. F. Folstein, S. E. Folstein, and P. R. McHugh, ""Mini-mental state". A practical method for grading the cognitive state of patients for the clinician," (in eng), *J Psychiatr Res,* vol. 12, no. 3, pp. 189-98, Nov 1975, doi: 10.1016/0022-3956(75)90026-6.

[98] Z. S. Nasreddine *et al.*, "The Montreal Cognitive Assessment, MoCA: a brief screening tool for mild cognitive impairment," (in eng), *J Am Geriatr Soc,* vol. 53, no. 4, pp. 695-9, Apr 2005, doi: 10.1111/j.1532-5415.2005.53221.x.

[99] D. Wechsler, *Manual for the Wechsler Adult Intelligence Scale* (Manual for the Wechsler Adult Intelligence Scale.). Oxford, England: Psychological Corp., 1955, pp. vi, 110-vi, 110.

[100] M. D. Lezak, D. B. Howieson, E. D. Bigler, and D. Tranel, *Neuropsychological assessment, 5th ed* (Neuropsychological assessment, 5th ed.). New York, NY, US: Oxford University Press, 2012, pp. xxv, 1161-xxv, 1161.

[101] R. C. Petersen, B. Caracciolo, C. Brayne, S. Gauthier, V. Jelic, and L. Fratiglioni, "Mild cognitive impairment: a concept in evolution," (in eng), *J Intern Med,* vol. 275, no. 3, pp. 214-28, Mar 2014, doi: 10.1111/joim.12190.

[102] G. B. Frisoni, N. C. Fox, C. R. Jack, Jr., P. Scheltens, and P. M. Thompson, "The clinical use of structural MRI in Alzheimer disease," (in eng), *Nat Rev Neurol,* vol. 6, no. 2, pp. 67-77, Feb 2010, doi: 10.1038/nrneurol.2009.215.

[103] B. Fischl, "FreeSurfer," (in eng), *Neuroimage,* vol. 62, no. 2, pp. 774-81, Aug 15 2012, doi: 10.1016/j.neuroimage.2012.01.021.

[104] L. Mosconi *et al.*, "Multicenter standardized 18F-FDG PET diagnosis of mild cognitive impairment, Alzheimer's disease, and other dementias," (in eng), *J Nucl Med,* vol. 49, no. 3, pp. 390-8, Mar 2008, doi: 10.2967/jnumed.107.045385.

[105] J. D. Doecke *et al.*, "Concordance Between Cerebrospinal Fluid Biomarkers with Alzheimer's Disease Pathology Between Three Independent Assay Platforms," (in eng), *J Alzheimers Dis,* vol. 61, no. 1, pp. 169-183, 2018, doi: 10.3233/JAD-170128.

[106] K. Blennow, M. J. de Leon, and H. Zetterberg, "Alzheimer's disease," (in eng), *Lancet,* vol. 368, no. 9533, pp. 387-403, Jul 2006, doi: 10.1016/s0140-6736(06)69113-7.

[107] N. J. Ashton *et al.*, "Plasma p-tau231: a new biomarker for incipient Alzheimer's disease pathology," (in eng), *Acta Neuropathol,* vol. 141, no. 5, pp. 709-724, May 2021, doi: 10.1007/s00401-021-02275-6.

[108] N. Mattsson, U. Andreasson, H. Zetterberg, K. Blennow, and A. s. D. N. Initiative, "Association of Plasma Neurofilament Light With Neurodegeneration in Patients With Alzheimer Disease," (in eng), *JAMA Neurol,* vol. 74, no. 5, pp. 557-566, May 01 2017, doi: 10.1001/jamaneurol.2016.6117.

[109] R. A. Sperling *et al.*, "Toward defining the preclinical stages of Alzheimer's disease: recommendations from the National Institute on Aging-Alzheimer's Association workgroups on diagnostic guidelines for Alzheimer's disease," (in eng), *Alzheimers Dement,* vol. 7, no. 3, pp. 280-92, May 2011, doi: 10.1016/j.jalz.2011.03.003.

[110] V. L. Villemagne *et al.*, "Amyloid β deposition, neurodegeneration, and cognitive decline in sporadic Alzheimer's disease: a prospective cohort study," (in eng), *Lancet Neurol,* vol. 12, no. 4, pp. 357-67, Apr 2013, doi: 10.1016/s1474-4422(13)70044-9.

[111] Y. I. Sheline *et al.*, "Amyloid plaques disrupt resting state default mode network connectivity in cognitively normal elderly," (in eng), *Biol Psychiatry,* vol. 67, no. 6, pp. 584-7, Mar 15 2010, doi: 10.1016/j.biopsych.2009.08.024.

[112] J. L. Cummings, T. Morstorf, and K. Zhong, "Alzheimer's disease drug-development pipeline: few candidates, frequent failures," (in eng), *Alzheimers Res Ther,* vol. 6, no. 4, p. 37, 2014, doi:

10.1186/alzrt269.
[113] R. Brookmeyer, N. Abdalla, C. H. Kawas, and M. M. Corrada, "Forecasting the prevalence of preclinical and clinical Alzheimer's disease in the United States," (in eng), *Alzheimers Dement,* vol. 14, no. 2, pp. 121-129, Feb 2018, doi: 10.1016/j.jalz.2017.10.009.
[114] M. Ganguli, H. H. Dodge, C. Shen, and S. T. DeKosky, "Mild cognitive impairment, amnestic type: an epidemiologic study," (in eng), *Neurology,* vol. 63, no. 1, pp. 115-21, Jul 13 2004, doi: 10.1212/01.wnl.0000132523.27540.81.
[115] S. Gauthier *et al.*, "Mild cognitive impairment," (in eng), *Lancet,* vol. 367, no. 9518, pp. 1262-70, Apr 15 2006, doi: 10.1016/s0140-6736(06)68542-5.
[116] R. C. Petersen, "Clinical practice. Mild cognitive impairment," (in eng), *N Engl J Med,* vol. 364, no. 23, pp. 2227-34, Jun 09 2011, doi: 10.1056/NEJMcp0910237.
[117] A. Ward, H. M. Arrighi, S. Michels, and J. M. Cedarbaum, "Mild cognitive impairment: disparity of incidence and prevalence estimates," (in eng), *Alzheimers Dement,* vol. 8, no. 1, pp. 14-21, Jan 2012, doi: 10.1016/j.jalz.2011.01.002.
[118] W. Bai *et al.*, "Worldwide prevalence of mild cognitive impairment among community dwellers aged 50 years and older: a meta-analysis and systematic review of epidemiology studies," (in eng), *Age Ageing,* vol. 51, no. 8, Aug 02 2022, doi: 10.1093/ageing/afac173.
[119] W. X. Song *et al.*, "Evidence from a meta-analysis and systematic review reveals the global prevalence of mild cognitive impairment," (in eng), *Front Aging Neurosci,* vol. 15, p. 1227112, 2023, doi: 10.3389/fnagi.2023.1227112.
[120] P. S. Sachdev *et al.*, "The Prevalence of Mild Cognitive Impairment in Diverse Geographical and Ethnocultural Regions: The COSMIC Collaboration," (in eng), *PLoS One,* vol. 10, no. 11, p. e0142388, 2015, doi: 10.1371/journal.pone.0142388.
[121] P. M. Rossini *et al.*, "The Italian INTERCEPTOR Project: From the Early Identification of Patients Eligible for Prescription of Antidementia Drugs to a Nationwide Organizational Model for Early Alzheimer's Disease Diagnosis," (in eng), *J Alzheimers Dis,* vol. 72, no. 2, pp. 373-388, 2019, doi: 10.3233/jad-190670.
[122] J. L. Liss *et al.*, "Practical recommendations for timely, accurate diagnosis of symptomatic Alzheimer's disease (MCI and dementia) in primary care: a review and synthesis," (in eng), *J Intern Med,* vol. 290, no. 2, pp. 310-334, Aug 2021, doi: 10.1111/joim.13244.
[123] E. V. Ward, C. J. Berry, and D. R. Shanks, "Age effects on explicit and implicit memory," (in eng), *Front Psychol,* vol. 4, p. 639, 2013, doi: 10.3389/fpsyg.2013.00639.
[124] A. J. Mitchell and M. Shiri-Feshki, "Rate of progression of mild cognitive impairment to dementia--meta-analysis of 41 robust inception cohort studies," (in eng), *Acta Psychiatr Scand,* vol. 119, no. 4, pp. 252-65, Apr 2009, doi: 10.1111/j.1600-0447.2008.01326.x.
[125] R. Roberts and D. S. Knopman, "Classification and epidemiology of MCI," (in eng), *Clin Geriatr Med,* vol. 29, no. 4, pp. 753-72, Nov 2013, doi: 10.1016/j.cger.2013.07.003.
[126] P. Garcia *et al.*, "Sex significantly predicts medial temporal volume when controlling for the influence of ApoE4 biomarker and demographic variables: A cross-ethnic comparison," (in eng), *J Int Neuropsychol Soc,* vol. 30, no. 2, pp. 128-137, Feb 2024, doi: 10.1017/S1355617723000358.
[127] M. M. Mielke, P. Vemuri, and W. A. Rocca, "Clinical epidemiology of Alzheimer's disease: assessing sex and gender differences," (in eng), *Clin Epidemiol,* vol. 6, pp. 37-48, 2014, doi: 10.2147/CLEP.S37929.
[128] N. L. Campbell, F. Unverzagt, M. A. LaMantia, B. A. Khan, and M. A. Boustani, "Risk factors for the progression of mild cognitive impairment to dementia," (in eng), *Clin Geriatr Med,* vol. 29, no. 4, pp. 873-93, Nov 2013, doi: 10.1016/j.cger.2013.07.009.
[129] A. M. Sanford, "Mild Cognitive Impairment," (in eng), *Clin Geriatr Med,* vol. 33, no. 3, pp. 325-337, Aug 2017, doi: 10.1016/j.cger.2017.02.005.
[130] "Estimation of the global prevalence of dementia in 2019 and forecasted prevalence in 2050: an analysis for the Global Burden of Disease Study 2019," (in eng), *Lancet Public Health,* vol. 7, no. 2, pp. e105-e125, Feb 2022, doi: 10.1016/s2468-2667(21)00249-8.
[131] J. Hugo and M. Ganguli, "Dementia and cognitive impairment: epidemiology, diagnosis, and treatment," (in eng), *Clin Geriatr Med,* vol. 30, no. 3, pp. 421-42, Aug 2014, doi:

10.1016/j.cger.2014.04.001.
[132] A. Patel and D. J. Chong, "Obstructive Sleep Apnea: Cognitive Outcomes," (in eng), *Clin Geriatr Med,* vol. 37, no. 3, pp. 457-467, Aug 2021, doi: 10.1016/j.cger.2021.04.007.
[133] B. Reisberg, S. H. Ferris, M. J. de Leon, and T. Crook, "Global Deterioration Scale (GDS)," (in eng), *Psychopharmacol Bull,* vol. 24, no. 4, pp. 661-3, 1988.
[134] R. C. Petersen, G. E. Smith, S. C. Waring, R. J. Ivnik, E. G. Tangalos, and E. Kokmen, "Mild cognitive impairment: clinical characterization and outcome," (in eng), *Arch Neurol,* vol. 56, no. 3, pp. 303-8, Mar 1999, doi: 10.1001/archneur.56.3.303.
[135] R. C. Petersen, "Mild Cognitive Impairment," (in eng), *Continuum (Minneap Minn),* vol. 22, no. 2 Dementia, pp. 404-18, Apr 2016, doi: 10.1212/con.0000000000000313.
[136] "StatPearls," 2025.
[137] R. C. Petersen, "Mild cognitive impairment as a diagnostic entity," (in eng), *J Intern Med,* vol. 256, no. 3, pp. 183-94, Sep 2004, doi: 10.1111/j.1365-2796.2004.01388.x.
[138] B. Winblad *et al.*, "Mild cognitive impairment--beyond controversies, towards a consensus: report of the International Working Group on Mild Cognitive Impairment," (in eng), *J Intern Med,* vol. 256, no. 3, pp. 240-6, Sep 2004, doi: 10.1111/j.1365-2796.2004.01380.x.
[139] B. Reisberg *et al.*, "The pre-mild cognitive impairment, subjective cognitive impairment stage of Alzheimer's disease," (in eng), *Alzheimers Dement,* vol. 4, no. 1 Suppl 1, pp. S98-S108, Jan 2008, doi: 10.1016/j.jalz.2007.11.017.
[140] A. C. van Harten *et al.*, "Preclinical AD predicts decline in memory and executive functions in subjective complaints," (in eng), *Neurology,* vol. 81, no. 16, pp. 1409-16, Oct 15 2013, doi: 10.1212/WNL.0b013e3182a8418b.
[141] R. Stewart *et al.*, "Longitudinal neuroimaging correlates of subjective memory impairment: 4-year prospective community study," (in eng), *Br J Psychiatry,* vol. 198, no. 3, pp. 199-205, Mar 2011, doi: 10.1192/bjp.bp.110.078683.
[142] K. Abdulrab and R. Heun, "Subjective Memory Impairment. A review of its definitions indicates the need for a comprehensive set of standardised and validated criteria," (in eng), *Eur Psychiatry,* vol. 23, no. 5, pp. 321-30, Aug 2008, doi: 10.1016/j.eurpsy.2008.02.004.
[143] F. Jessen *et al.*, "A conceptual framework for research on subjective cognitive decline in preclinical Alzheimer's disease," (in eng), *Alzheimers Dement,* vol. 10, no. 6, pp. 844-52, Nov 2014, doi: 10.1016/j.jalz.2014.01.001.
[144] A. J. Mitchell, H. Beaumont, D. Ferguson, M. Yadegarfar, and B. Stubbs, "Risk of dementia and mild cognitive impairment in older people with subjective memory complaints: meta-analysis," (in eng), *Acta Psychiatr Scand,* vol. 130, no. 6, pp. 439-51, Dec 2014, doi: 10.1111/acps.12336.
[145] R. Buckley *et al.*, "Self and informant memory concerns align in healthy memory complainers and in early stages of mild cognitive impairment but separate with increasing cognitive impairment," (in eng), *Age Ageing,* vol. 44, no. 6, pp. 1012-9, Nov 2015, doi: 10.1093/ageing/afv136.
[146] B. Dubois, "The Emergence of a New Conceptual Framework for Alzheimer's Disease," (in eng), *J Alzheimers Dis,* vol. 62, no. 3, pp. 1059-1066, 2018, doi: 10.3233/JAD-170536.
[147] B. Dubois *et al.*, "Preclinical Alzheimer's disease: Definition, natural history, and diagnostic criteria," (in eng), *Alzheimers Dement,* vol. 12, no. 3, pp. 292-323, Mar 2016, doi: 10.1016/j.jalz.2016.02.002.
[148] J. P. Holland *et al.*, "Alternative approaches for PET radiotracer development in Alzheimer's disease: imaging beyond plaque," (in eng), *J Labelled Comp Radiopharm,* vol. 57, no. 4, pp. 323-31, Apr 2014, doi: 10.1002/jlcr.3158.
[149] K. E. Pike *et al.*, "Names and numberplates: quasi-everyday associative memory tasks for distinguishing amnestic mild cognitive impairment from healthy aging," (in eng), *J Clin Exp Neuropsychol,* vol. 34, no. 3, pp. 269-78, 2012, doi: 10.1080/13803395.2011.633498.
[150] S. Kasper *et al.*, "Management of mild cognitive impairment (MCI): The need for national and international guidelines," (in eng), *World J Biol Psychiatry,* vol. 21, no. 8, pp. 579-594, Oct 2020, doi: 10.1080/15622975.2019.1696473.
[151] M. S. Albert *et al.*, "The diagnosis of mild cognitive impairment due to Alzheimer's disease:

recommendations from the National Institute on Aging-Alzheimer's Association workgroups on diagnostic guidelines for Alzheimer's disease," (in eng), *Alzheimers Dement,* vol. 7, no. 3, pp. 270-9, May 2011, doi: 10.1016/j.jalz.2011.03.008.

[152] J. C. Morris, "The Clinical Dementia Rating (CDR): current version and scoring rules," (in eng), *Neurology,* vol. 43, no. 11, pp. 2412-4, Nov 1993, doi: 10.1212/wnl.43.11.2412-a.

[153] J. K. Kueper, M. Speechley, and M. Montero-Odasso, "The Alzheimer's Disease Assessment Scale-Cognitive Subscale (ADAS-Cog): Modifications and Responsiveness in Pre-Dementia Populations. A Narrative Review," (in eng), *J Alzheimers Dis,* vol. 63, no. 2, pp. 423-444, 2018, doi: 10.3233/JAD-170991.

[154] M. R. Ralph, "Validity of the Trail Making Test as an Indicator of Organic Brain Damage," *Perceptual and Motor Skills,* vol. 8, no. 3, pp. 271-276, 1958, doi: 10.2466/pms.1958.8.3.271.

[155] R. I. Pfeffer, T. T. Kurosaki, C. H. Harrah, J. M. Chance, and S. Filos, "Measurement of functional activities in older adults in the community," (in eng), *J Gerontol,* vol. 37, no. 3, pp. 323-9, May 1982, doi: 10.1093/geronj/37.3.323.

[156] M. P. Lawton and E. M. Brody, "Assessment of older people: self-maintaining and instrumental activities of daily living," (in eng), *Gerontologist,* vol. 9, no. 3, pp. 179-86, Autumn 1969.

[157] J. L. Cummings, M. Mega, K. Gray, S. Rosenberg-Thompson, D. A. Carusi, and J. Gornbein, "The Neuropsychiatric Inventory: comprehensive assessment of psychopathology in dementia," (in eng), *Neurology,* vol. 44, no. 12, pp. 2308-14, Dec 1994, doi: 10.1212/wnl.44.12.2308.

[158] J. W. Britton *et al.*, in *Electroencephalography (EEG): An Introductory Text and Atlas of Normal and Abnormal Findings in Adults, Children, and Infants*, E. K. St. Louis and L. C. Frey Eds. Chicago: American Epilepsy Society

[159] H. Berger, "Über das Elektrenkephalogramm des Menschen," *Archiv für Psychiatrie und Nervenkrankheiten,* vol. 87, no. 1, pp. 527-570, 1929/12/01 1929, doi: 10.1007/BF01797193.

[160] C. Babiloni *et al.*, "Alpha rhythm and Alzheimer's disease: Has Hans Berger's dream come true?," (in eng), *Clin Neurophysiol,* vol. 172, pp. 33-50, Apr 2025, doi: 10.1016/j.clinph.2025.02.256.

[161] J. Santamaria and K. H. Chiappa, "The EEG of drowsiness in normal adults," (in eng), *J Clin Neurophysiol,* vol. 4, no. 4, pp. 327-82, Oct 1987.

[162] J. Malmivuo and R. Plonsey, "257Electroencephalography," in *Bioelectromagnetism: Principles and Applications of Bioelectric and Biomagnetic Fields*: Oxford University Press, 1995, sec. Oxford Academic, p. 0.

[163] S. Hestrin and W. E. Armstrong, "Morphology and physiology of cortical neurons in layer I," (in eng), *J Neurosci,* vol. 16, no. 17, pp. 5290-300, Sep 01 1996, doi: 10.1523/JNEUROSCI.16-17-05290.1996.

[164] A. Proekt, "Brief Introduction to Electroencephalography," (in eng), *Methods Enzymol,* vol. 603, pp. 257-277, 2018, doi: 10.1016/bs.mie.2018.02.009.

[165] J. M. Bekkers, "Pyramidal neurons," (in eng), *Curr Biol,* vol. 21, no. 24, p. R975, Dec 20 2011, doi: 10.1016/j.cub.2011.10.037.

[166] Y. Kawaguchi, "Groupings of nonpyramidal and pyramidal cells with specific physiological and morphological characteristics in rat frontal cortex," (in eng), *J Neurophysiol,* vol. 69, no. 2, pp. 416-31, Feb 1993, doi: 10.1152/jn.1993.69.2.416.

[167] A. M. Feyissa and W. O. Tatum, "Adult EEG," (in eng), *Handb Clin Neurol,* vol. 160, pp. 103-124, 2019, doi: 10.1016/B978-0-444-64032-1.00007-2.

[168] M. S. Hämäläinen and R. J. Ilmoniemi, "Interpreting magnetic fields of the brain: minimum norm estimates," (in eng), *Med Biol Eng Comput,* vol. 32, no. 1, pp. 35-42, Jan 1994, doi: 10.1007/bf02512476.

[169] A. B. Usakli, "Improvement of EEG signal acquisition: an electrical aspect for state of the art of front end," (in eng), *Comput Intell Neurosci,* vol. 2010, p. 630649, 2010, doi: 10.1155/2010/630649.

[170] A. Ebner, G. Sciarretta, C. M. Epstein, and M. Nuwer, "EEG instrumentation. The International Federation of Clinical Neurophysiology," (in eng), *Electroencephalogr Clin Neurophysiol Suppl,* vol. 52, pp. 7-10, 1999.

[171] U. R. Acharya, F. Molinari, S. V. Sree, S. Chattopadhyay, K.-H. Ng, and J. S. Suri, "Automated diagnosis of epileptic EEG using entropies," *Biomedical Signal Processing and Control,* vol. 7, no. 4, pp. 401-408, 2012/07/01/ 2012, doi: https://doi.org/10.1016/j.bspc.2011.07.007.
[172] V. Jurcak, D. Tsuzuki, and I. Dan, "10/20, 10/10, and 10/5 systems revisited: their validity as relative head-surface-based positioning systems," (in eng), *Neuroimage,* vol. 34, no. 4, pp. 1600-11, Feb 2007, doi: 10.1016/j.neuroimage.2006.09.024.
[173] K. Natarajan, U. R. Acharya, F. Alias, T. Tiboleng, and S. K. Puthusserypady, "Nonlinear analysis of EEG signals at different mental states," (in eng), *Biomed Eng Online,* vol. 3, no. 1, p. 7, Mar 16 2004, doi: 10.1186/1475-925x-3-7.
[174] J. N. Acharya and V. J. Acharya, "Overview of EEG Montages and Principles of Localization," (in eng), *J Clin Neurophysiol,* vol. 36, no. 5, pp. 325-329, Sep 2019, doi: 10.1097/WNP.0000000000000538.
[175] H. H. Jasper, "The ten-twenty electrode system of the International Federation," *Electroencephalogr Clin Neurophysiol,* vol. 10, pp. 371-375, 1958.
[176] Y. Kuroiwa and G. G. Celesia, "Clinical significance of periodic EEG patterns," (in eng), *Arch Neurol,* vol. 37, no. 1, pp. 15-20, Jan 1980, doi: 10.1001/archneur.1980.00500500045005.
[177] P. Gloor, G. Ball, and N. Schaul, "Brain lesions that produce delta waves in the EEG," (in eng), *Neurology,* vol. 27, no. 4, pp. 326-33, Apr 1977.
[178] S. Kubicki, W. M. Herrmann, K. Fichte, and G. Freund, "Reflections on the topics: EEG frequency bands and regulation of vigilance," (in eng), *Pharmakopsychiatr Neuropsychopharmakol,* vol. 12, no. 2, pp. 237-45, Mar 1979, doi: 10.1055/s-0028-1094615.
[179] A. A. Borbély, F. Baumann, D. Brandeis, I. Strauch, and D. Lehmann, "Sleep deprivation: effect on sleep stages and EEG power density in man," (in eng), *Electroencephalogr Clin Neurophysiol,* vol. 51, no. 5, pp. 483-95, May 1981, doi: 10.1016/0013-4694(81)90225-x.
[180] H. Soininen, J. Partanen, A. Pääkkonen, E. Koivisto, and P. J. Riekkinen, "Changes in absolute power values of EEG spectra in the follow-up of Alzheimer's disease," *Acta Neurologica Scandinavica,* vol. 83, no. 2, pp. 133-136, 1991, doi: 10.1111/j.1600-0404.1991.tb04662.x.
[181] L. S. Leung, "Theta rhythm during REM sleep and waking: correlations between power, phase and frequency," (in eng), *Electroencephalogr Clin Neurophysiol,* vol. 58, no. 6, pp. 553-64, Dec 1984, doi: 10.1016/0013-4694(84)90045-2.
[182] W. Klimesch, "EEG alpha and theta oscillations reflect cognitive and memory performance: a review and analysis," (in eng), *Brain Res Brain Res Rev,* vol. 29, no. 2-3, pp. 169-95, Apr 1999.
[183] M. M. Widagdo, J. M. Pierson, and R. D. Helme, "Age-related changes in qEEG during cognitive tasks," (in eng), *Int J Neurosci,* vol. 95, no. 1-2, pp. 63-75, Jul 1998, doi: 10.3109/00207459809000650.
[184] W. Klimesch, P. Sauseng, and S. Hanslmayr, "EEG alpha oscillations: the inhibition-timing hypothesis," (in eng), *Brain Res Rev,* vol. 53, no. 1, pp. 63-88, Jan 2007, doi: 10.1016/j.brainresrev.2006.06.003.
[185] W. Klimesch, "Memory processes, brain oscillations and EEG synchronization," (in eng), *Int J Psychophysiol,* vol. 24, no. 1-2, pp. 61-100, Nov 1996, doi: 10.1016/s0167-8760(96)00057-8.
[186] M. R. Brier *et al.*, "Frontal theta and alpha power and coherence changes are modulated by semantic complexity in Go/NoGo tasks," *International Journal of Psychophysiology,* vol. 78, no. 3, pp. 215-224, 2010/12/01/ 2010, doi: https://doi.org/10.1016/j.ijpsycho.2010.07.011.
[187] O. M. Bazanova and D. Vernon, "Interpreting EEG alpha activity," (in eng), *Neurosci Biobehav Rev,* vol. 44, pp. 94-110, Jul 2014, doi: 10.1016/j.neubiorev.2013.05.007.
[188] A. Athanasiou, M. A. Klados, C. Styliadis, N. Foroglou, K. Polyzoidis, and P. D. Bamidis, "Investigating the Role of Alpha and Beta Rhythms in Functional Motor Networks," (in eng), *Neuroscience,* vol. 378, pp. 54-70, 05 15 2018, doi: 10.1016/j.neuroscience.2016.05.044.
[189] L. M. Doyle, K. Yarrow, and P. Brown, "Lateralization of event-related beta desynchronization in the EEG during pre-cued reaction time tasks," (in eng), *Clin Neurophysiol,* vol. 116, no. 8, pp. 1879-88, Aug 2005, doi: 10.1016/j.clinph.2005.03.017.
[190] C. C. Chen *et al.*, "Complexity of subthalamic 13-35 Hz oscillatory activity directly correlates with clinical impairment in patients with Parkinson's disease," (in eng), *Exp Neurol,* vol. 224, no. 1, pp. 234-40, Jul 2010, doi: 10.1016/j.expneurol.2010.03.015.

[191] A. G. Guggisberg, S. S. Dalal, A. M. Findlay, and S. S. Nagarajan, "High-frequency oscillations in distributed neural networks reveal the dynamics of human decision making," (in eng), *Front Hum Neurosci,* vol. 1, p. 14, 2007, doi: 10.3389/neuro.09.014.2007.
[192] J. Kaiser, T. Heidegger, and W. Lutzenberger, "Behavioral relevance of gamma-band activity for short-term memory-based auditory decision-making," (in eng), *Eur J Neurosci,* vol. 27, no. 12, pp. 3322-8, Jun 2008, doi: 10.1111/j.1460-9568.2008.06290.x.
[193] T. P. Jung *et al.*, "Removing electroencephalographic artifacts by blind source separation," (in eng), *Psychophysiology,* vol. 37, no. 2, pp. 163-78, Mar 2000.
[194] J. Iriarte *et al.*, "Independent component analysis as a tool to eliminate artifacts in EEG: a quantitative study," (in eng), *J Clin Neurophysiol,* vol. 20, no. 4, pp. 249-57, 2003 Jul-Aug 2003, doi: 10.1097/00004691-200307000-00004.
[195] W. O. Tatum, B. A. Dworetzky, and D. L. Schomer, "Artifact and recording concepts in EEG," (in eng), *J Clin Neurophysiol,* vol. 28, no. 3, pp. 252-63, Jun 2011, doi: 10.1097/WNP.0b013e31821c3c93.
[196] J. A. Urigüen and B. Garcia-Zapirain, "EEG artifact removal-state-of-the-art and guidelines," (in eng), *J Neural Eng,* vol. 12, no. 3, p. 031001, Jun 2015, doi: 10.1088/1741-2560/12/3/031001.
[197] X. Jiang, G. B. Bian, and Z. Tian, "Removal of Artifacts from EEG Signals: A Review," (in eng), *Sensors (Basel),* vol. 19, no. 5, Feb 26 2019, doi: 10.3390/s19050987.
[198] V. Asadpour and A. Engelbrecht, *Brain-Computer Interface*. IntechOpen, 2022.
[199] A. M. Husain, *Practical Epilepsy*. Springer Publishing Company, 2015.
[200] F. Miraglia, F. Vecchio, P. Bramanti, and P. M. Rossini, "EEG characteristics in "eyes-open" versus "eyes-closed" conditions: Small-world network architecture in healthy aging and age-related brain degeneration," (in eng), *Clin Neurophysiol,* vol. 127, no. 2, pp. 1261-1268, Feb 2016, doi: 10.1016/j.clinph.2015.07.040.
[201] G. Barbati, C. Porcaro, F. Zappasodi, P. M. Rossini, and F. Tecchio, "Optimization of an independent component analysis approach for artifact identification and removal in magnetoencephalographic signals," (in eng), *Clin Neurophysiol,* vol. 115, no. 5, pp. 1220-32, May 2004, doi: 10.1016/j.clinph.2003.12.015.
[202] A. Delorme and S. Makeig, "EEGLAB: an open source toolbox for analysis of single-trial EEG dynamics including independent component analysis," (in eng), *J Neurosci Methods,* vol. 134, no. 1, pp. 9-21, Mar 2004, doi: 10.1016/j.jneumeth.2003.10.009.
[203] C. Babiloni *et al.*, "What electrophysiology tells us about Alzheimer's disease: a window into the synchronization and connectivity of brain neurons," *Neurobiology of Aging,* vol. 85, pp. 58-73, 2020/01/01/ 2020, doi: https://doi.org/10.1016/j.neurobiolaging.2019.09.008.
[204] J. Jeong, "EEG dynamics in patients with Alzheimer's disease," (in eng), *Clin Neurophysiol,* vol. 115, no. 7, pp. 1490-505, Jul 2004, doi: 10.1016/j.clinph.2004.01.001.
[205] P. M. Rossini, S. Rossi, C. Babiloni, and J. Polich, "Clinical neurophysiology of aging brain: from normal aging to neurodegeneration," (in eng), *Prog Neurobiol,* vol. 83, no. 6, pp. 375-400, Dec 2007, doi: 10.1016/j.pneurobio.2007.07.010.
[206] E. Basar, *Memory and brain dynamics: Oscillations integrating attention, perception, learning, and memory*. CRC press, 2004.
[207] D. V. Moretti, "Conversion of mild cognitive impairment patients in Alzheimer's disease: prognostic value of Alpha3/Alpha2 electroencephalographic rhythms power ratio," (in eng), *Alzheimers Res Ther,* vol. 7, p. 80, Dec 29 2015, doi: 10.1186/s13195-015-0162-x.
[208] S. S. Poil, W. de Haan, W. M. van der Flier, H. D. Mansvelder, P. Scheltens, and K. Linkenkaer-Hansen, "Integrative EEG biomarkers predict progression to Alzheimer's disease at the MCI stage," (in eng), *Front Aging Neurosci,* vol. 5, p. 58, 2013, doi: 10.3389/fnagi.2013.00058.
[209] S. Basharpoor, F. Heidari, and P. Molavi, "EEG coherence in theta, alpha, and beta bands in frontal regions and executive functions," (in eng), *Appl Neuropsychol Adult,* vol. 28, no. 3, pp. 310-317, 2021 May-Jun 2021, doi: 10.1080/23279095.2019.1632860.
[210] F. Vecchio, F. Miraglia, E. Judica, M. Cotelli, F. Alù, and P. M. Rossini, "Human brain networks: a graph theoretical analysis of cortical connectivity normative database from EEG data in healthy elderly subjects," (in eng), *Geroscience,* Mar 2020, doi: 10.1007/s11357-020-

00176-2.
[211] K. Zawiślak-Fornagiel *et al.*, "Quantitative EEG Spectral and Connectivity Analysis for Cognitive Decline in Amnestic Mild Cognitive Impairment," (in eng), *J Alzheimers Dis,* vol. 97, no. 3, pp. 1235-1247, 2024, doi: 10.3233/JAD-230485.
[212] J. Zhou, S. Liu, K. K. Ng, and J. Wang, "Applications of Resting-State Functional Connectivity to Neurodegenerative Disease," (in eng), *Neuroimaging Clin N Am,* vol. 27, no. 4, pp. 663-683, Nov 2017, doi: 10.1016/j.nic.2017.06.007.
[213] T. Koenig *et al.*, "Decreased EEG synchronization in Alzheimer's disease and mild cognitive impairment," (in eng), *Neurobiol Aging,* vol. 26, no. 2, pp. 165-71, Feb 2005, doi: 10.1016/j.neurobiolaging.2004.03.008.
[214] F. Vecchio *et al.*, "Human Brain Networks in Physiological and Pathological Aging: Reproducibility of Electroencephalogram Graph Theoretical Analysis in Cortical Connectivity," (in eng), *Brain Connect,* vol. 12, no. 1, pp. 41-51, Feb 2022, doi: 10.1089/brain.2020.0824.
[215] F. Vecchio, F. Miraglia, P. Bramanti, and P. M. Rossini, "Human brain networks in physiological aging: a graph theoretical analysis of cortical connectivity from EEG data," (in eng), *J Alzheimers Dis,* vol. 41, no. 4, pp. 1239-49, 2014, doi: 10.3233/JAD-140090.
[216] A. R. McIntosh, V. Vakorin, N. Kovacevic, H. Wang, A. Diaconescu, and A. B. Protzner, "Spatiotemporal dependency of age-related changes in brain signal variability," (in eng), *Cereb Cortex,* vol. 24, no. 7, pp. 1806-17, Jul 2014, doi: 10.1093/cercor/bht030.
[217] Z. Wang and A. Alzheimer's Disease Neuroimaging Initiative, "Brain Entropy Mapping in Healthy Aging and Alzheimer's Disease," (in eng), *Front Aging Neurosci,* vol. 12, p. 596122, 2020, doi: 10.3389/fnagi.2020.596122.
[218] A. Cacciotti, C. Pappalettera, F. Miraglia, P. M. Rossini, and F. Vecchio, "EEG entropy insights in the context of physiological aging and Alzheimer's and Parkinson's diseases: a comprehensive review," (in eng), *Geroscience,* vol. 46, no. 6, pp. 5537-5557, Dec 2024, doi: 10.1007/s11357-024-01185-1.
[219] C. Pappalettera, A. Cacciotti, L. Nucci, F. Miraglia, P. M. Rossini, and F. Vecchio. (2022). Approximate Entropy analysis across electroencephalographic rhythmic frequency bands during physiological aging of human brain.
[220] R. V. L. Hartley, "Transmission of information," *The Bell System Technical Journal,* vol. 7, no. 3, pp. 535-563, 1928, doi: 10.1002/j.1538-7305.1928.tb01236.x.
[221] H. Nyquist, "Certain factors affecting telegraph speed," *The Bell System Technical Journal,* vol. 3, no. 2, pp. 324-346, 1924, doi: 10.1002/j.1538-7305.1924.tb01361.x.
[222] C. Bandt and B. Pompe, "Permutation entropy: a natural complexity measure for time series," (in eng), *Phys Rev Lett,* vol. 88, no. 17, p. 174102, Apr 29 2002, doi: 10.1103/PhysRevLett.88.174102.
[223] S. Pincus, "Approximate entropy (ApEn) as a complexity measure," (in eng), *Chaos,* vol. 5, no. 1, pp. 110-117, Mar 1995, doi: 10.1063/1.166092.
[224] J. S. Richman and J. R. Moorman, "Physiological time-series analysis using approximate entropy and sample entropy," (in eng), *Am J Physiol Heart Circ Physiol,* vol. 278, no. 6, pp. H2039-49, Jun 2000, doi: 10.1152/ajpheart.2000.278.6.H2039.
[225] M. Costa, A. L. Goldberger, and C. K. Peng, "Multiscale entropy analysis of biological signals," (in eng), *Phys Rev E Stat Nonlin Soft Matter Phys,* vol. 71, no. 2 Pt 1, p. 021906, Feb 2005, doi: 10.1103/PhysRevE.71.021906.
[226] S. M. Pincus, "Approximate entropy as a measure of system complexity," (in eng), *Proc Natl Acad Sci U S A,* vol. 88, no. 6, pp. 2297-301, Mar 15 1991, doi: 10.1073/pnas.88.6.2297.
[227] D. Salmaso and A. M. Longoni, "Problems in the assessment of hand preference," (in eng), *Cortex,* vol. 21, no. 4, pp. 533-49, Dec 1985.
[228] F. Miraglia, F. Vecchio, and P. M. Rossini, "Brain electroencephalographic segregation as a biomarker of learning," (in eng), *Neural Netw,* vol. 106, pp. 168-174, Oct 2018, doi: 10.1016/j.neunet.2018.07.005.
[229] R. Sun, W. W. Wong, J. Wang, and R. K. Tong, "Changes in Electroencephalography Complexity using a Brain Computer Interface-Motor Observation Training in Chronic Stroke

Patients: A Fuzzy Approximate Entropy Analysis," (in eng), *Front Hum Neurosci,* vol. 11, p. 444, 2017, doi: 10.3389/fnhum.2017.00444.
[230] D. Abásolo, R. Hornero, P. Espino, J. Poza, C. I. Sánchez, and R. de la Rosa, "Analysis of regularity in the EEG background activity of Alzheimer's disease patients with Approximate Entropy," (in eng), *Clin Neurophysiol,* vol. 116, no. 8, pp. 1826-34, Aug 2005, doi: 10.1016/j.clinph.2005.04.001.
[231] C. Arti Patle and Deepak Singh, "SVM kernel functions for classification," *2013 International Conference on Advances in Technology and Engineering (ICATE),* pp. 1-9, 2013.
[232] F. Vecchio *et al.*, "Classification of Alzheimer's Disease respect to physiological aging with innovative EEG Biomarkers in a machine learning implementation. (i*n press)*," *Journal of Alzheimer's Disease,* 2020.
[233] A. Sarica, A. Cerasa, and A. Quattrone, "Random Forest Algorithm for the Classification of Neuroimaging Data in Alzheimer's Disease: A Systematic Review," (in eng), *Front Aging Neurosci,* vol. 9, p. 329, 2017, doi: 10.3389/fnagi.2017.00329.
[234] N. Raz, F. M. Gunning-Dixon, D. Head, J. H. Dupuis, and J. D. Acker, "Neuroanatomical correlates of cognitive aging: evidence from structural magnetic resonance imaging," (in eng), *Neuropsychology,* vol. 12, no. 1, pp. 95-114, Jan 1998, doi: 10.1037//0894-4105.12.1.95.
[235] C. R. Jack *et al.*, "Tracking pathophysiological processes in Alzheimer's disease: an updated hypothetical model of dynamic biomarkers," (in eng), *Lancet Neurol,* vol. 12, no. 2, pp. 207-16, Feb 2013, doi: 10.1016/S1474-4422(12)70291-0.
[236] F. Vecchio *et al.*, "Human brain networks in physiological and pathological aging: reproducibility of EEG graph theoretical analysis in cortical connectivity," (in eng), *Brain Connect,* Apr 02 2021, doi: 10.1089/brain.2020.0824.
[237] F. Vecchio *et al.*, "Human brain networks in cognitive decline: a graph theoretical analysis of cortical connectivity from EEG data," (in eng), *J Alzheimers Dis,* vol. 41, no. 1, pp. 113-27, 2014, doi: 10.3233/jad-132087.
[238] C. J. Stam and J. C. Reijneveld, "Graph theoretical analysis of complex networks in the brain," (in eng), *Nonlinear Biomed Phys,* vol. 1, no. 1, p. 3, Jul 05 2007, doi: 10.1186/1753-4631-1-3.
[239] R. L. Carhart-Harris, "The entropic brain - revisited," (in eng), *Neuropharmacology,* vol. 142, pp. 167-178, 11 2018, doi: 10.1016/j.neuropharm.2018.03.010.
[240] T. Mizuno *et al.*, "Assessment of EEG dynamical complexity in Alzheimer's disease using multiscale entropy," (in eng), *Clin Neurophysiol,* vol. 121, no. 9, pp. 1438-1446, Sep 2010, doi: 10.1016/j.clinph.2010.03.025.
[241] D. Abásolo, R. Hornero, C. Gómez, M. García, and M. López, "Analysis of EEG background activity in Alzheimer's disease patients with Lempel-Ziv complexity and central tendency measure," (in eng), *Med Eng Phys,* vol. 28, no. 4, pp. 315-22, May 2006, doi: 10.1016/j.medengphy.2005.07.004.
[242] J. H. Cole and K. Franke, "Predicting Age Using Neuroimaging: Innovative Brain Ageing Biomarkers," (in eng), *Trends Neurosci,* vol. 40, no. 12, pp. 681-690, Dec 2017, doi: 10.1016/j.tins.2017.10.001.
[243] O. Al Zoubi *et al.*, "Predicting Age From Brain EEG Signals-A Machine Learning Approach," (in eng), *Front Aging Neurosci,* vol. 10, p. 184, 2018, doi: 10.3389/fnagi.2018.00184.
[244] E. Mioshi, K. Dawson, J. Mitchell, R. Arnold, and J. R. Hodges, "The Addenbrooke's Cognitive Examination Revised (ACE-R): A brief cognitive test battery for dementia screening," *International Journal of Geriatric Psychiatry,* vol. 21, no. 11, pp. 1078-1085, 2006, doi: 10.1002/gps.1610.
[245] F. Vecchio *et al.*, "Prognostic Role of Hemispherical Functional Connectivity in Stroke: A Study via Graph Theory Versus Coherence of Electroencephalography Rhythms," (in eng), *Stroke,* Nov 23 2022, doi: 10.1161/STROKEAHA.122.040747.
[246] V. Miskovic and A. Keil, "Reliability of event-related EEG functional connectivity during visual entrainment: magnitude squared coherence and phase synchrony estimates," (in eng), *Psychophysiology,* vol. 52, no. 1, pp. 81-9, Jan 2015, doi: 10.1111/psyp.12287.
[247] V. Longo *et al.*, "Transcranial Direct Current Stimulation Enhances Neuroplasticity and Accelerates Motor Recovery in a Stroke Mouse Model," (in eng), *Stroke,* p.

STROKEAHA121034200, Mar 16 2022, doi: 10.1161/STROKEAHA.121.034200.
[248] D. S. Bassett and E. Bullmore, "Small-world brain networks," (in eng), *Neuroscientist,* vol. 12, no. 6, pp. 512-23, Dec 2006, doi: 10.1177/1073858406293182.
[249] O. Kramer, "Scikit-Learn," in *Machine Learning for Evolution Strategies*, O. Kramer Ed. Cham: Springer International Publishing, 2016, pp. 45-53.
[250] S. Badillo *et al.*, "An Introduction to Machine Learning," *Clinical Pharmacology & Therapeutics,* vol. 107, no. 4, pp. 871-885, 2020/04/01 2020, doi: https://doi.org/10.1002/cpt.1796.
[251] S. Khalid, T. Khalil, and S. Nasreen, "A survey of feature selection and feature extraction techniques in machine learning," *2014 Science and Information Conference,* pp. 372-378, 2014.